

INVESTIGATING THE ROLE OF SHROOM3 IN KIDNEY DEVELOPMENT

INVESTIGATING THE ROLE OF SHROOM3 IN KIDNEY DEVELOPMENT

By Ashmeet Hunjan, B.Sc. (Hons.)

A Thesis Submitted to the School of Graduate Studies in Partial Fulfillment of the
Requirements for the Degree Master of Science

McMaster University © Copyright by Ashmeet Hunjan, August 2021

TITLE: Investigating the Role of Shroom3 in Kidney Development

AUTHOR: Ashmeet Hunjan B.Sc. (Hons.), McMaster University

PROGRAM: Medical Sciences Graduate Program, Division of Cancer and Genetics,
McMaster University, Hamilton, Ontario Canada

SUPERVISOR: Darren Bridgewater, PhD

SUPERVISORY COMMITTEE: Dr. Joan Krepinsky and Dr. Peter Margetts

NUMBER OF PAGES: xiii, 117

ABSTRACT

Nephrons develop from a specialized group of mesenchyme cells known as the nephron progenitors. Nephron progenitors can very dynamic as they can self-renew, migrate, and change their cell morphology. These alterations are essential for orientating and organizing select cells for progression through various stages of nephrogenesis. However, the underlying mechanisms that drive these dynamic morphological changes are not fully understood. Shroom3 is an actin-binding protein that regulates cell shape changes by modulating the actin cytoskeleton. In mice and humans, mutations in Shroom3 are associated with poor nephron function and chronic kidney disease. Despite these findings, the underlying mechanisms of Shroom3 function and how genetic mutations contribute to abnormal nephron formation are unclear. Here, we investigated functional roles for Shroom3 in the nephron progenitor population by analyzing E13.5 and E18.5 Wildtype and Shroom3 deficient mice (termed Shroom3^{-/-}). First, using in-situ hybridization (ISH) and immunofluorescence (IF), we confirm Shroom3 expression in select nephron progenitors. Next, we demonstrated abnormal cell shape and abnormal nephron progenitor cell clustering using H&E staining and Pax2 immunofluorescence. We showed a reduction in nephron progenitor cell numbers and decreased cell length in E13.5 Shroom3^{-/-} kidneys. Using markers of cell orientation, we discovered altered cell orientation in some but not all nephron progenitor cells. While analyzing the cell cytoskeleton, we also demonstrated the abnormal distribution of F-actin in Shroom^{-/-} nephron progenitors. Lastly, immunofluorescence and transmission electron microscopy analysis of Shroom3^{-/-} nephron progenitors confirmed the abnormal shape and reduced filopodia-like thin actin-

based membrane protrusions. Our findings conclude that Shroom3 is essential for maintaining and regulating nephron progenitor cell morphology. Taken together, these findings could help explain why Shroom3 mutations are highly associated with kidney disease.

ACKNOWLEDGMENTS

First and foremost, I would like to express my sincerest gratitude and a thank you to my supervisor, Dr. Darren Bridgewater, for his ongoing mentorship. Thank you for challenging me and always encouraging me to reach my full potential. Your enthusiasm towards research and your work ethic has inspired me throughout my journey. I could not have asked for a better mentor. Thank you for giving me this opportunity and making it a great learning experience.

To my committee members Dr. Joan Krepisnsky and Dr. Peter Margetts, thank you for your invaluable advice and guidance through my study to my supervisory committee. I appreciated all your feedback.

I am very grateful to Joanna Cunanan, our incredible lab technician. I appreciate everything you have done for me from the beginning of my journey to the end. The time and energy you have invested into helping me with my project have been pivotal in my progress. Your constant support throughout my journal will be cherished as you played an essential part in my project. You are indeed one of the most hardworking and intelligent people I have encountered. I wish you all the best in all your future endeavours.

To Kristina Cunanan, I admire you for getting involved and challenging yourself early in your undergraduate studies. You constantly strive to give your 100% in your written work, your experiments, and your coursework. Our time together fell short because of the pandemic, but I still enjoyed having you at our Zoom lab meetings.

To Lily Morikawa, your knowledge, skills, and techniques in histology are astonishing. You have been a great help to me, and I am grateful to have worked with someone as sweet as you.

To Marcia, your expert advice and assistance with all the practical aspects of Electron Microscope is greatly appreciated.

I would also like to thank Aftab for his help with the cryosections and for always being so supportive. I always appreciated your kindness your willingness to support my success.

Finally, to my parents, sister, and brother, thank you for all your support. A big thank you to my friends who always who have been my biggest supporters throughout my journey.

TABLE OF CONTENTS

DESCRIPTIVE NOTES.....	iii
ABSTRACT.....	iv
ACKNOWLEDGEMENTS.....	vi
TABLE OF CONTENTS.....	viii
LIST OF SUPPLEMENTARY FIGURES.....	ix
LIST OF FIGURES.....	x
DECLARATION OF ACADEMIC ACHIEVEMENT.....	xiii
1. BACKGROUND	1
1.1 Kidney anatomy and function	1
1.1.1 Gross anatomy of the mammalian kidney	1
1.1.2 Kidney and the Nephron: Structure and Function	2
1.2 Kidney Development	4
1.2.1 Pre-Metanephric-Development.....	4
1.2.2 Metanephros and development of the Mammalian kidney	5
1.2.3 Initiation of Nephrogenesis.....	6
1.2.4 Nephron Progenitor Cells	11
1.2.5 Nephron progenitor cells	12
1.2.6 Cell Signaling and Specialization.....	13
1.2.7 Nephron progenitors and Cellular Projections.....	16
1.3 Shroom3.....	21
1.3.1 Shroom3 Protein	21
1.3.2 Shroom3 Function	23
1.3.3 Shroom3 and Chronic Kidney Disease	25

1.3.4	Shroom3 in Kidney Disease and Development	26
1.3.5	Shroom3 in embryonic kidney development	28
2.	HYPOTHESIS & OBJECTIVES	31
2.1	Overall Hypothesis	31
2.2	Study Objectives	31
3.	Methods and Materials	32
4.	Results	39
4.1	Shroom3 protein is localized in nephron progenitor cells.....	39
4.2	Shroom3 mutation results in abnormal nephron progenitor cell morphology	44
4.3	Shroom3 knockout in embryonic kidneys results in reduced nephron progenitor cell number and cell length	51
4.4	Shroom3 mutant nephron progenitors display altered cell orientation	58
4.5	Shroom3 mutation leads to changes in F-actin distribution	68
4.6	Shroom3 mutant Nephron progenitors lack cellular projections	73
4.7	Lack of cellular projections in the absence of Shroom3.....	78
5.	DISCUSSION	86
	Overall Findings	86
5.1	Spatial expression pattern of Shroom3 in select nephron progenitor cells may influence specific cell fate changes during nephron formation	86

5.2	Shroom3 might regulate the balance between nephron progenitor self-renewal and differentiation.....	89
5.3	Shroom3 influences nephron progenitor cell orientation	91
5.4	Shroom3 mutation may be disrupting ECM dynamics and cross talk between cells 92	
5.5	Shroom3 modulates nephron progenitor cell cytoskeleton and influences nephron projection formation.....	94
5.6	Potential Mechanism of Shroom3	95
5.7	Future directions and implications	98
6.	Conclusions:.....	100
7.	References	101

LIST OF SUPPLEMENTARY FIGURES

Supplementary Figure 1: Anatomy of the Kidney	2
Supplementary Figure 2: Basic structure of the nephron.	4
Supplementary Figure 3: Stages of kidney development.	5
Supplementary Figure 4: Schematic diagram illustrating morphological changes leading to nephron formation.....	9
Supplementary Figure 5: Nephrogenic Zone of the developing kidney.....	10
Supplementary Figure 6: Localization of the progenitor cell population.....	12
Supplementary Figure 7: Nephron progenitor and sub-domains	13
Supplementary Figure 8: Types of Progenitor cells and cell signalling.	16
Supplementary Figure 9: Nephron Progenitors are a dynamic group of cells.....	19
Supplementary Figure 10: Types of cellular projections.....	20
Supplementary Figure 11: Shroom3 gene structure and protein function	21
Supplementary Figure 12: Shroom3 in cell elongation and apical constriction.	25
Supplementary Figure 13: Expression of Shroom3 in the Adult Kidney	27
Supplementary Figure 14: Abnormal Glomeruli in Shroom3 Mutant Kidney.....	28
Supplementary Figure 15: Shroom3 expression in the developing kidneys.....	29
Supplementary Figure 16: Abnormal Renal Vesicles formation in Shroom3 mutants. 30	

LIST OF FIGURES

Figure 1: Detecting Shroom3 mRNA localization by in-Situ Hybridization	40
Figure 2: Magnified images of Shroom3 In-Situ Hybridization.....	41
Figure 3: Shroom3 N-Term antibody	42
Figure 4: Optimizing the N-term Shroom3 antibody in adult kidneys	43
Figure 5: Shroom3 protein is found in select nephron progenitor cells.....	44
Figure 6: Mouse Model and Genotyping.....	46
Figure 7: Shroom3 knockout E13.5 kidneys display abnormal nephron progenitor cell not clustering and spacing	47
Figure 8: Shroom3 Knockout E18.5 kidneys display abnormal nephron progenitor organization	48
Figure 9: Pax2 immunofluorescence of E13.5 mouse kidneys display nephron progenitors abnormally spaced apart from the ureteric epithelium	49
Figure 10: Shroom3 knockout E18.5 kidneys display abnormal spacing between nephron progenitors and ureteric epithelium	50
Figure 11: Six2 immunofluorescence of E13.5 mouse kidneys	53
Figure 12: High power images of E13.5 mouse kidneys with Six2 staining.....	54
Figure 13: Statistical analysis of Six2+ cell in of Shroom3 knockout E13.5 mouse kidneys	55
Figure 14: Ncam immunofluorescence of Shroom3 knockout E13.5 mouse kidneys display reduced number of nephron progenitors	56

Figure 15: Ncam immunofluorescence of Shroom3 knockout E18.5 mouse kidneys displays no difference in nephron progenitor cell number	57
Figure 16: Six2 and GM130 co-immunofluorescence of E13.5 Shroom3 mutant kidneys suggests no differences in cell orientation	60
Figure 17: Six2 and GM130 co-immunofluorescence of E18.5 Shroom3 mutant suggests no differences in cell orientation.....	61
Figure 18: Shroom3 mutant E13.5 mice display altered GM130 expression pattern.....	62
Figure 19: Shroom3 mutant E18.5 mice kidneys display altered GM130 expression pattern	63
Figure 20: High power images of E18.5 mice kidney highlight altered nephron GM130 expression	64
Figure 21: Integrin-a8 immunofluorescence in E13.5 kidneys.....	66
Figure 22: Expression of integrin-a8 at E13.5 is unchanged in Shroom3 ^{-/-} kidneys.....	67
Figure 23: Shroom3 mutated E18.5 kidneys display altered expression of Integrin- α 8...	68
Figure 24: F-actin distribution in Shroom3 mutant embryonic kidneys is disrupted	70
Figure 25: High power image of E13.5 kidneys display abnormal F-actin distribution...	72
Figure 26: Lack of cellular projections in Shroom3 mutant E13.5 nephron progenitors .	75
Figure 27: Ncam immunofluorescence on E13.5 kidneys to detect cellular projections..	76
Figure 28: Ncam immunofluorescence on E18.5 kidneys display no change in projection formation.....	77
Figure 29: Transmission Electron Microscopy of E18.5 Shroom3 mutant nephron progenitors display irregular cell shape and organization	80
Figure 30: Embryonic kidneys display presence of Lamellipodia-like thick protrusions	81
Figure 31: Transmission Electron Microscopy of the E18.5 Shroom3 mutant kidney show lack of cellular projection formation	82
Figure 32: Shroom3 mutant E13.5 nephron progenitors display increased ECM and decreased filipodia formation	84
Figure 33: Shroom3 mutant E13.5 display increased extracellular matrix.....	85
Figure 34: Model of Shroom3 function in nephron progenitors.....	97

DECLARATION OF ACADEMIC ACHIEVEMENT

I personally accomplished all the research and necessary tasks for Figure 3 through Figure 34. Hadiseh Khalili previously conducted the experiments for Figures 1 Figure 2, but I personally imaged all the slides to create the figures.

1. BACKGROUND

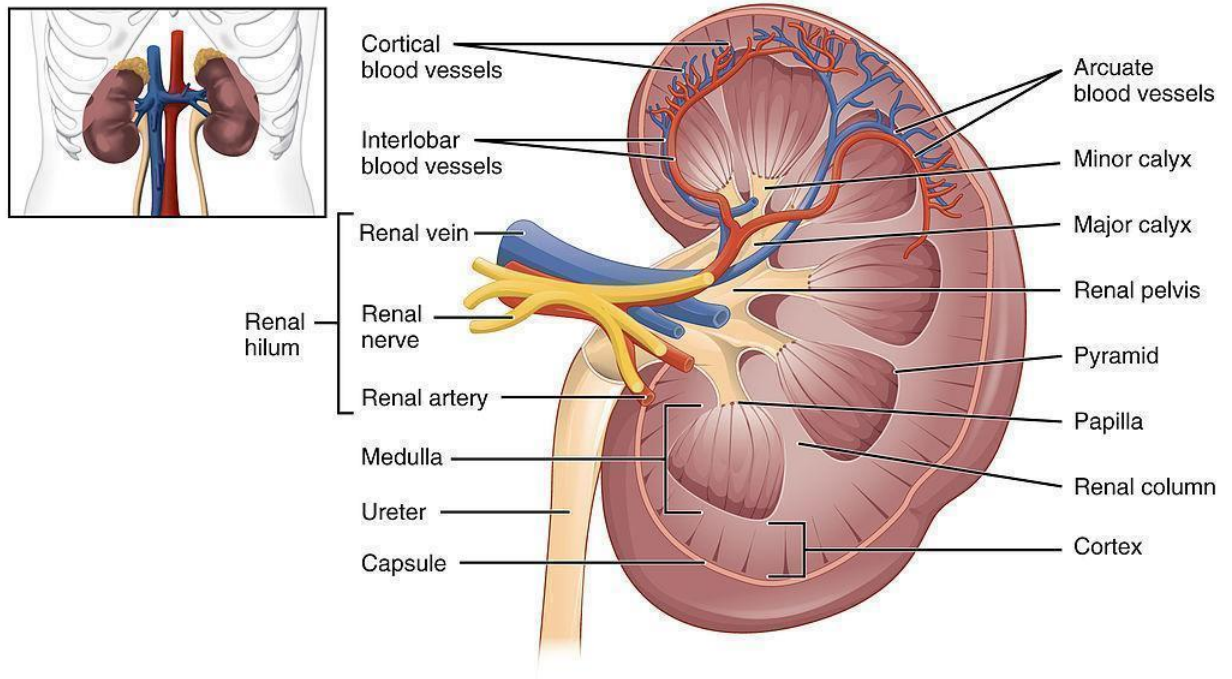
1.1 Kidney anatomy and function

1.1.1 Gross anatomy of the mammalian kidney

Kidneys are a pair of bilateral bean-shaped organs located posterior to the abdomen, sitting on either side of the vertebral column (Supplementary 1). Located in middle of the kidney is the renal sinus, renal pelvis, renal calyces, vasculature, nervous and adipose tissue. As blood enters the kidney through the renal artery it gets filtered and exits via the renal veins. Whereas the filtered plasma (urine) exits the kidney through the ureter to the urinary bladder.

A bisected kidney displays three distinct regions: the outer cortex, the inner medulla, and the renal pelvis (Brenner & Rector, 2012). The cortex contains the renal corpuscles and convoluted tubules. Located at the medulla tips are the renal pyramids composed of the renal papillae and the collecting ducts that drain into the minor calyces and major calyces. The urine travels through the minor to major calyces and then drains the renal pelvis that connects to the ureter.

Supplementary 1: Anatomy of the Kidney



Anatomy of the Kidney. Sagittal section of adult kidney illustrating the cortex, medulla, renal pelvis, artery and vein and the ureter.

1.1.2 Kidney and the Nephron: Structure and Function

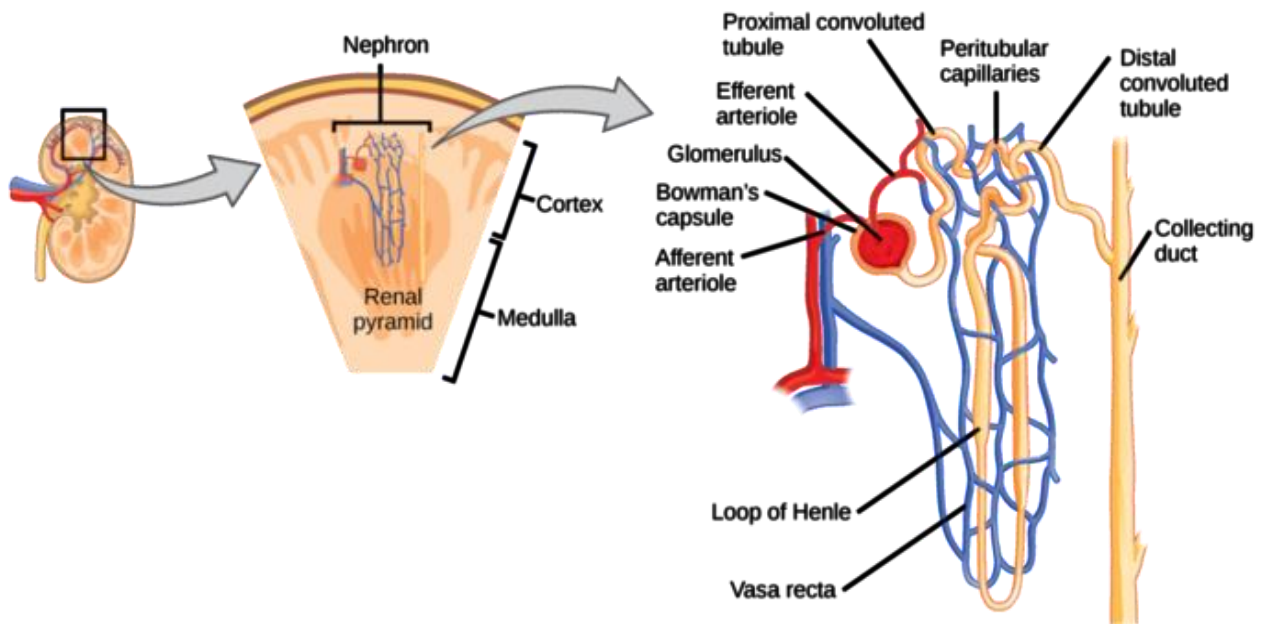
Nephrons are the functioning units of the kidney that filter, reabsorb and secrete solutes ions such as glucose and salt and excrete harmful toxins into the urine. An adult human kidney is composed of an average of 200,000 to 2 million nephrons, whereas a mouse kidney is composed of around 12,000 nephrons. Each nephron is composed of specialized functional segments critical to regulating blood volume, blood pressure and blood plasma osmolarity. Each segment of the nephron possesses tubular epithelial cells that differ in shape, size, and specializations, which is necessary for the many unique functions of the tubular segments. A single nephron can be divided into the renal corpuscle and the renal tubule (Brenner & Rector, 2012, Supplementary 2). The glomerulus is part of the renal corpuscle and contains capillaries composed of endothelial cells linked up by several

fenestrations and cells known as podocytes. During blood filtration, the blood passes through the capillaries and the glomerular basement membrane (GBM) of the endothelial cells. Next, the filtrate passed through the podocytes into the bowman's capsule (BC). After being filtered in the bowman's capsule, the fluid enters the renal tubule, the site of urine formation.

The renal tubule consists of three distinct regions, the proximal convoluted tubule (PCT), the loop of Henle (LOH), and the distal convoluted tubule (DCT). Each region is composed of specialized epithelial cells that alter in cell shape and function. For instance, the proximal convoluted tubule comprises tall cuboidal epithelium cells containing a subcellular microvillus, which helps increase the surface area for fluid reabsorption. When the filtrate passes the BC, it enters the PCT, where the microvilli reabsorb 90% of fluid and ions into the bloodstream.

After leaving the PCT, the filtrate enters the loop of Henle (LOH) which consists of descending and ascending loop. The descending LOH is composed of simple squamous epithelium, which passively allows water to exit the bloodstream. The ascending LOH contains a thin and thick loop that filters sodium chloride (NaCl) back into the bloodstream. The thick ascending LOH, lined by thicker simple cuboidal epithelium, represents the distal convoluted tubule (DCT), which effectively transports sodium, chloride, and potassium. The DCT is also the last segment of the nephron as the fluid from the DCT eventually drains into the collecting duct (CD) system, where final fluid modification occurs. Once modified, the filtrate drains into the ureter. Therefore, each segment of the nephron plays a distinct and vital role in ensuring proper filtration and reabsorption.

Supplementary 2: Basic structure of the nephron.



Basic structure of the nephron. The glomerulus, Bowman's capsule, proximal convoluted tubule, the loop of Henle, and the distal convoluted tubule are the functional segments of the kidney. The flow of filtrate begins at the Bowman's capsule travelling

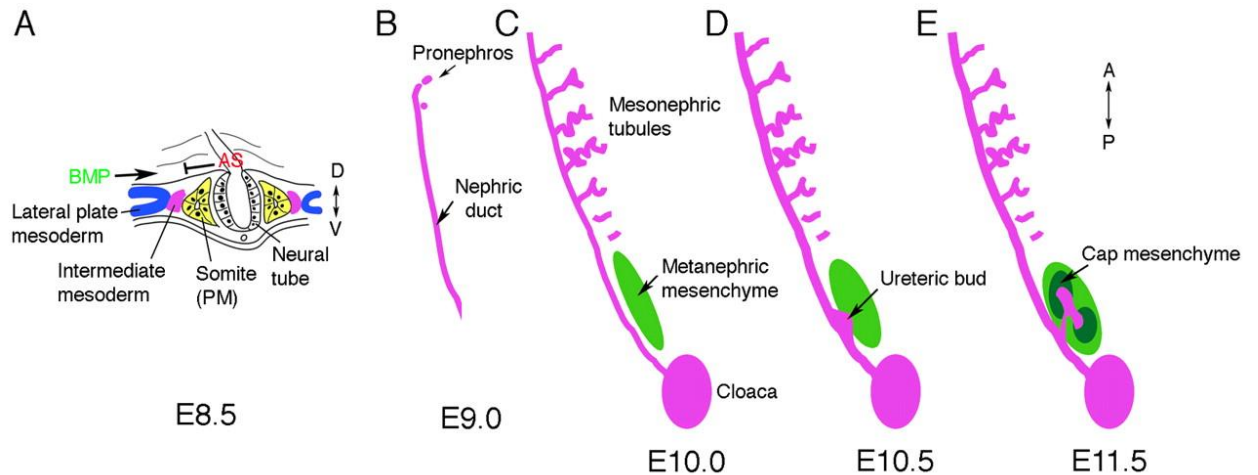
1.2 [Kidney Development](#)

1.2.1 Pre-Metanephric-Development

The urogenital system, comprising the kidneys, the gonads, and respective ductal systems, is generated from the intermediate mesoderm (Vize et al., 2003). The Wolffian duct, also known as the pronephric duct, arises from the dorsal intermediate mesoderm, while the nephrogenic cord arises from the ventral intermediate mesoderm (Supplementary 3). Development begins at gestational day 22 in humans and embryonic day 8 in the mouse with the formation of the pronephric duct (also known as the Nephric or Wolffian duct; Supplementary 3). At E8.5, cells of the Wolffian duct start migrating caudally along the dorsal end of the body, inducing the formation of mesonephros (Seely, 2017). Past the embryonic period, the pronephros and mesonephros become non-functional structures in

mammals. At the 4th week of embryonic development, the pronephros completely disappears (Vize et al., 2003). The mesonephric holds a functional filtering capacity at 4-8 weeks and degenerates before birth. The development of a functioning kidney is dependent on the accurate formation and degradation of pronephros and mesonephros.

Supplementary 3: Stages of kidney development.



Stages of kidney development. Diagram illustrates the development of the pronephros, the mesonephros, and the metanephros. Metanephros begins at E10.5 when signals from the metanephric mesenchyme (green) cause the nephric duct (pink) to form an outgrowth.

1.2.2 Metanephros and development of the Mammalian kidney

The formation of the permanent kidney, the metanephros, is initiated after the degradation of the pronephros and mesonephros. At 5-weeks of gestation in humans and 10.5 days post-coitus in mice, signals from the metanephric mesenchyme (MM) induce outgrowth of the ureteric bud epithelium (UB). As the MM sends out signals such as *Gdnf* and *Fgf10*, cells in the caudal-most portion of the Nephric duct proliferate and grow towards the MM, creating a UB (Brenner & Rector, 2012). The UB signals to the MM, allowing the mesenchymal cells to cap around the ureteric bud tips (Supplementary 3). As the MM aggregates around the tips, it forms nodules known as the cap mesenchyme. At

E11.5, the process of UB tip cell proliferation repeats, known as bifurcation, and the result is the creation of A T-shaped structure (Supplementary 4). The continuation of these bifurcation events is known as branching morphogenesis, where the final product is the formation of the renal collecting system. This system consists of the collecting ducts, major and minor calyces, renal pelvis, and ureter. Thus, branching morphogenesis is initiated and regulated by the signalling molecules from the metanephros mesenchyme during development.

A developing kidney is composed of the ureteric bud epithelium, also known as the ureteric epithelium (UE), the metanephric mesenchyme, later known as nephron progenitors (NP), and the stromal cells (SC) (Supplementary 6). Each type of cell gives rise to different parts of the functioning kidney. The UE cells undergo branching morphogenesis to create the renal collecting system. The nephron progenitors undergo nephrogenesis to create all the nephron segments. Finally, the stromal progenitors mature into the kidney interstitium, mesangial cells, pericytes, and part of the kidney vasculature (O'Brien and McMahon, 2014).

1.2.3 Initiation of Nephrogenesis

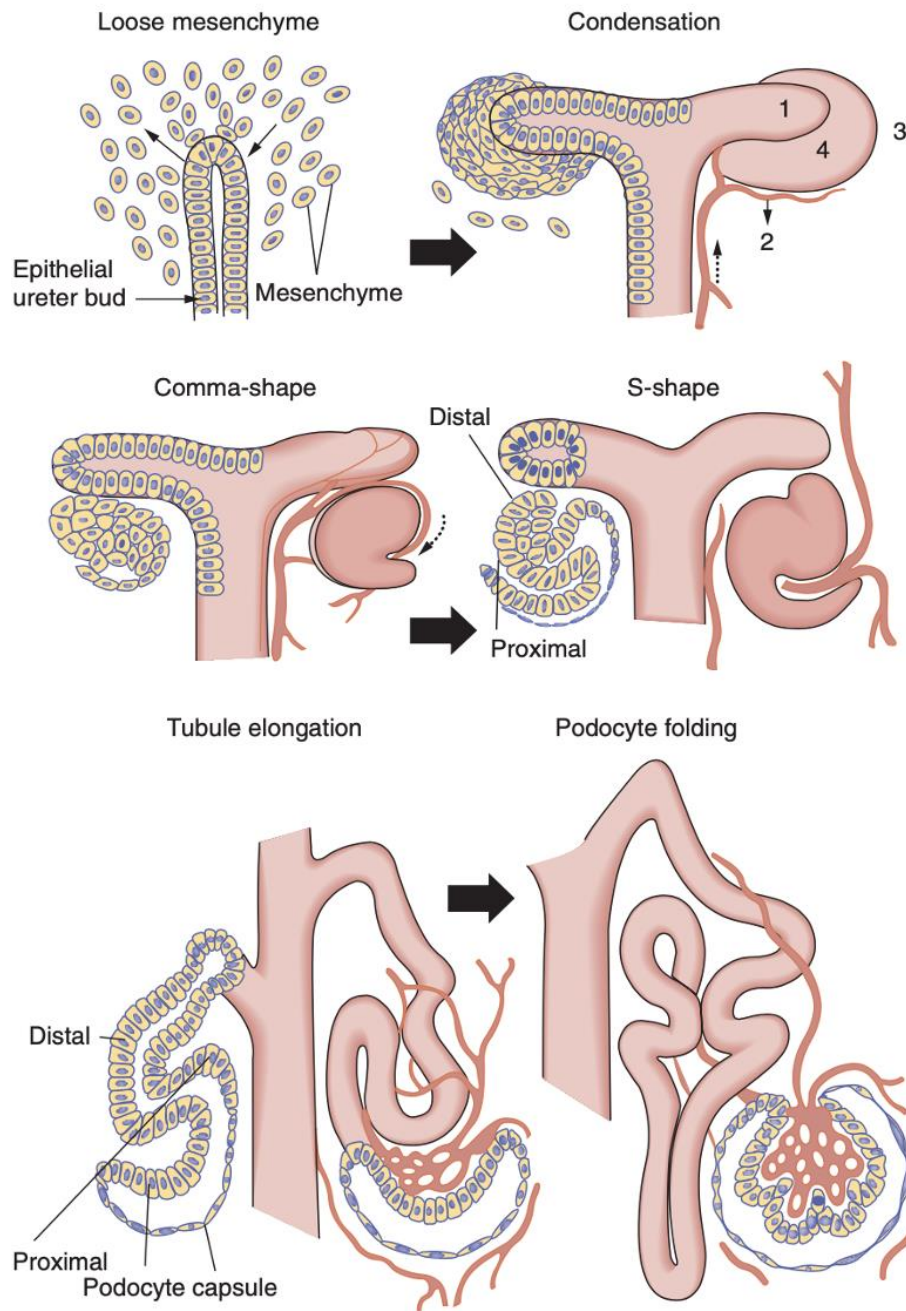
Nephrons are the functional units of the kidney, and the nephron formation is known as nephrogenesis. Nephron formation relies on accurate reciprocal cellular communications between the nephron progenitor and ureteric epithelium. Before nephrogenesis, select nephron progenitors cluster together near the ureteric trunk, a region of the ureteric epithelium. The nephron progenitors cluster further under the ureteric trunk and undergo a mesenchymal-to-epithelial transition to form the pretubular aggregates. Nephrogenesis begins when the pretubular aggregates rearrange and transition into a polarized spherical

structure known as the renal vesicles. The renal vesicles will further change their shape and differentiate into distinct morphological structures through elongation and form the comma-shaped body. These cell bodies will undergo further structural transformation and develop into an S-shape body and finally into the capillary loop and mature nephron stage (Supplementary 4). At the final stage, cells of the developing bodies will develop into either the columnar or cuboidal epithelium of specific nephron segments, such as the proximal and distal convoluted tubules of a mature nephron.

During nephron formation, a proximal-to-distal pattern is established, which plays a vital role in determining the fate of the cells. For instance, after renal vesicle formation, the structure elongates and develops a distal and proximal end. In a developed nephron, the proximal side of the renal vesicles will become the glomerulus. The podocytes start to appear as a columnar-shaped epithelial cell layer during the S-shape stages. As these structures change shape, the presumptive podocyte layer will separate from the distal cells and become a part of the proximal tubule. Concurrently, the parietal epithelial cells of the developing bodies differentiate to form the BC while the endothelial cells migrate to the vascular cleft. Initially connected by tight junctions, the podocytes then develop actin-based foot processes towards the capillary. At the capillary loop stage, apoptosis of a subset of endothelial cells forms the capillary lumen. At this stage, the glomerular endothelial cells develop their fenestrae transmembrane pores giving them their semi-permeable characteristic. It is thus critical that nephron progenitors undergo precise morphological changes during development to allow for structural transformation and formation of proximal-to-distal patterning required to develop a functioning nephron (Brenner & Rector, 2012). Nephrogenesis is induced in the peripheral regions of the kidney, and for this reason, the most mature nephrons are in the kidney's innermost regions. The nephrogenic zone in

a human and mouse embryonic kidney is the outermost kidney region comprised of the ureteric epithelium, stromal cells, and nephron progenitors (Supplementary 5). At postnatal days 4-6, all the nephron progenitor cells are exhausted, and nephrogenesis is complete (Cebrian et al., 2014).

Supplementary 4: Schematic diagram illustrating morphological changes leading to nephron formation.

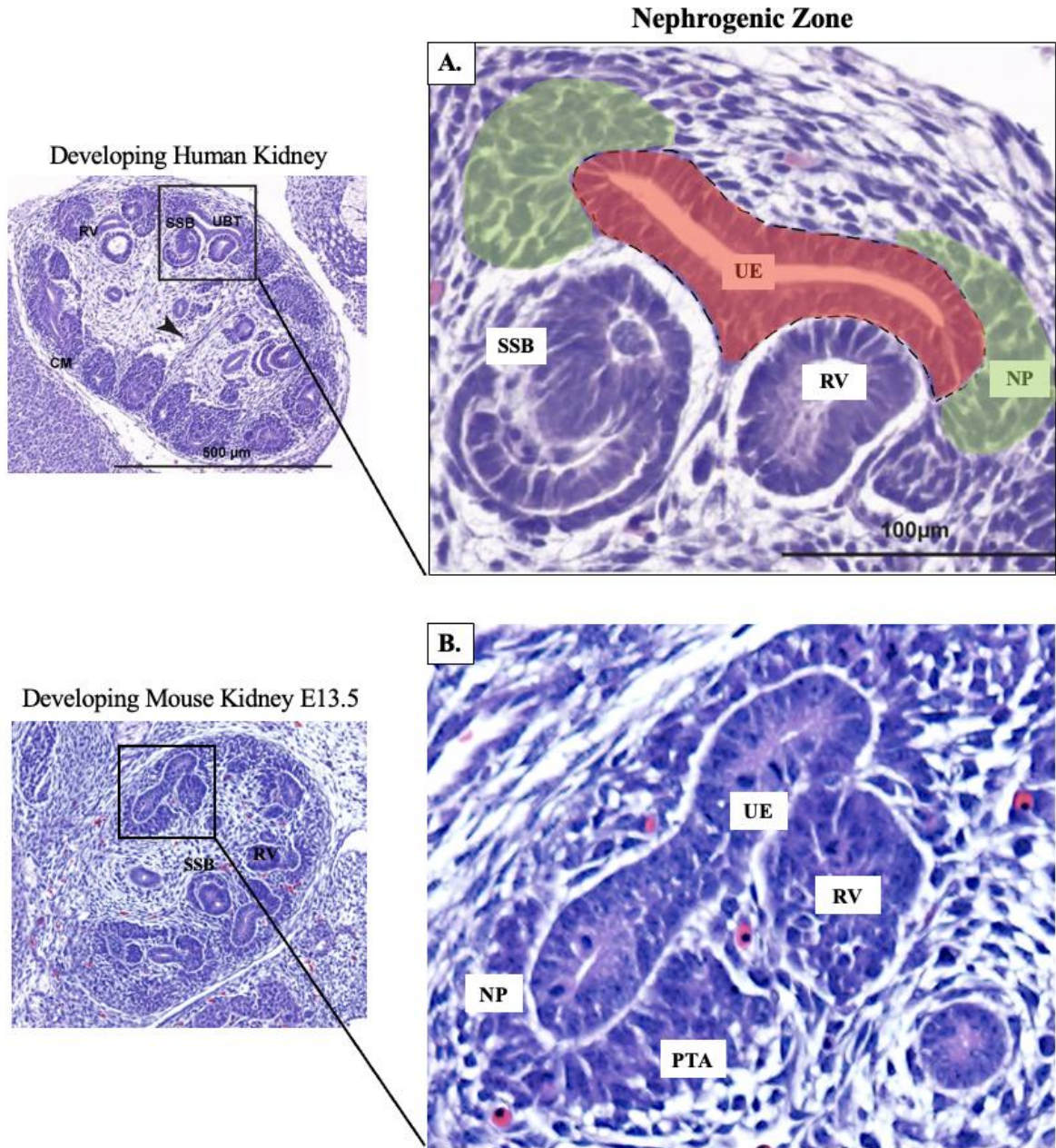


Schematic diagram illustrating morphological changes leading to nephron formation.

The four different cell lineages are the ureteric epithelial cells (1), the blood vessels (2), the uninduced mesenchyme (3), and the induced mesenchyme (4). The reciprocal interactions between ureteric epithelial and mesenchyme cells induce nephron progenitor's morphological changes. First, the mesenchyme undergoes condensation, then

mesenchymal to epithelial transition to develop into epithelial of the mature nephron. (Image from Brenner & Rector, 2012).

Supplementary 5: Nephrogenic Zone of the developing kidney.



Nephrogenic Zone of the developing kidney. A) Hematoxylin and eosin staining of embryonic human kidney show nephrogenic zone where nephrogenesis occurs in the developing kidney (Image adapted from Nils O. Lindström et al.) B) Schematic illustrating stage of nephrogenesis as seen in H&E. NP- nephron progenitors; UE- ureteric epithelium

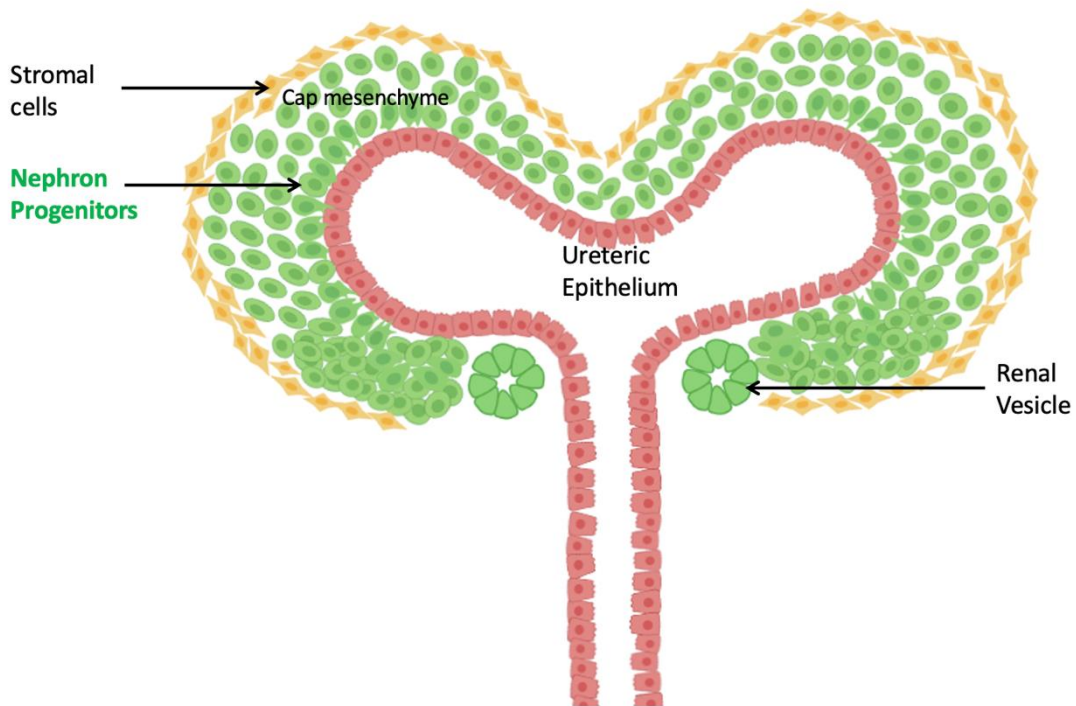
(includes the ureteric bud). Different stages: PTA-pretubular aggregate; RV- renal vesicle; CSB- comma-shaped; SSB- S-shape body.

Nephron progenitors

1.2.4 Nephron Progenitor Cells

Nephron progenitors, found in the cap mesenchyme, are a highly dynamic group of self-renewing cells that give rise to all the nephron segments (Supplementary 6). Nephron progenitors can either undergo cell proliferation or cell differentiation depending on the signals communicated to them from the ureteric bud tips. These signals enable cells to communicate their location, orientation, and physical interaction with adjacent cells. The transcriptional regulator Six2 for instance regulates nephron progenitor cell proliferation, and self-renewal. During cell differentiation, select nephron progenitor cells transition into epithelial cells through when they undergo mesenchymal to epithelial transition. This transition to epithelial cells requires changes in cell morphology dependent on changes to the intracellular actin dynamics which are regulated by cell signalling events during development (Brown et al., 2013).

Supplementary 6: Localization of the progenitor cell population.



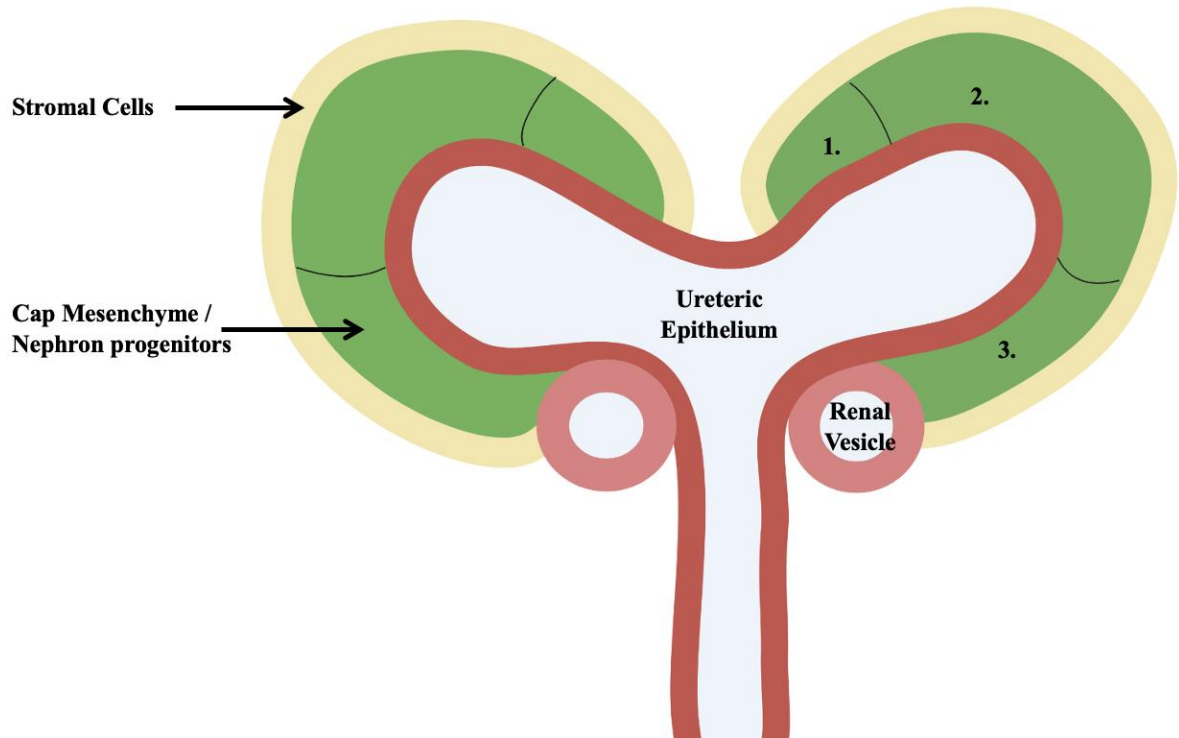
Localization of the progenitor cell population. Diagram illustrates the arrangement of the 3 different types of progenitors found in the developing kidney. Ureteric epithelium, Nephron progenitors, and Stromal cells.

1.2.5 Nephron progenitor cells

Nephron progenitors can be characterized into three sub-domains that each express various signalling molecules. The first domain is the “cap mesenchyme,” representing the entire population of self-renewing nephron progenitors expressing the transcription factor Six2 (Supplementary 7). The “capping mesenchyme” represents the second domain and consists of uninduced nephron progenitors that are both transcription factor Six2 and regulatory factor Cited1 positive (+). The “induced mesenchyme” is the third domain consisting of Six2 and Wnt4 positive nephron progenitors, which will differentiate and develop into nephrons (Mugford et al., 2009). During development, nephron progenitors can move from the uninduced region (top of the ureteric epithelium) to the site where

nephrons are formed (bottom of the ureteric epithelium). Although it is unclear how these cells travel from one domain to another, one possible mechanism is directional migration due to cell signalling (Combs, 2011), which requires changes in the nephron progenitor cell shape controlled by the actin dynamics.

Supplementary 7: Nephron progenitor and sub-domains



Nephron progenitor and sub-domains. The cap mesenchyme can be divided into three domains consisting of: (1) Six2+ cells (2) Cited1+, Six2+, Meox1+, Eya+ cells (3) Six2+, Wnt4+, Eya1+ cells. (Image adapted from Mugford et al. 2009)

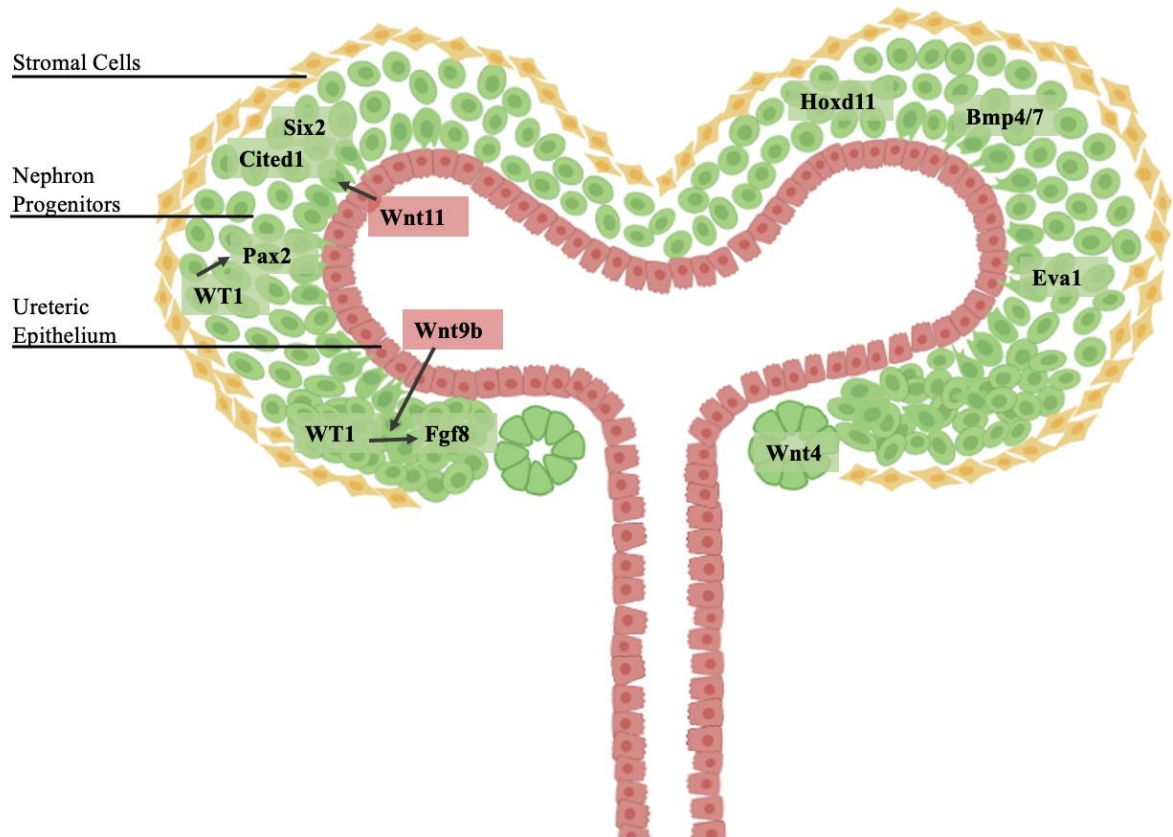
1.2.6 Cell Signaling and Specialization

Nephron progenitors and their cell signalling molecules can be categorized based on their location, uninduced region or the induced region. The uninduced region contains molecules that regulate nephron progenitor proliferation and survival, whereas the induced region generally consists of signalling molecules that regulate nephron progenitor differentiation. Some signaling factors that regulate nephron progenitor cell fate are the wingless-type mouse mammary tumor virus integration site family members (WNTs), bone

morphogenetic proteins (BMPs), fibroblast growth factors (FGFs) (Brown et al., 2013) (Supplementary 8). Among the family of proteins, WNT proteins in the nephron progenitor cells are most established and known to play a role in cell proliferation and differentiation. For instance, Wnt proteins regulate a crucial step to nephrogenesis, mesenchymal to epithelial transition (MET) (Torres et al., 2000). Wnt9b and Wnt11 are Wnt proteins produced by the ureteric epithelium, yet they regulate nephron progenitor cell fate. WNT9b regulates nephron progenitor self-renewal and differentiation, whereas Wnt11 regulates cell polarity, cytoskeletal organization, adhesive properties, and cell motility (Reidy & Rosenblum, 2009). Wnt9b is dependent on activation by β -catenin and follows a canonical signalling pathway. In contrast, Wnt11 does not require β -catenin and follows a non-canonical pathway. In the absence of Wnt9b, nephron progenitors fail to undergo MET (Carroll & Das, 2013). Wnt9b also plays a role in stimulating the activation of Wnt-4, which is another protein that induces nephron progenitors cell differentiation. Studies show that the absence of Wnt4 causes abnormal nephron progenitor cell differentiation, leading to the formation of fewer pretubular aggregates and renal vesicles that lack cell polarity (Dressler, 2006). Another molecule that stimulates Wnt-4 expression is Paired box protein (Pax2) (Dressler, 2006). Pax2 is an essential protein self-renewal and specification as it is expressed by both the nephron progenitors and ureteric epithelial cells. Pax2 activates signalling factors Six2 and glial cell line-derived neurotrophic factor (GDNF) in the nephron progenitors. GDNF signals to the ureteric epithelium to undergo branching morphogenesis through the GDNF receptor (RET) (Brophy et al., 2001). During kidney development, a knockout of the Pax2 gene results in abnormal branching morphogenesis and nephron specification (Cai et al., 2005). The nephron progenitors contain another signalling factor, Hox11, which interacts with Pax2 to induce transcription of two direct

downstream targets Six2 and GDNF (Wellik et al., 2002; Gong et al., 2007). Hox11 functions to help generate the NP cells, stromal progenitor cells and induce branching morphogenesis. Studies show that a double mutation of Hox11 paralogous group genes Hoxa11 and Hoxd11 results in kidney hypoplasia (Wellik et al., 2002). While Six2 is controlled by upstream signalling protein complex Pax2/Eya1/Hox11, Six2 itself functions to help maintain an undifferentiated state of the cell by preventing WNT signalling inducing nephron progenitor cell differentiation (Gong et al., 2007). Other essential signaling molecules that regulate nephron progenitors are Osr1 and WT1. OSR1 is essential to establish the metanephric mesenchyme (Mugford et al., 2008b) and interact with Six2 and Wilm's tumour (WT1), another transcription factor, to modulate nephron progenitor maintenance and specification (Xu et al., 2014, 2016). WT1 is another protein essential for nephron progenitor cell renewal, mesenchymal to epithelial transmission, and differentiation (Hartwig et al., 2010; Fanni et al., 2011). WT1 promotes proliferation by directly activating FGFs, such as Fgf8, through the phosphoinositide 3-kinase (PI3K)-Akt signalling pathway. In all, these signalling molecules are essential for controlling their cell fate, cell-cell communication, and morphology of nephron progenitors. The absence of these signals can lead to abnormal kidney development because their absence can lead to premature nephron progenitor cell depreciation or differentiation, leading to abnormalities such as renal agenesis or hypoplasia. Although many signalling factors that control nephron progenitor cell fate and morphology are recognized in the literature, many still factors remain unidentified (Karner et al., 2011).

Supplementary 8: Types of Progenitor cells and cell signalling.



Types of Progenitor cells and cell signalling. Diagram illustrates the arrangement of the 3 different types of progenitors found in the developing kidney. Stromal or interstitial cells (yellow), Ureteric epithelium (red) nephron progenitors (green). The diagram illustrates localization of some key signaling factors that regulate nephron progenitor cell function and fate.

1.2.7 Nephron progenitors and Cellular Projections

Nephron progenitors are highly motile cells that undergo significant cell shape changes as they move between adjacent ureteric buds and attach and detach with the ureteric epithelial cells. Recent studies have shown that nephron progenitors change shape and form membrane projections that elongate towards the ureteric epithelium (Supplementary 9, Minuth & Denk et al., 2013). These projections are critical during the first stages of nephrogenesis because they influence cell-cell interaction and cellular signalling and play a role in the transition of nephron progenitors to polarized epithelial

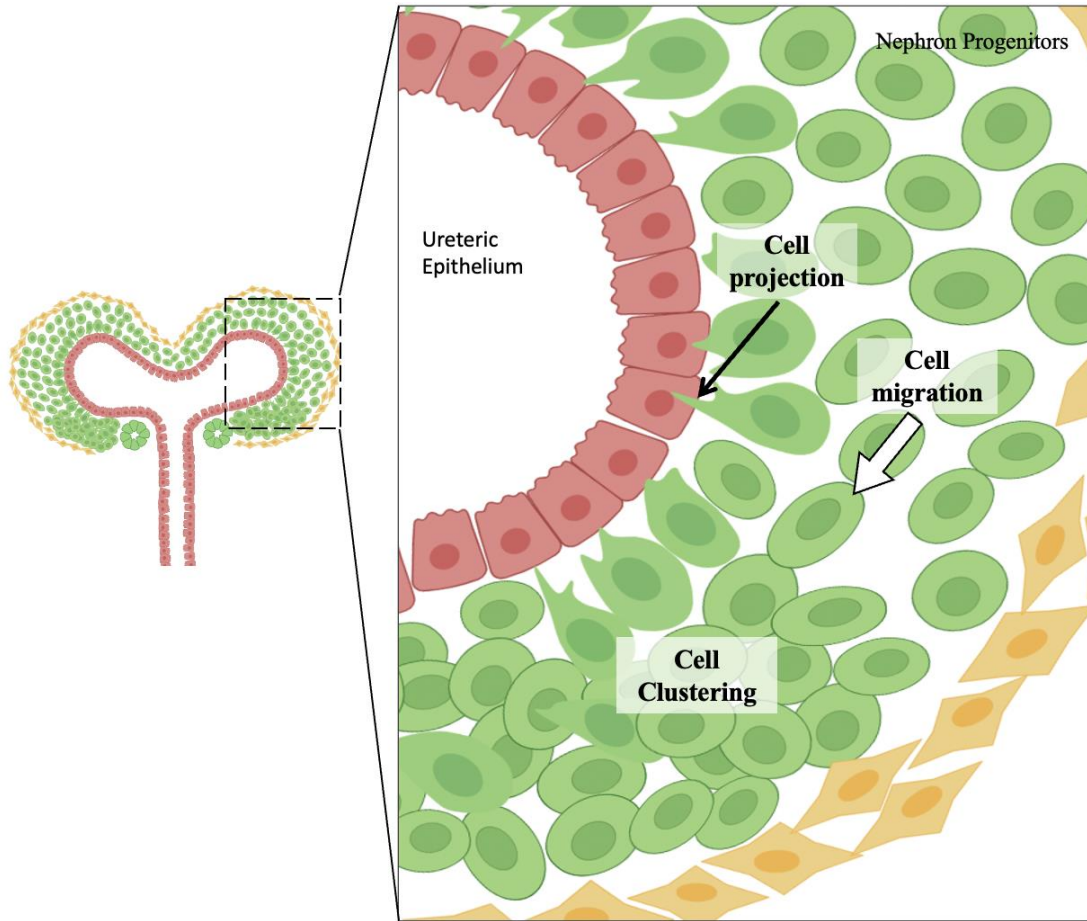
cells. In the absence of the projections, nephron progenitor can lose the ability to attach to the ureteric epithelial and, as a result, can undergo accelerated differentiation and premature depletion (O'Brien et al., 2019). Although recent studies show that nephron progenitors generate these projections, their function and regulation during development remain unclear.

There are several types of cellular projections, such as lamellipodia, filopodia, blebs and invadopodia (Supplementary 10). Each has a unique morphology and intracellular machinery that regulate its formation and function. A lamellipodium or lamellipodia is a broad fan-shaped protrusion with a Filamentous (F)-actin leading edge. In a lamellipodium, branched networks of actin drive cell mobility as an accumulation of F-actin physically pushes the membrane forward in the direction of migration (Svitkina, 2018). The formation of lamellipodia is regulated by the Arp2/3 complex (Johnson et al., 2015). The Arp2/3 complex controls the rate of actin polymerization as it nucleates the assembly of new actin filaments from existing filaments. The Arp2/3 complex activity is controlled by signalling molecules such as small GTPase Rac and phospholipid phosphatidylinositol (3,4,5)-trisphosphate (PIP3). Prime examples of cells that display this migratory behaviour due to protrusion formation are fibroblasts and tumour cells. The epithelial to mesenchymal transition (EMT) of tumour cells results from actin-dependent protrusions that propel cell migration (Shankar et al., 2010). While lamellipodia are large and thick protrusions, filopodia are narrower, thinner, and longer finger-like protrusions 0.1–0.2- μm in diameter. Filopodia are composed of long parallel actin bundles oriented with their fast-growing filament “+ ends” toward the tip (Kim et al., 2019). While lamellipodia are Arp2/3 dependent, the filopodia protrusion is Arp2/3-independent and signals via formins. Filopodia take part in neuronal communication and development, epithelial cell-cell

adhesion, and cell motility. However, it is essential to note that filopodia alone cannot drive cell mobility, they require existence of lamellipodia. For instance, mesenchymal (fibroblast-like) cells require the formation of lamellipodia and filopodia for migration (Supplementary 10A). Human skin fibroblast cells contain multiple lamellipodia, giving the cell a weakly polarized morphology (Supplementary 10B.a). Human lung fibroblasts cells contain filopodia that assist with directional migration (Supplementary 9B.b). Blebs are specialized rounded membrane protrusions found in migrating stromal cells and occur when there is an increase in intracellular pressure which can occur due to the activation of small GTPase Rho or myosin II (Kardash et al., 2010).

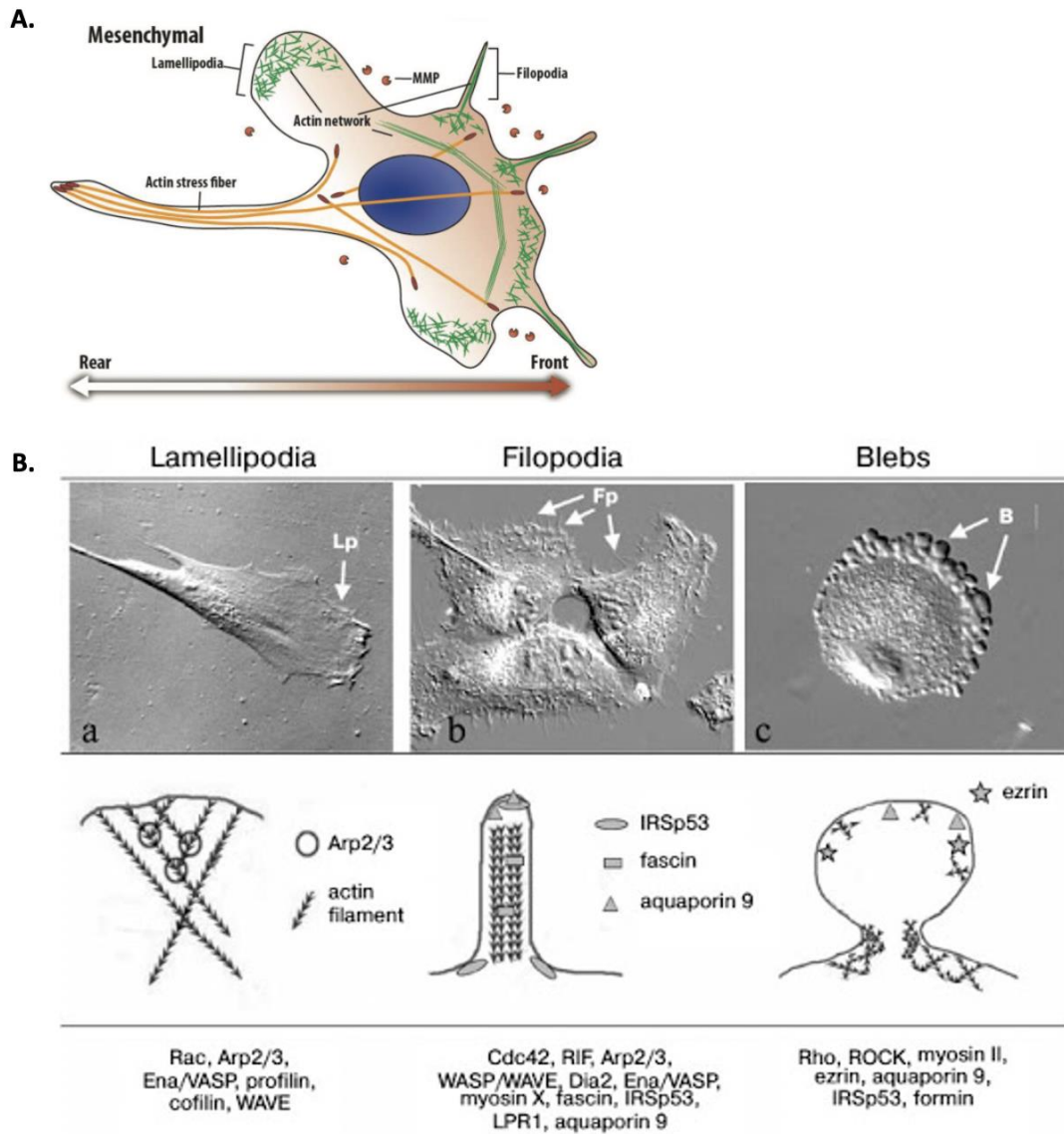
Additionally, the actin cytoskeleton is at the heart of cell morphology, mobility, and projection formation. The underlying mechanism that controls protrusion formation, such as filopodia and lamellipodia, blebbing and invadopodium, is the polymerization and accumulation of F-actin filaments at the membrane which exerts a mechanical force to generate projections (Kardash et al., 2010, Supplementary 10B). In cancer cells, epithelial to mesenchymal transition (EMT) occurs due to actin-dependent protrusions that propel migration (Shankar et al., 2010). In some cases, polarized cells also display a migrating behaviour due to nucleation and polymerization of actin at the leading edge of cells. In other cases, adhesion to substratum and cell mechanical properties are also highly regulated by integrins. Since nephron progenitors are motile cells that display attachment and detachment from the ureteric bud (Combs, 2011), this behaviour may be due to internal cell polarized, which influences F-actin rearrangement cell shape, and cell orientation.

Supplementary 9: Nephron Progenitors are a dynamic group of cells.



Nephron Progenitors are a dynamic group of cells. Schematic representing key nephron progenitor (NP) cell characteristics. In the blown-up image, select nephron progenitors have cellular projections (black arrow) elongating towards the ureteric epithelium (UE). Some cells are migrating (white arrow) to form a clustered groups of nephron progenitors.

Supplementary 10: Types of cellular projections.



Types of cellular projections. A) lamellipodia and filopodia formation during mesenchymal cell migration. A lamellipodium is a fan-shaped broad F-actin dense protrusion. A filopodia is a thin protrusion composed of long parallel actin bundles in the cell's leading edge (front). Mesenchymal migration involves forming a projected actin network in the frontal side and organizing multiple focal adhesions for the physical connection between the cell and the extracellular matrix (bottom). Image adapted from (Kim et al., 2019). B) Examples of different cell types producing various protrusions for cell migration. a) Represents lamellipodia in human skin fibroblast cells. b) Filopodia in human lung fibroblast cells. c) Blebbing in stromal cells. The bottom row illustrates the organization of the actin cytoskeleton and man proteins involved in forming cellular projections (Image from Alexandria, 2014).

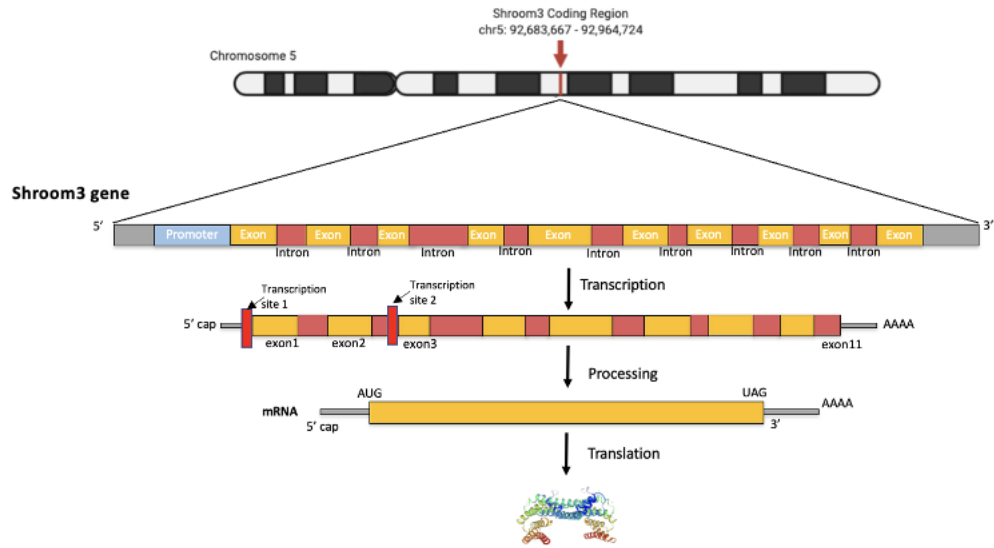
1.3 [Shroom3](#)

1.3.1 Shroom3 Protein

Although regulation of actin dynamics is necessary for proper cell shape and cell migration, it is still poorly understood in the nephron progenitor cell population. Shroom3 is a cytoskeleton regulator and part of a Shroom family of proteins (Shroom1, Shroom2 and Shroom4) (Halabi, 2013). The gene that encodes for Shroom3 is found on Chromosome 4 in humans and 5 in the mouse. In mice, 11 exons can encode for two Shroom3 isoforms, each in base pair number and amino acid (AA) sequence. The first isoform has 6765 base pairs and is 1996 AA long, while the second isoform has 6,435 base pairs and is 1808 AA long (Supplementary 11). The differences in the AA number are due to alternative transcription start sites, which generate different Shroom3 isoforms. The longer isoform has a transcription site located before exon one. In contrast, the shorter isoform (lacking the PDZ domain) of Shroom3 has a transcription site between exons two and three of the long isoform (Supplementary 11A). The long isoform of Shroom3 contains three domains, PDZ, ASD1 and ASD2, whereas the shorter isoform contains two domains ASD1 and ASD2 (Supplementary 11B). The PDZ domain of the long isoform is located at the N-terminal of Shroom3, consisting of amino acid sequence 25-110. In comparison, the ASD1 (Shroom-Domain 1) and C-terminal ASD2 (Shroom-domain2) are found between amino acid sequence 928-1030 and 1669-1957 of Shroom3 protein, respectively. The ASD1 domain directly binds to F-actin filaments, and the ASD2 domain binds to Rho-associated kinases (ROCK1 and ROCK2), which activate non-muscle myosin II (Supplementary 11C, Hildebrand et al., 1999).

Supplementary 11: Shroom3 gene structure and protein function

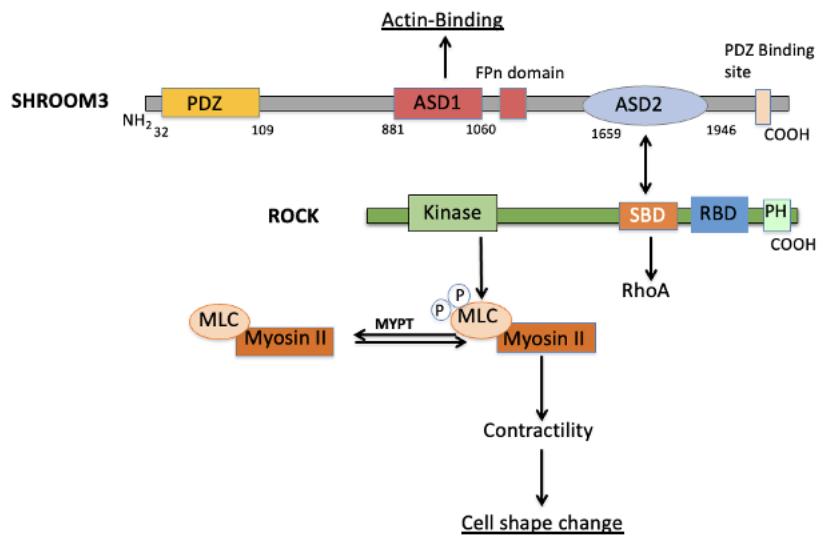
A. Shroom3 Gene on Chromosome 5 (mouse)



B. Shroom3 Isoforms



C. Shroom3 protein interaction and function



Shroom3 gene structure and protein function. A) The gene that encodes for Shroom3 is located on Chromosome 5 in the mouse and is composed of 11 exons. B) Once translated, Shroom3 protein is found in a longer and shorter isoform. While the longer isoform of

Shroom3 has three active domains: N-terminal PDZ, actin-binding ASD1, and C-terminal ASD2, the shorter isoform lacks PDZ.C) To initiate apical constriction, the Shroom binding domain (SBD) of Rock directly binds to the ASD2 domain of Shroom3 and phosphorylates the myosin light chain. This results in the activation of myosinII, leading to apical constriction and a change in cell shape.

1.3.2 Shroom3 Function

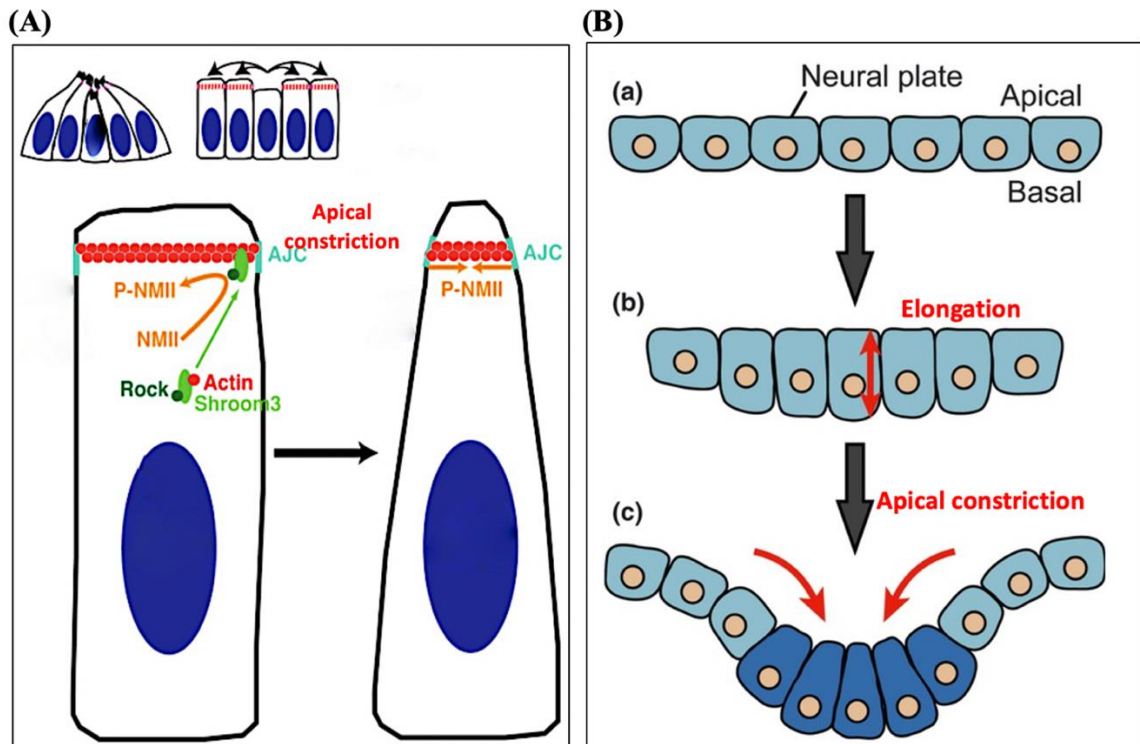
Shroom3 is a cytoskeletal-associated protein that regulates actin dynamics, tissue morphogenesis and apical constriction (Halabi, 2013). Shroom3 drives cell morphogenesis as it induces cell shape changes during neural tube formation through a process known as apical constriction (Supplementary 12). During apical constriction, the apical surface of epithelial cells constricts to decrease the apical surface area forcing the cell into a wedged shape. Morphogenetic events such as gastrulation, tube formation and neurulation require epithelial cells to apically constrict. Tissue folding at specified hinge points is dependent on the apical constriction, and thus, it is essential during morphogenesis and development. For instance, the absence of apical constriction neural tube closure events can lead result in congenital disabilities (Sawyer et al., 2010).

Shroom3 carries out apical constriction through the RhoA/Rock pathway. Once activated by RhoA, the ASD2 domain of Shroom3 directly binds to Rock1. Rock1 then activates non-muscle MyosinII in one of two ways, either by phosphorylating the serine-19 residue on the myosin light chain or indirectly inhibiting the myosin phosphatase activity. At the apical end of the cell, the activated myosin moves along the F-actin filaments already localized to the apical end. The movement of myosin on F-actin filaments is crucial because it facilitates the pull on apical cellular junctions to create a contractile actomyosin ring (Supplementary 12A). Actomyosin contractility is critical for neural tube formation, invagination of the lens pit and gut morphogenesis as it facilitates tissue development (Sawyer et al., 2010). In a developing embryo, Shroom3 mutation prevents

neural folds from converging at the dorsal midline leading to a “mushroom” phenotype of the brain region (Hildebrand & Soriano, 1999). The absence of Shroom3 prevents proper neural tube development, which leads to anencephaly, craniofacial clefting, spina bifida, and herniation. Studies also show that a mutation of Shroom3 in mice and zebrafish leads to expanded apical domains of the retinal neuroepithelial (Clark et al., 2012). Whereas, in lens morphogenesis, Shroom3 plays a role in inducing epithelial cells to undergo apical constriction to create the lens pit (Plageman et al., 2010; Plageman et al., 2011a)

In addition to regulating the actin cytoskeleton, Shroom3 also controls the microtubule cytoskeleton (Lee et al., 2007). Microtubules are linear filaments involved in cellular processes such as cell division, organization, movement, and cell shape changes. Microtubules are composed of repeating α/β tubulin heterodimers (Wiese & Zheng, 2006), and the addition of these heterodimers to existing monomers is a process known as microtubule nucleation. Microtubule nucleation can result in cells shape changes as it influences a process known as apicobasal elongation (Supplementary 12B.b). During apicobasal elongation, cells become more elongated as they transition from cuboidal to a columnar cell shape (Kondo & Hayashi, 2015). Shroom3 helps carry out apicobasal cell elongation by repositioning an important microtubule nucleator known as γ -tubulin to the apical end of the cell (Lee et al., 2007). For instance, during gut morphogenesis, Shroom3 helps maintain pseudostratification of the intestinal epithelium by recruiting γ -tubulin to the apical region during microtubule assembly (Chung et al., 2010). Therefore, Shroom3 regulates cytoskeletal dynamics by localizing F-actin and γ -tubulin to the apical regions of cells. However, although many studies have identified Shroom3 in the gut and neural tube morphogenesis, the role of Shroom3 during kidney morphogenesis remains a mystery.

Supplementary 12: Shroom3 in cell elongation and apical constriction.



Shroom3 in cell elongation and apical constriction. A) Model of the Shroom3-driven apical constriction mechanism in epithelial cells. Shroom3 localizes to the apical part of the cells where it interacts with Rock. At the apical side, Rock activates non-muscle myosin, leading to actin contraction and apical junction complex (AJC). B) Diagram represents apical constriction: a) cuboidal shaped epithelial cells of the neural plate have an apical and basal side; b) Shroom3 is involved in elongating cells to change from cuboidal to columnar; c) Shroom3 is involved in cell constriction where cells adapt a wedge-like shape. (Image from Suzuki et al., 2012 and Ernst et al., 2012).

1.3.3 Shroom3 and Chronic Kidney Disease

In an effort to find genes associated with kidney disease, several genome-wide association studies (GWAS) have identified Shroom3 to be associated with kidney dysfunction and chronic kidney disease (CKD). Using a large group of individuals of European background, a study by GWAS identified four risk loci to have the highest association with estimated creatinine glomerular filtration rate (eGFR_{crea}) and CKD (Kottgen et al., 2009). In addition, they identified an intronic SNP at rs17319721 of the SHROOM3 gene on Chromosome 4 to have the highest association with CKD (Kottgen et

al., 2009). The increased risk of CKD due to the missense mutation occurs during the transition of allele G to allele A. In an earlier study, researchers showed that Fawn-hooded hypertensive (FHH) rats, a model of CKD, contain mutations in the ASD1 binding domain of Shroom3 correlate with foot process effacement and glomerulosclerosis. The study further demonstrated that these glomerular defects could be rescued by integrating the wildtype Shroom3 gene into FHH rates. Overall, these studies suggest a crucial role of Shroom3 in kidney disease.

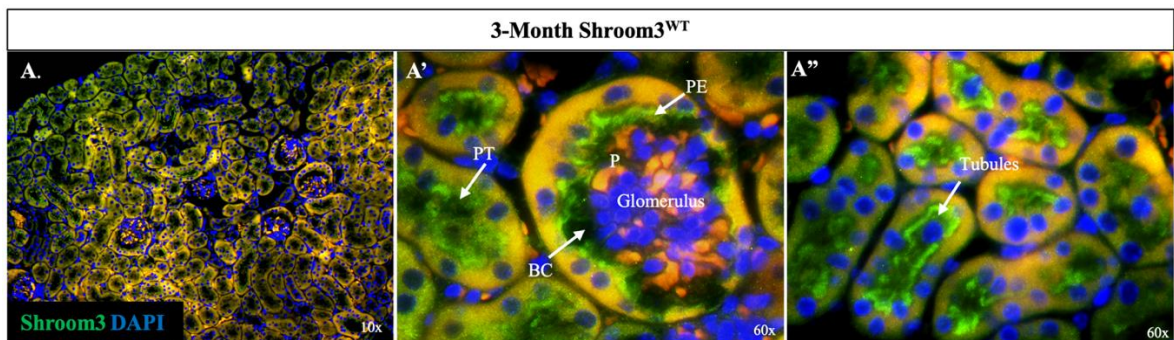
1.3.4 Shroom3 in Kidney Disease and Development

A study by Menon et al. (2015) investigated the effects of intronic rs17319721 single nucleotide polymorphism (SNP) of Shroom3, which generates an enhancer element for transcription factor 7-like-2 (TCF7L2), resulting in upregulation of Shroom3 transcription and increases the production of factor-beta 1 (TGF- β 1) which increased Shroom3. The donor kidneys with this SNP have a reduced eGFR, tubulointerstitial fibrosis, and allograft rejection at 12 months post-transplantation. Furthermore, a marked reduction of Shroom3 can also lead to a decreased profibrotic gene expression in vitro in renal epithelial cells and decreased interstitial fibrosis in vivo in a murine kidney injury model (Menon et al., 2015). In all, these studies suggest that the proper dose and regulation of Shroom3 function is essential for kidney development and repair.

In an adult kidney, Shroom3 protein is localized in the medullary collecting ducts and podocytes of the glomeruli (Supplementary 13). During Shroom3 haploinsufficiency (Shroom3 +/-), kidneys display abnormal actin cytoskeleton organization, glomerulosclerosis, foot process effacement, and increased proteinuria levels. A study by Khalili et al. showed localization of Shroom3 in the condensing mesenchyme, podocytes,

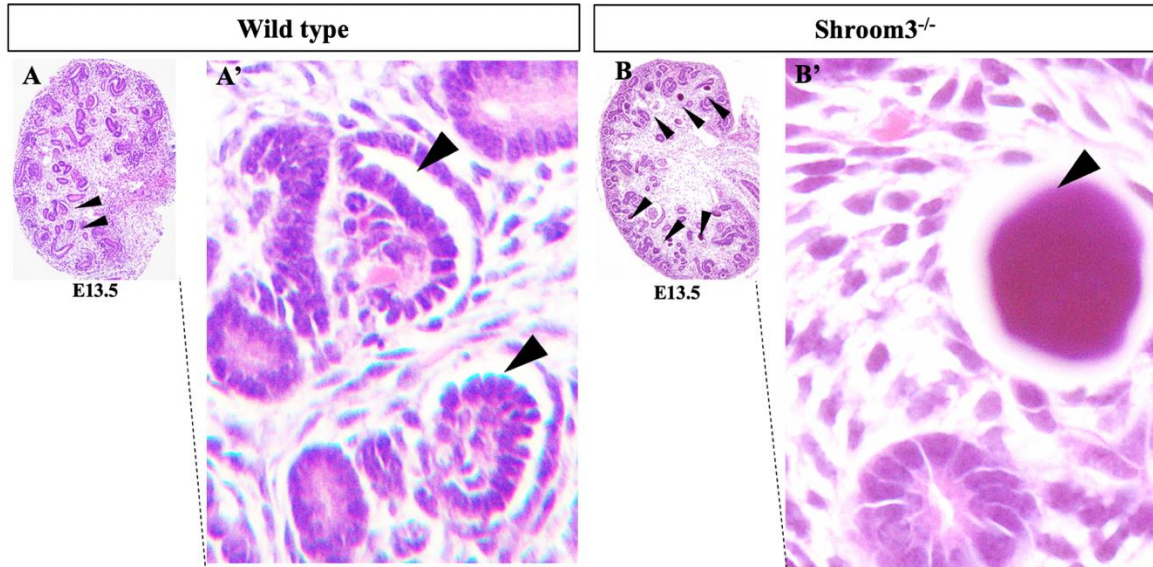
and collecting ducts of a developing kidney (Khalili et al., 2016). However, since Shroom3 homozygous mice (Shroom3^{-/-}) did not survive past birth, past studies could only examine Shroom3^{-/+} embryonic kidneys. In this study, Shroom3^{-/+} kidneys demonstrated cystic and collapsing glomeruli, an abnormally large space in the Bowman's capsule, and podocytes hypo-cellularity (Supplementary 14). In addition to that, Shroom3^{+/-} mice also displayed loss of Rock1 expression in the apical regions, suggesting that Shroom3 haploinsufficiency affects Rock/MyoII signalling pathways. The disrupted Rock/MyoII signalling damages the actin cytoskeleton of the cells and could account the damaged podocyte shape and function which would affect nephron function. Overall, findings from these studies provide an understanding of Shroom3 protein localization and understanding into the phenotypic abnormalities observed in the absence of Shroom3.

Supplementary 13: Expression of Shroom3 in the Adult Kidney



Expression of Shroom3 in the Adult Kidney. Immunofluorescence expression analysis **Shroom3** (Green), **DAPI** (blue), and no-stain (Red/orange) of the adult 3-month-old wildtype kidney (A) Low power image of the kidney. (A'-A'') High power images showing Shroom3 expression (arrow) in the proximal tubules (PT), the parietal epithelial cells (PE) of Bowman's capsule (BC), proximal tubules (PT), and podocytes (P).

Supplementary 14: Abnormal Glomeruli in Shroom3 Mutant Kidney.



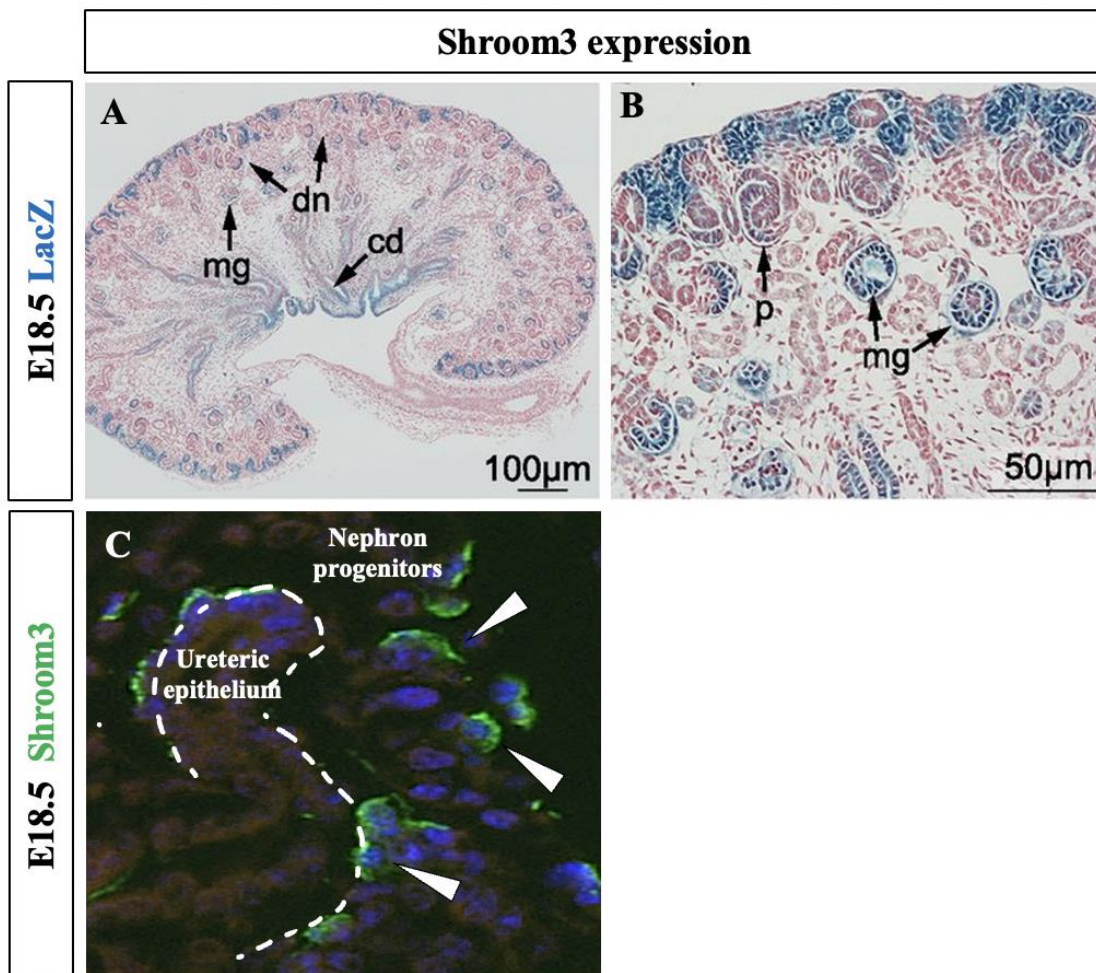
Abnormal Glomeruli in Shroom3 Mutant Kidney. Hematoxylin and Eosin staining of WT and Shroom3 mutants of the E13.5. Comparing WT glomeruli (A') to the mutant glomeruli (B') are collapsing and display larger areas of separation (Taken from Khalili et al. 2016).

1.3.5 Shroom3 in embryonic kidney development

Data from our lab shows that Shroom3 is expressed in the developing kidney (Supplementary 15A). Previous work in our lab also shows that mutant embryonic kidneys display abnormally organized and clustered nephron progenitor which are found at large distances from the neighbouring ureteric epithelium (Kitala et al. 2019). Research from our lab also shows the abnormal formation of renal vesicles of Shroom3 mutant developing kidneys, as the renal vesicles show lack a proper wedge cell shape and lack of proper localization of Par3 protein at the apical end of the cells (Supplementary 16A,D). Since renal vesicles have an internal cell polarity and an apical and basal side, disrupted localization of Par3 suggests a lack of cellular polarity of the epithelial cells in the absence of Shroom3.

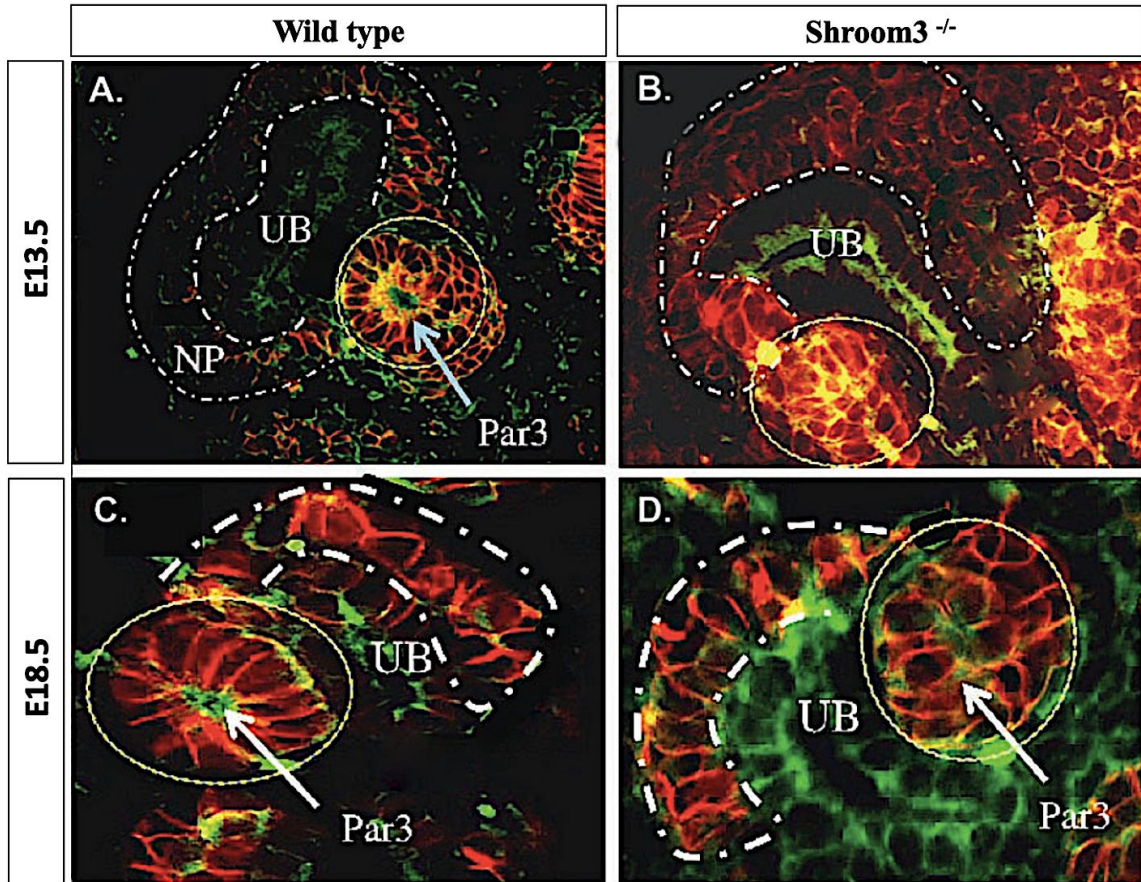
The events leading up to nephrogenesis and proper nephrogenesis are essential for kidney function. The observed changes to nephron progenitor cell shapes and organization in Shroom3 mutated kidneys can explain the development of abnormally structured renal vesicles and collapsing glomeruli in the developing kidney. Research shows that abnormalities during nephron development can increase a kidney's susceptibility to disease and the formation of damaged kidneys. With our study, we aim to investigate the role of Shroom3 during kidney development to decipher why Shroom3 variants are associated with chronic kidney disease.

Supplementary 15: Shroom3 expression in the developing kidneys.



Shroom3 expression in the developing kidneys. (A–F) X-Gal staining of E13.5 and E18.5 kidneys representing Shroom3 endogenous gene expression. In embryonic kidneys at E13.5 and E18.5, Shroom3 is expressed in the medullary collecting duct, condensing mesenchyme adjacent to the ureteric epithelium, developing nephrons, and maturing glomeruli a pattern consistent with the podocyte cell layer (Image from Khalili et al. 2016). G) In E18.5 WT kidneys, **Shroom3** (green) is expressed in select nephron progenitors (arrows) (Image from Kitata et al. 2019).

Supplementary 16: Abnormal Renal Vesicles formation in Shroom3 mutants.



Abnormal Renal Vesicles formation in Shroom3 mutants. Immunofluorescence expression analysis of **Par3** (green) and **NCAM** (red) in Shroom3 WT and Shroom3^{-/-} mutant in E13.5 and E18.5 kidneys. (A, C) Renal vesicles found Wild Type containing a central lumen (green) and apically constricted cells (red). (B, D) The improper development of renal vesicles in Shroom3^{-/-} kidneys. No central lumen is observed in E13.5 renal vesicles. Par3 is expressed throughout the whole renal vesicle, and NCAM highlights non-apical constricted cells. (White dashed line – nephron progenitors (NP), Yellow circle – renal vesicle, UB- ureteric bud) (Image from Kitata et al. 2019).

2. HYPOTHESIS & OBJECTIVES

Nephron progenitors undergo significant cell shape changes to regulate cell migration, cell movements, and cell projection formation. The changes in cell properties are critical as it sets the foundation for proper nephron function. Shroom3 is an actin-binding protein that changes cell morphology by modulating the actin cytoskeleton. Examination of Shroom3 deficient embryonic mice revealed abnormal nephron development. However, how Shroom3 contributes to the abnormal developing nephron is unknown. In my research, I investigated the role of Shroom3 in early kidney development, specifically in the nephron progenitor cells. In this study, we hypothesized that Shroom3 regulates nephron progenitor cell morphology.

2.1 Overall Hypothesis

Shroom3 regulates nephron progenitor cell shape and organization.

2.2 Study Objectives

1. Investigate Shroom3 expression in Nephron Progenitors

Hypothesis: Shroom3 is expressed in specific nephron progenitor cells

2. Investigate the orientation of Nephron Progenitors

Hypothesis: Shroom3 regulates nephron progenitors cell orientation.

3. Determine if Shroom3 is important for cellular projection formation

Hypothesis: Shroom3 regulates progenitor projection formation

3. Methods and Materials

Mouse Models

Shroom3 heterozygous mutant mice Shroom3Gt(ROSA)53Sor/J (or Shroom3Gt/+) were gifted from Dr. Thomas Drysdale at the University of Western Ontario. The mouse's genetic background was originally generated by Hildebrand and Soriano (1999) on a C57BL/6 background. However, since the C57BL/6 mice are resistant to kidney disease, the phenotype was very mild, making it challenging to understand the mechanism of Shroom3 in the kidney. Since CD1 background mice are more susceptible to kidney disease, likely due to their genetic variability, we crossed the C57BL/6 mice onto CD1 background mice. As a result of this cross, the phenotype becomes more robust, which helped us better understand the role of Shroom3 in the kidney. The original Shroom3 Knockout mice were generated by inserting a SA β galCrepA gene-trap cassette between exons 3 and 4 of the Shroom3 gene. The gene trap has many different components, such as the adenovirus splice acceptor (SA) to ensure the production of a fusion transcript, a Cre recombinase (Cre) which helps mediate site-specific recombination, and an MC1 polyadenylation (pA) tail which helps generate a stop codon. Since the gene trap contains a splice acceptor (SA) and premature stop codon (pA), inserting the trap in the gene's coding region, between exon 3 and 4, generated a truncated and non-functional null Shroom3 protein (Thomas and Capecchi, 1987). To generate Shroom3 heterozygous mice, Shroom3 null CD1 mice were crossed with a Wildtype CD1.

Mouse kidney dissection

To obtain the kidney tissues, we first crossed a Shroom3 heterozygous (Shroom3^{+/-}) female and male mice and checked for plugs the next day between 7-8 AM. Next, we

resected mouse embryos from pregnant mice at embryonic stage (E)13.5 and E18.5 under an Olympus SZ61 microscope. Then, using Dumont #5 INOX surgical forceps in cold Phosphate-buffered saline (PBS) pH 7.4, the E13.5 and E18.5 kidneys are dissected and fixed in 4% paraformaldehyde at 4°C. After 48 hours, the kidneys were prepared for histology.

PCR Genotyping:

DNA was isolated by lysing embryo heads, tail, or adult male ear notch at 75 2 minutes and 95°C for 5 minutes in the lysis buffer. Lysates were centrifuged at 12,500 rpm for 2 minutes. Genotyping was performed for mutant alleles were detected using primer sequences: forward primer, 5'-GGTGACTGAGGAGTAGAGTCC-3' and a reverse primer 5'- GAG TTT GTG CTC AAC CGC GAG-3'. The PCR conditions amplification were set at 94°C for 45 seconds, 58°C for 40 seconds, and 72°C for 40 seconds, for 35 cycles. PCR products were run on a 1% agarose gel with five µL RedSafe (Sigma Aldrich) in a 1X Tris-acetate-EDTA (TAE) buffer at 135V for 50 minutes.

Hematoxylin and Eosin

Paraffin-embedded kidneys were sectioned on a microtome (Leica) into five µm-thick sections, mounted onto Superfrost microscope slides (VWR), and dried at room temperature for 24 hours. Paraffin-embedded kidney sections were dried overnight at room temperature. For preparation for histological staining, the kidneys sections were deparaffinized through serial xylene and ethanol. They rehydrated using graded ethanol washes (100%, 95%, 70%, 50%, PBS) followed by staining with Hematoxylin and Eosin (Sigma Aldrich). Slides were fixed using a non-aqueous vectamount mounting medium

(Vector Labs) and imaged using an Olympus BX80 light microscope and CellSens image acquisition software.

In situ hybridization:

In situ hybridization (FISH) was performed by Hadiseh, using the Affymetrix QuantiGene ViewRNA according to manufacturer's protocol (please see Khalili et al., 2016 for the protocol) Immunofluorescence (Paraffin) Kidney sections were deparaffinized and rehydrated using xylene and graded ethanol washes (100%, 95%, 70%, and 50%). Next, the samples were washed in PBS and then placed in a pressure cooker containing the sodium citrate (pH 6.0) buffer for 5 minutes for antigen retrieval. Next, the samples were washed in PBS. A hydrophobic barrier (Vector Labs, H-4000) was used around the tissue samples. Samples were blocked with 10% normal goat serum or 10% donkey serum and 5% bovine serum albumin at room temperature for 1 hour. Tissue samples were incubated with primary antibodies Shroom3 (gifted from Timothy Plageman, 1:200), Pax2 (1:200), N-cam (Sigma,1:200), F-actin (1:200), GM130 (1:200), Integrin-a8 (1:400), overnight at 4°C. The slides with no primary antibody served as the negative control for the experiments. After overnight incubation, the next day, the slides underwent a serial wash with PBS. Next, slides were incubated in Alexa Fluor 488 or 568-conjugated secondary antibodies in a blocking buffer (1:1000) for 1 hour at room temperature. This step was followed by another wash in PBS and stained with Dapi (Sigma, 1:1000 dilution) for 5 minutes. Slides were fixed using Fluoromount mounting medium (Sigma, F4680) and imaged using either Olympus BX80 light microscope CellSens image acquisition software.

Immunofluorescence (Frozen tissue)

Embryonic kidneys were dissected and fixed in 4% formaldehyde in PBS overnight at 4°C. The following day, kidneys were transferred into a 30% sucrose solution in PBS overnight. The next day, kidneys were transferred into a solution containing a 1:1 ratio of OCT and sucrose and 15 minutes into a 3:1 ratio. Using an OCT embedding compound, the tissue was mounted and stored at -80°. Next, the Lecia cryostat cut 10µm sections of the kidney onto charged Superfrost/Plus slides. For immunofluorescence, the slides were first thawed on the benchtop for ten and then rinsed in PBS for 5 minutes. Next, using a pressure cooker containing the sodium citrate (pH 6.0), heat and pressure-induced antigen retrieval for performed on the tissue on a low heat for 4 minutes. After the antigen retrieval, the samples were washed in PBS and blocked with 10% normal goat serum at room temperature for 1 hour. After the blocking step, the tissue samples were incubated with primary antibodies Shroom3 (gifted from Timothy Plageman, 1:200). Slides were washed with blocking solution and incubated with Alexa Fluor 488 conjugated secondary antibodies (Invitrogen, 1:1000) for 1 hour at room temperature. Slides were fixed using Gold Antifade mounting medium and imaged using either Olympus BX80 light microscope CellSens image acquisition software.

Nephron progenitor Cell Count

To determine the number of nephron progenitors in the embryonic E13.5 and E18.5 wildtype and Shroom3^{-/-} kidneys, the Six2 positive stained embryonic kidneys (1:200) were first imaged at 10x and 20x magnification. Using the 8th section of each embryonic kidney, the cell number was counted using ImageJ version 1.53a (2020). For this analysis, the image threshold was first adjusted to black and white, and the background was removed.

Using the watershed tool, which allows for 1-pixel lines, allowed for clear distinction between each cell as it separated the overlapping cells. The average number of cells per cap mesenchyme of each kidney (n=3) was then graphed, and statistical analysis was performed using a 2-tailed t-test.

Nephron progenitor Cell Length

To determine the nephron progenitor cell length, embryonic kidneys were stained with NCAM (1:200), which marked the cell membrane of all the nephron progenitors and early developing structures of the nephron. To be consistent, only nephron progenitors found closest to the ureteric epithelium (the first layer of cells) were analyzed for cell length. To measure the cell lengths, 10x images set to scale. Next, ten cells of each cap mesenchyme region were analyzed on ImageJ using Wand Tracing Tool which measured the cell length in um. This process was repeated four times for each kidney, and a total of 3 kidneys were analyzed (n=3). Using excel, the cell length from each cap mesenchyme was averaged from E13.5 and E18.5 wildtype and Shroom3^{-/-} kidneys. Prism8 was used to graph the data. A 2-tailed t-test was performed for statistical analysis.

GM130 Localization and Cell count

The expression of GM130 was labelled as either being in the proximal or distal side of the nephron progenitors at E18.5 and E13.5 kidneys. The first layer of nephron progenitors was counted in the cap mesenchyme for proximal and distal localization of GM130 in Wildtype and Shroom3^{-/-}. For our analysis, we used five different cap mesenchyme regions from 4 different E13.5 kidneys. For the E18.5 kidneys, we analyzed ten different randomly selected regions. In total, kidneys from 4 different litters were analyzed (n=4). The average

number of cells per cap mesenchyme was then graphed, and statistical analysis was performed using a 2-tailed t-test.

Electron Microscopy

The Electron Microscopy Facility performed tissue preparation for TEM in the Health Science Centre at McMaster University. Using a transmission electron microscope, the nephron progenitor was analyzed for the presence of cellular projections in the nephron progenitors of Shroom3^{-/-} and wildtype embryonic kidneys. First, whole embryonic kidneys from Wildtype and Shroom3^{-/-} at E18.5 were fixed with 2.5% glutaraldehyde in 0.1M sodium cacodylate buffer (provided by EM Facility). The Kidneys were postfixed in a buffer containing 1% osmium tetroxide. Using a series of graded ethanol washes, the tissues were dehydrated and then embedded in epoxy resin. The tissue will be sectioned using an ultramicrotome stained with uranyl acetate. Images were viewed using JEOL JEM 1200 EM TEMSCAN (Tokyo, Japan). Images were captured using an AMT 4-megapixel digital camera.

Nephron progenitor and Cellular projections

To determine the cellular projections from E13.5 and E18.5 wildtype and Shroom3^{-/-} kidneys, 40x images from NCAM immunofluorescence and transmission electron microscopy were analyzed. Using 40x images of the NCAM stained kidneys, the number of thin projections from each cell was manually quantified on excel and averaged. A total of 3 wildtypes and 2 Shroom3^{-/-} kidneys were used (n=3). Next, using low-power TEM images from E13.5 and E18.5 kidneys, thin-filipodia-like projections were manually analyzed from 5 different cap mesenchyme regions from 2 kidneys (n=2). The cellular

projections were quantified by averaging the number of projections per nephron progenitor. This analysis was all performed blinded. The percentage of cells with projections was then graphed using Prism8. A 2-tailed t-test was performed for statistical analysis.

Ethics Statement: All studies were performed following animal care and guidelines by the Canadian Council for Animal Care and McMaster's Animal Research Ethics Board (AREB) (Animal Utilization Protocol #100855) and approved the project described in this study.

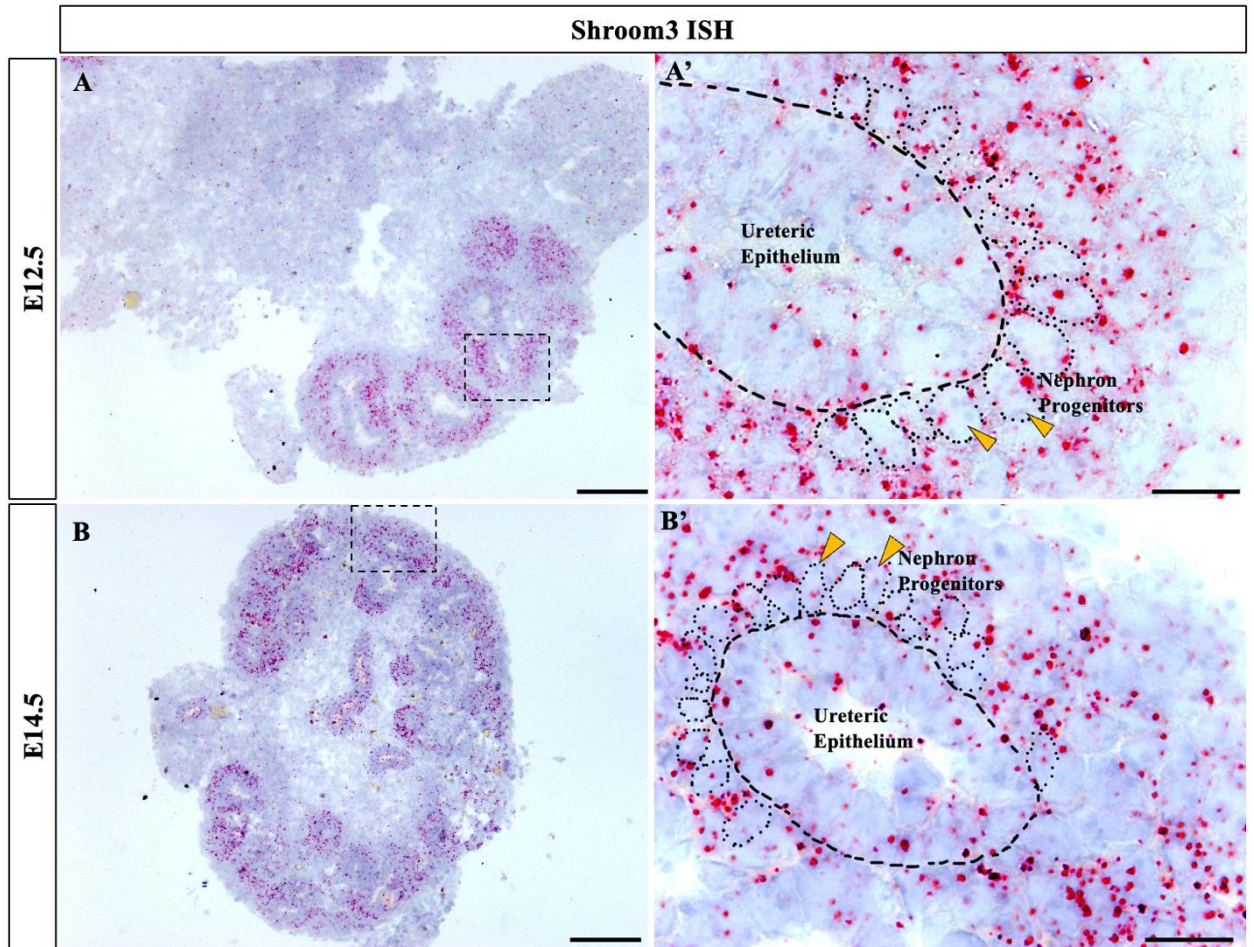
4. Results

4.1 Shroom3 protein is localized in nephron progenitor cells

Before understanding the function of Shroom3 in nephron progenitor cells, we first studied the protein localization of Shroom3 in the embryonic kidney. In previous studies from our lab, immunofluorescence using Shroom3 antibody (Dr. Plageman's laboratory in 2019) on Frozen sections demonstrated localization of Shroom3 protein in the cap mesenchyme cell population (Supplementary Figure 14, Kitala et al., 2016). However, this data was not able to be replicated by others under similar experimental conditions. Recognizing the importance of the location of Shroom3, I first analyzed the Shroom3 protein in embryonic kidneys in situ using Affymetrix QuantiGene ViewRNA ISH Tissue 2-Plex Assay, which was previously performed by Hadiseh Khalili. The assay provided in situ detection of two target mRNAs 1) Wilms Tumor Suppressor-1(Wt-1), which marks the podocytes and nephron progenitors, and 2) Shroom3 using TYPE 1 and TYPE 6 probes which generated red (Shroom3) and blue (Wt-1) signals. While Hadiseh detected Shroom3 in the condensing mesenchyme, glomerulus, and collecting ducts of the embryonic kidney, her studies focused on the glomerulus. I further examined the localization of Shroom3 protein in the cap mesenchyme by closely analyzing the nephrogenic region using Olympus 360 microscope. Upon analysis of the nephrogenic zone, I confirmed the Shroom3 in the Wt-1 positive nephron progenitor cells. However, I also noted localization of Shroom3 protein was limited or absent in some nephron progenitor cells. At the same time, it was almost undetected in the ureteric epithelium compared to the progenitors (red dots, Fig.1). I also detected the presence of Shroom3 mRNA concentrated to certain areas of select

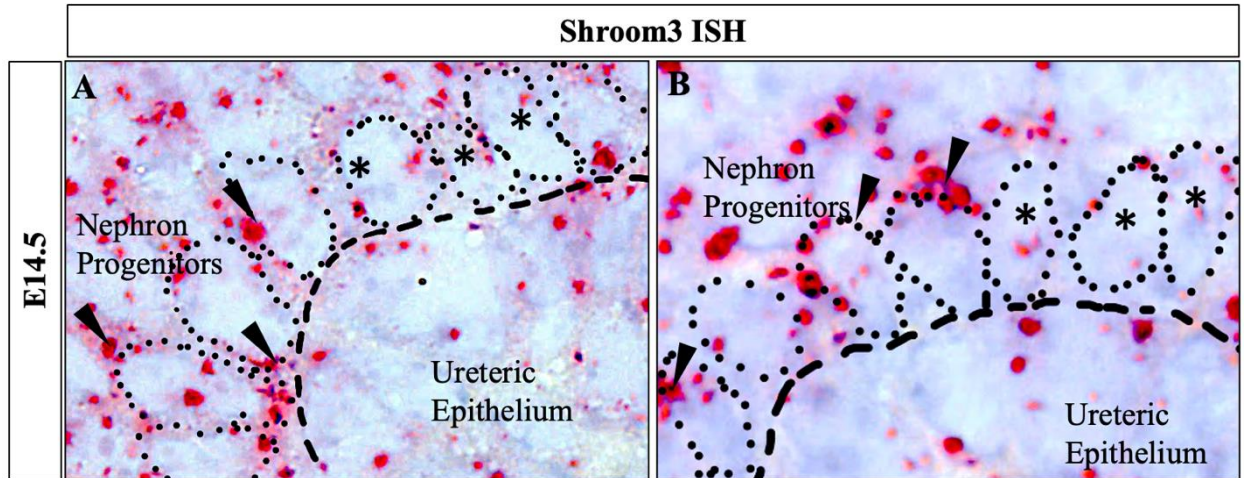
nephron progenitor cells (arrow, Fig.2). No signal was generated when a probe that is non-specific to any mRNA was used as a negative control for this study.

Figure 1: Detecting Shroom3 mRNA localization by in-Situ Hybridization



Detecting Shroom3 mRNA localization by in-Situ Hybridization. The Red dots indicate mRNA localization (A-A') E12.5 kidneys (B-B') E14.5 kidneys display Shroom3 mRNA (red dots) in the nephron progenitors. The black arrow highlights area of nephron progenitor with concentrated Shroom3 mRNA localization. The asterisk indicates lack of Shroom3 in select nephron progenitors.

Figure 2: Magnified images of Shroom3 In-Situ Hybridization

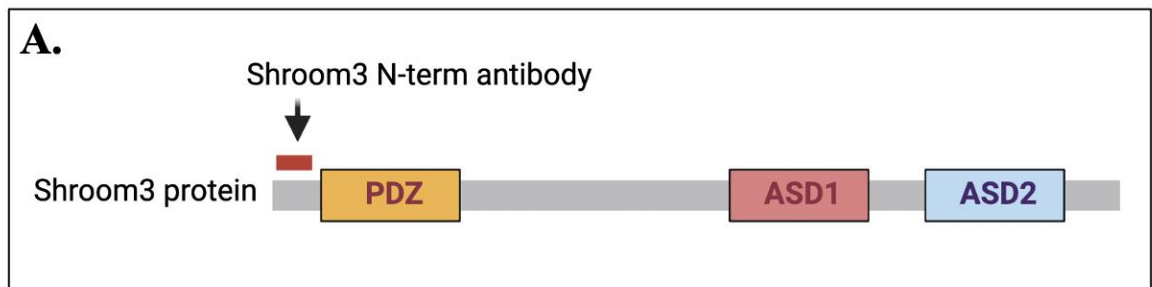


Magnified images of Shroom3 In-Situ Hybridization. (A-B) The Red dots indicate Shroom3 mRNA localization in select nephron progenitors of E14.5 kidneys. The black arrow highlights Shroom3 mRNA to one side of the nephron progenitors. The asterisk indicates lack of protein localization, in particular nephron progenitors.

Next, I examined the localization of Shroom3 protein in the embryonic kidneys. Since the Shroom3 antibody is not commercially available, we used the antibody generously gifted by Dr. Timothy Plageman. We were provided with two antibodies that recognized targeted amino acid sequence CLLEGMRQADIRYVK of Shroom3 protein isoform 1 or 2. While the N-terminus Shroom3 antibody detected the longest isoform of Shroom3, the second antibody Rabbit anti-Shroom3 150, recognized a shorter isoform of Shroom3 (Supplementary Fig. 3B). First, to verify if the antibodies are detecting pattern of Shroom3 protein as seen in the past, I performed IF on Wildtype 3-month-old kidney tissue. Both antibodies demonstrated Shroom3 protein localized to the apical border of the Bowman's capsule and in select tubules (Fig. 4), a pattern that was consistent with previous studies in postnatal kidney tissue. After confirming the validity of the antibody, I examined localization of Shroom3 protein using immunofluorescence on paraffin embryonic tissue. However, I was unsuccessful at detecting a signal. Next, I performed immunofluorescence

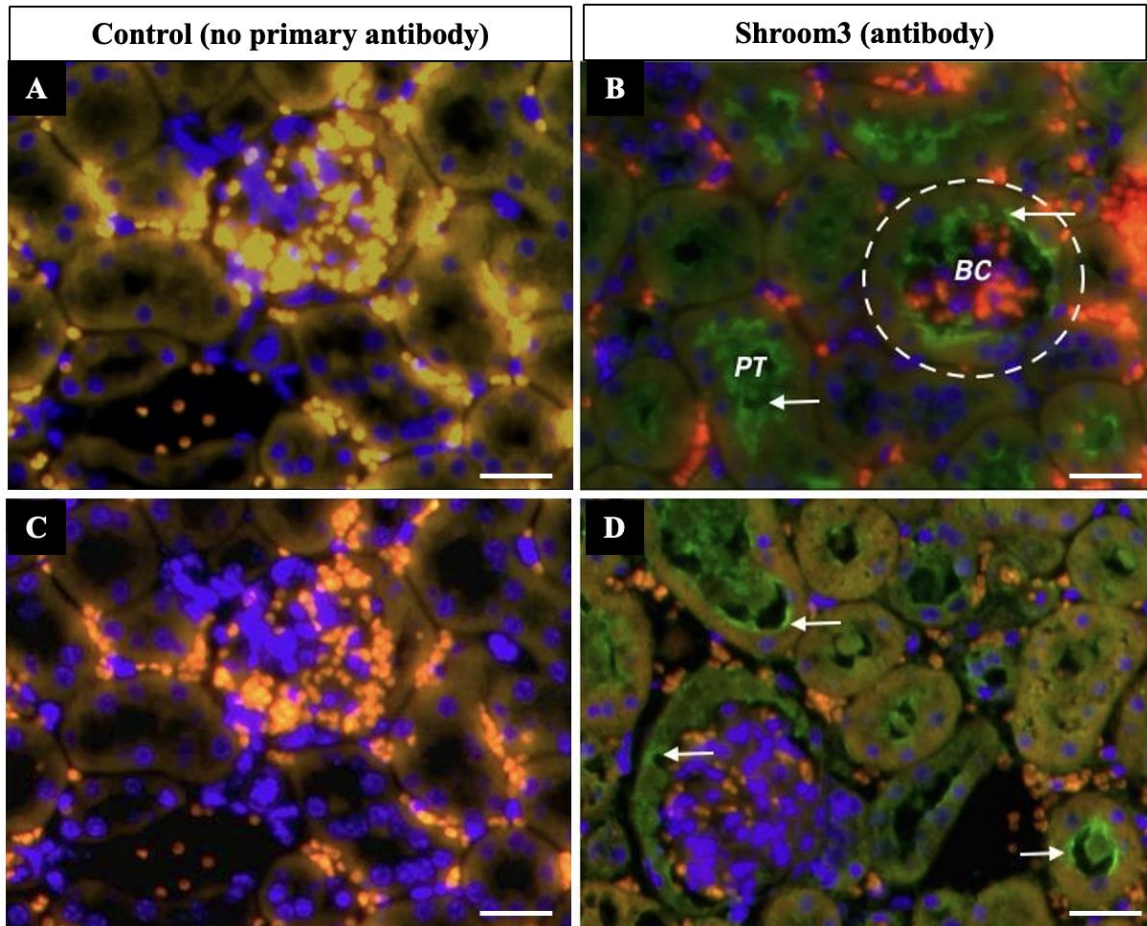
on frozen embryonic kidney sections. After multiple rounds of troubleshooting, I noticed the antibody specific to the N-terminus of the protein (Shroom3 N-terminus), which detected Shroom3 in a pattern observed as Shroom3 mRNA (Fig. 1B). Consistent with ISH results, Shroom3 was highly expressed in most nephron progenitors and slightly in the ureteric epithelium in frozen IF (Fig. 4). The closer analysis also revealed Shroom3 protein was localized to one end of select nephron progenitor cells (Fig. 4). These results highlight not all Shroom3 mRNAs translates into a protein. This data demonstrates that Shroom3 protein is localized some but not all nephron progenitor cells suggesting a very specific role for Shroom3 in this cell population.

Figure 3: Shroom3 N-Term antibody



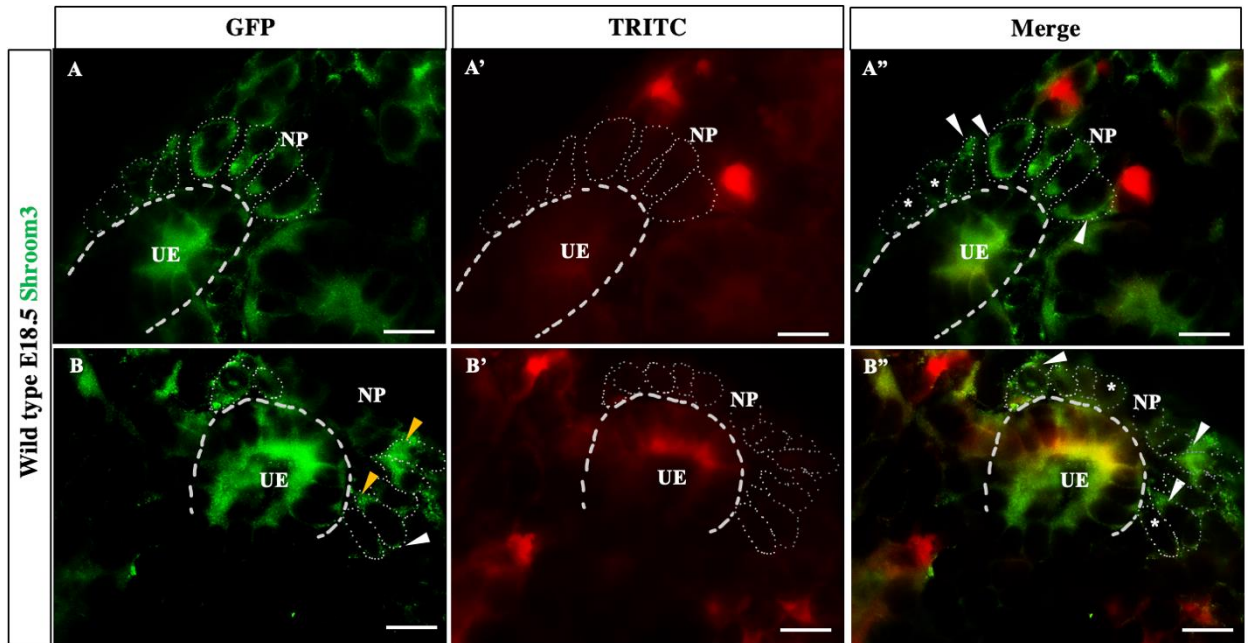
Shroom3 N-Term antibody: The N-term Shroom3 antibody (rabbit) detects the long isoform of Shroom3 at the N-terminal end of the protein (red line and arrow).

Figure 4: Optimizing the N-term Shroom3 antibody in adult kidneys



Optimizing the N-term Shroom3 antibody in adult kidneys: Immunofluorescence of Shroom3 antibody. (A,C). The overlay of the TRITC channel (red) and green channel show autofluorescence of red blood cells (orange). The controls indicate no non-specific binding occurred. (B, D) *Shroom3* protein was localized to in the apical border of Bowman's capsule and proximal tubules. (Green, arrow), DAPI (blue).

Figure 5: Shroom3 protein is found in select nephron progenitor cells



Shroom3 protein is found in select nephron progenitor cells. (A, B) Shroom3 protein localization (green) (A'-B'). Overlay of TRITC channel (red) and green channel show no non-specific binding in the nephron progenitors. Tissue with no primary antibodies was used as controls (A''-B'') Merged (A and A') panels display localization of Shroom3 protein to one side of select nephron progenitors (white arrow). The absence of Shroom3 in select nephron progenitors is represented with an asterisk.

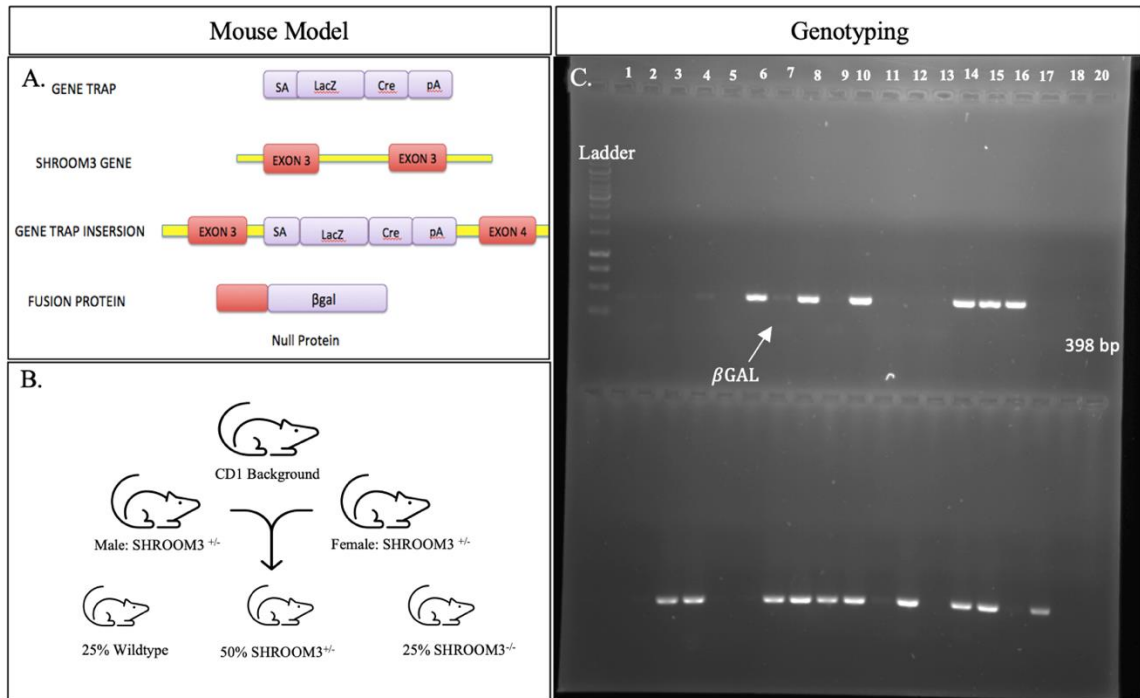
4.2 Shroom3 mutation results in abnormal nephron progenitor cell morphology

Our lab's previous analysis of Shroom3 homozygous (Shroom3^{-/-}) embryonic kidneys revealed abnormal podocytes and renal vesicle cell morphology (Supplementary Fig.13). Since nephrogenesis begins when nephron progenitors differentiate into the epithelial cells of the renal vesicles, abnormal regularities with the nephron progenitor can lead to improper development of the nephron. Abnormal nephron formation is something we observed in our Shroom3 knockout kidneys. To determine whether Shroom3 affects nephron progenitor cell morphology and overall organization, I first analyzed Wildtype and Shroom3^{-/-} kidneys at two different embryonic stages, E13.5 and E18.5. I used the

Shroom3^{Gt(ROSA)53Sor/J} mice containing a gene trap at the Shroom3 promoter region that truncates the protein and creates Shroom3 null embryos (Fig.6).

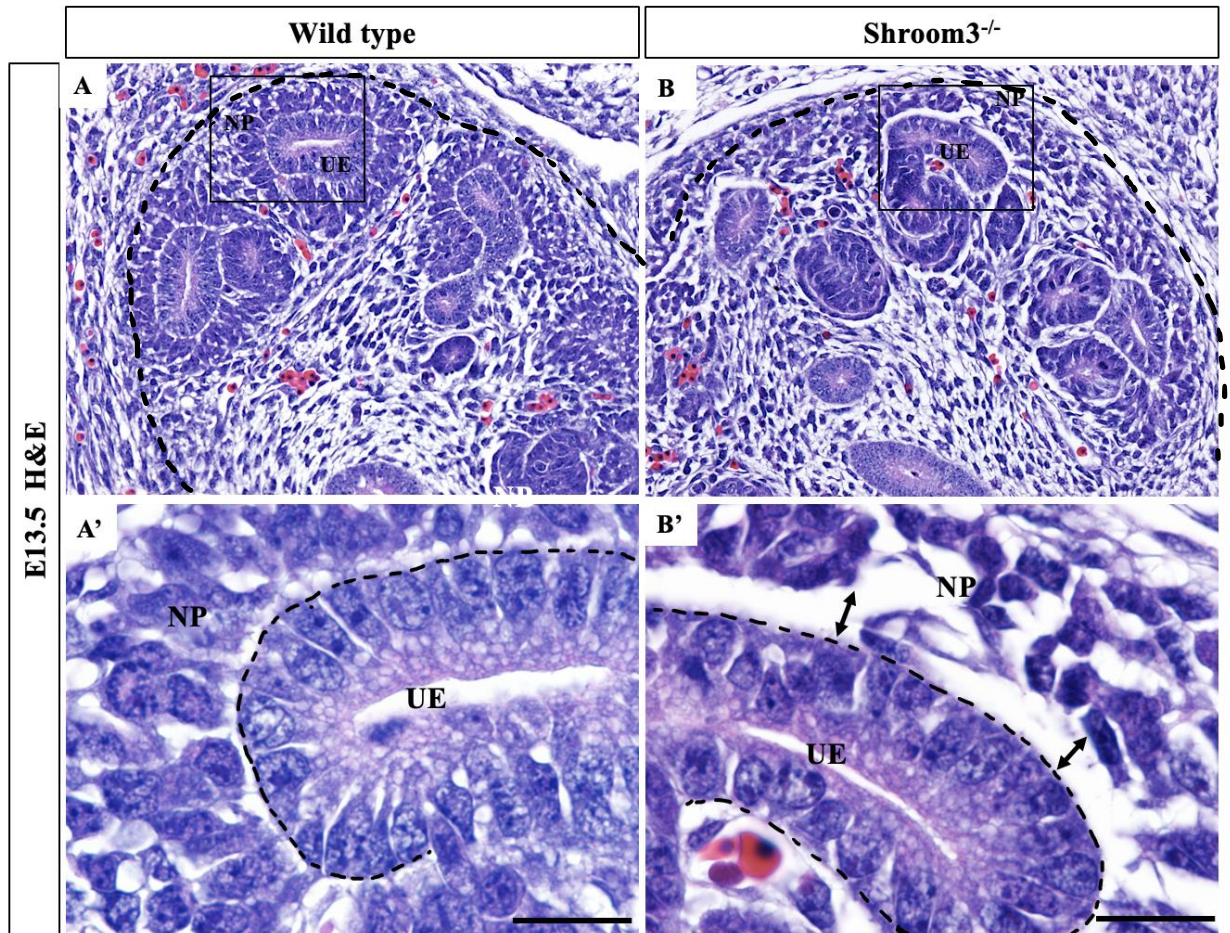
The histological analysis of E13.5 Shroom3^{-/-} by H&E staining demonstrated abnormally shaped and clustered nephron progenitor which were also largely spaced apart from ureteric epithelium bud tips (Fig. 7B'). Analysis of H&E stained E13.5 Shroom3^{-/-} kidneys also revealed a similar phenotype where the nephron progenitors had an abnormal cell shape and space between the nephron progenitors and the ureteric bud epithelium. However, the phenotype observed in the E18.5 Shroom3^{-/-} kidneys was less severe than the E13.5 Shroom3^{-/-}. This is interesting and suggests Shroom3 may be playing a more critical role early on in development than a late development stage. Next, using Pax2, a transcription factor found in the nephron progenitors and ureteric bud epithelium, I confirmed the presence of round and abnormally clustered nephron progenitors that do not condense around the ureteric bud epithelium of Shroom3^{-/-} E13.5 and E18.5 kidneys (Fig.9 D, Fig.10 C'-D'). The results from H&E and Pax2 analysis confirm previous findings and suggest that Shroom3 plays an essential role in regulating nephron progenitor clustering and morphology which is an essential step for initiating nephron formation.

Figure 6: Mouse Model and Genotyping



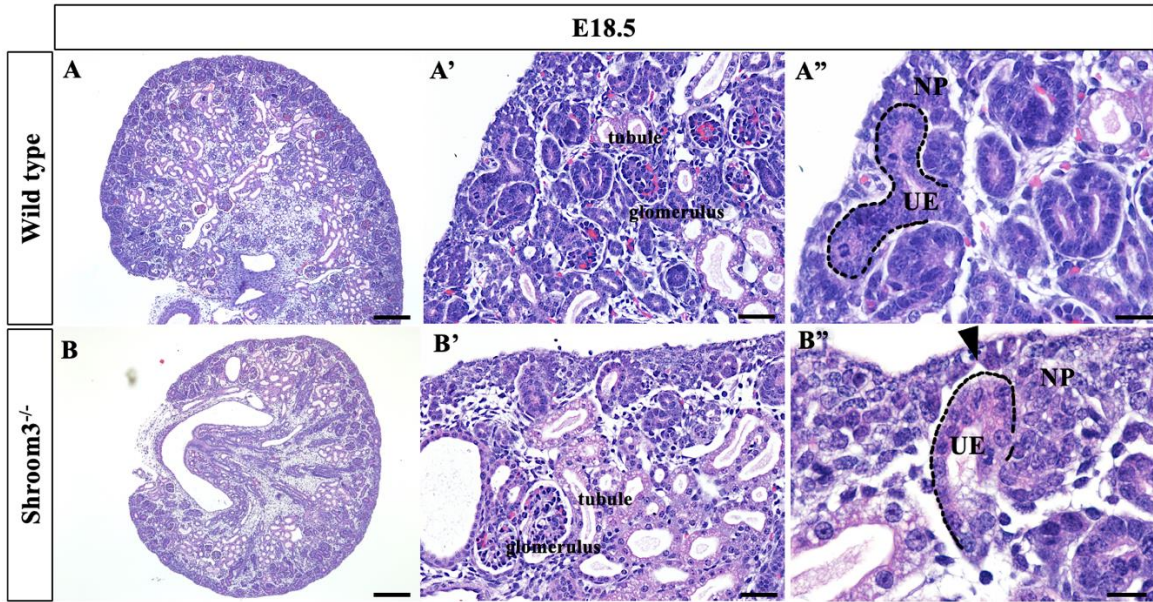
Mouse Model and Genotyping. A) Shroom3 mouse model was generated by Hildebrand and Soriano, 1999. To create the model, a gene trap containing sequence SA β galCre pA (adenovirus splice acceptor, β -galactosidase, Cre recombinase, MC1 polyadenylation) was inserted in between Exon 3 and 4 of Shroom3 gene. This intervention created a bifunctional gene encoding the fusion between and resulting in a non-functional protein. B) The Shroom3 heterozygous mutant mice (Shroom3^{Gt(ROSA)53Sor}/J) were crossed to generate wildtype, heterozygous and homozygous mice. C) PCR genotyping was performed confirm the presence of the LacZ allele using the forward primer and reverse primer. The bands (arrow) represent the Shroom3 heterozygous embryos with LacZ, whereas the no bands represented the wildtype embryos.

Figure 7: Shroom3 knockout E13.5 kidneys display abnormal nephron progenitor cell not clustering and spacing



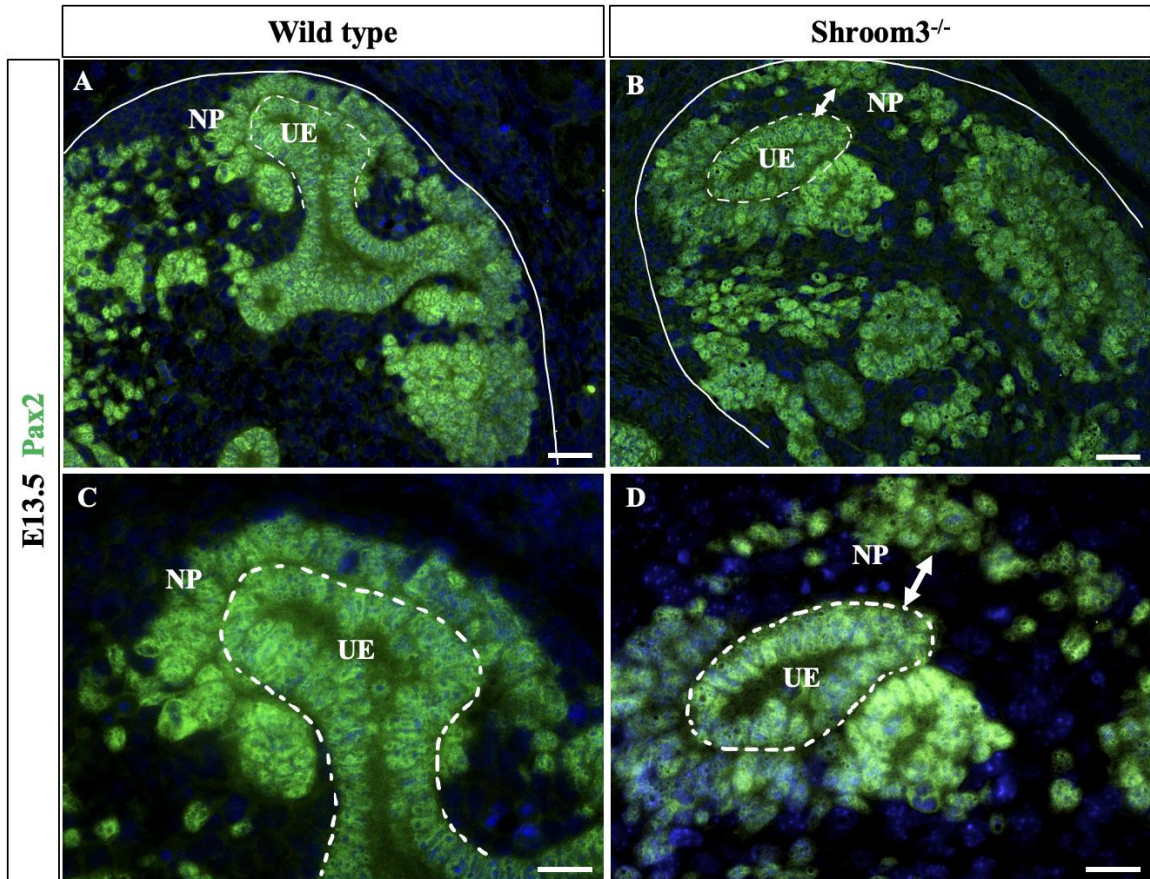
Shroom3 knockout E13.5 kidneys display abnormal nephron progenitor cell clustering and spacing: Histological analysis of the nephrogenic region of wildtype and Shroom3^{-/-} E13.5 kidneys using Hematoxylin and Eosin staining. (A-A') Wildtype E13.5 kidneys display organized, and clustered nephron progenitors (NP) around the ureteric epithelium (UE). (B-B') Shroom3^{-/-} kidneys display abnormally clustered, loosely packed nephron progenitor with an abnormal large space between UE and NP (black arrow).

Figure 8: Shroom3 Knockout E18.5 kidneys display abnormal nephron progenitor organization



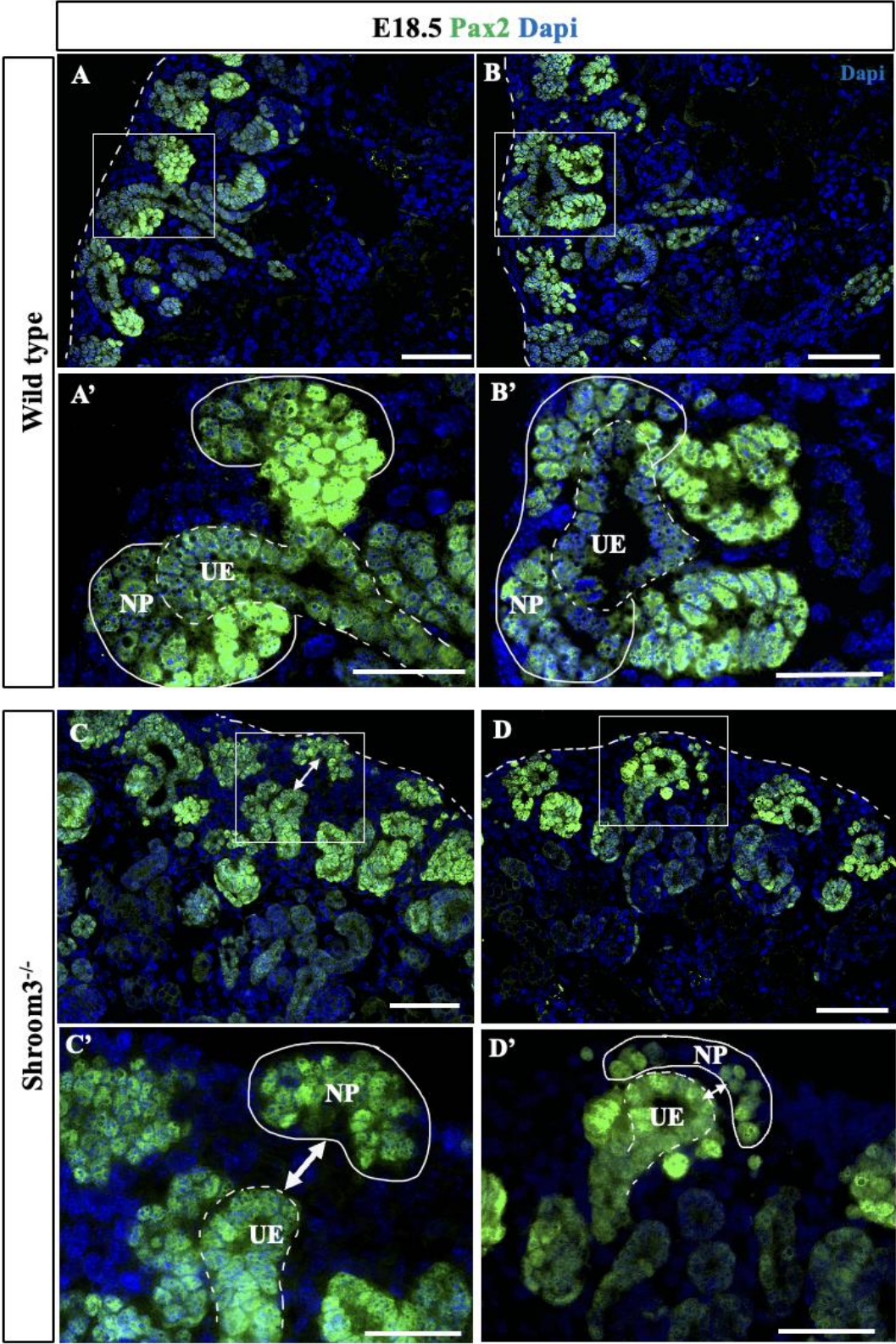
Shroom3 Knockout E18.5 kidneys display abnormal nephron progenitor organization: Histological analysis of nephrogenesis of E18.5 wildtype and Shroom3^{-/-} kidney tissue at Hematoxylin and Eosin staining. (A-A'') E13.5 Shroom3 wildtype kidneys reveal nephron progenitors aggregated and capped around UE tips (dashed lines). Shroom3^{-/-} kidneys display abnormal spacing (arrow) between UE and NP and disorganized NP cells. NP – Nephron progenitor, UE – Ureteric epithelium.

Figure 9: Pax2 immunofluorescence of E13.5 mouse kidneys display nephron progenitors abnormally spaced apart from the ureteric epithelium



Pax2 Immunofluorescence of Shroom3 E13.5 kidneys display nephron progenitors abnormally spaced apart from the ureteric epithelium: (A-C) Pax2 IF of Wildtype nephron progenitors show clustering and properly organized cells around the ureteric epithelium. (B-D) Pax2 expression in Shroom3 mutants illustrate abnormal nephron progenitor organization, clustering, and abnormally large gaps (arrow). NP – Nephron progenitor, UE – Ureteric epithelium.

Figure 10: Shroom3 knockout E18.5 kidneys display abnormal spacing between nephron progenitors and ureteric epithelium



Shroom3 E18.5 knockout kidneys display abnormalities: Pax2 Immunofluorescence of two wildtype and two Shroom3^{-/-} kidneys.(A-B) Low power images of Pax2 stained kidneys. (A'-B') High power Pax2 stained Wildtype kidneys display properly condensing nephron progenitors around the ureteric bud epithelium (UE). (C-D) Low power images of Shroom3^{-/-} kidneys. (C'-D') Higher power images show abnormal spacing between the NP and UE.

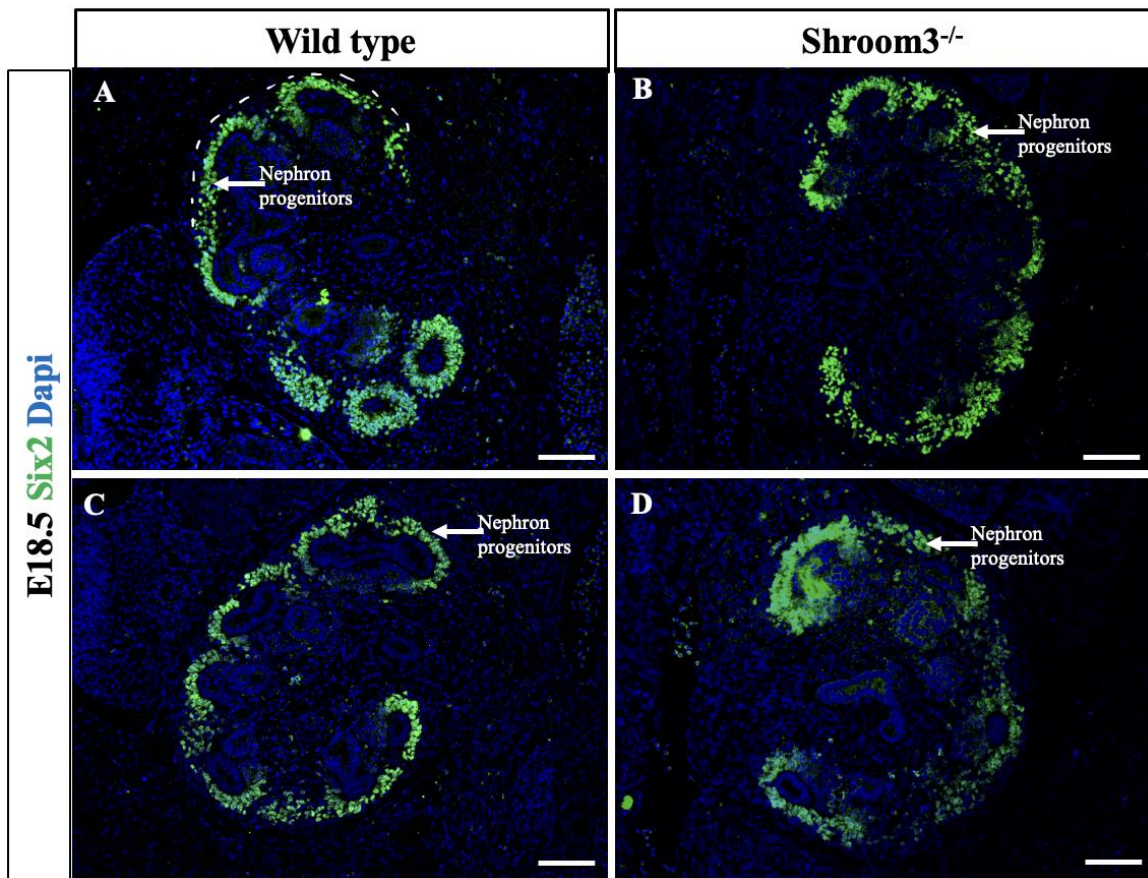
4.3 Shroom3 knockout in embryonic kidneys results in reduced nephron progenitor cell number and cell length

Preliminary data from H&E and Pax2 analysis displays irregular nephron progenitor cell phenotype in Shroom3^{-/-} embryonic kidneys. To further examine the phenotype, I stained the wildtype and Shroom3^{-/-} embryonic kidneys with Six2, which is a transcription factor that marks all the nephron progenitors (Fig.11, Fig12). Using the ImageJ software, I counted the number of Six2 positive cells in the kidney (for the quantification protocol, see materials and methods). Quantification of Six2⁺ cells from six Shroom3^{-/-} E13.5 kidneys demonstrated a significant decrease in the number of nephron progenitors compared to the wildtypes. (n= 6, p=0.0177, Fig. 13A). However, quantitative analysis of Six2⁺ cells in E18.5 Shroom3^{-/-} using a similar method, revealed no significant difference in the number of Six2⁺ cells (Fig. 13B). This analysis demonstrates that a loss of Shroom3 is associated with a reduced nephron progenitor cells population in the earlier stages of kidney development.

Since Shroom3 is a regulator of the actin cytoskeleton (Hildebrand & Soriano,1999) we were interested in analyzing Shroom3 also modulates nephron progenitor undergo cell shape changes. To analyze the shape of the cells, I stained the embryonic kidneys with a neural cell adhesion molecule (NCAM) that marks the cell membrane of nephron progenitors. The wildtype E13.5 and E18.5 nephron progenitor were elongated and closely condensed cells around the ureteric epithelium (Fig.14 and 15). Whereas Shroom3^{-/-}

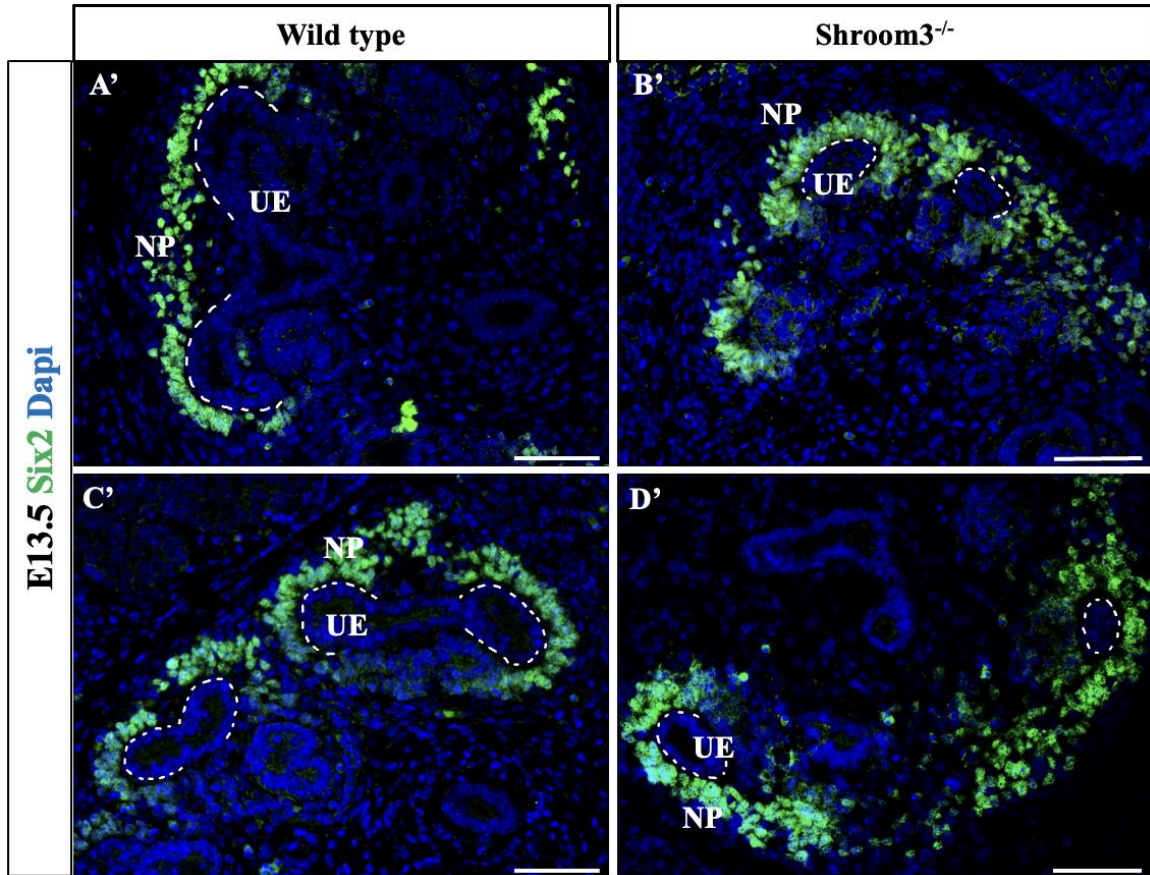
nephron progenitors exhibited a round morphology and disorganized cells. Next, I examined differences in cell length by randomly selecting ten nephron progenitor cells from the cap mesenchyme of 7 different kidneys. I then averaged the cell length using the ImageJ software. The wildtype E13.4 nephron progenitors averaged a length of 0.5412 μm , while the *Shroom3*^{-/-} E13.5 averaged length of 0.3963 μm . Statistical analysis revealed that *Shroom3*^{-/-} nephron progenitors were significantly smaller in cell length than the wildtypes (Fig.14E). However, there was no difference in E18.5 *Shroom3*^{-/-} kidneys (Fig. 15E). Interestingly, the analysis of both *Six2* and *Ncam* stained E18.5 tissue display no significant changes in cell number and cell length at the later stage of development E18.5 (Fig.11B, Fig.13E). This data demonstrates that *Shroom3* regulates the cell shape at E13.5. This is a novel finding, as studies have not examined differences in nephron progenitor cell length concerning *Shroom3*. Overall, these findings imply a critical role of *Shroom3* in regulating cell shape by maintaining nephron progenitor cell length.

Figure 11: Six2 immunofluorescence of E13.5 mouse kidneys



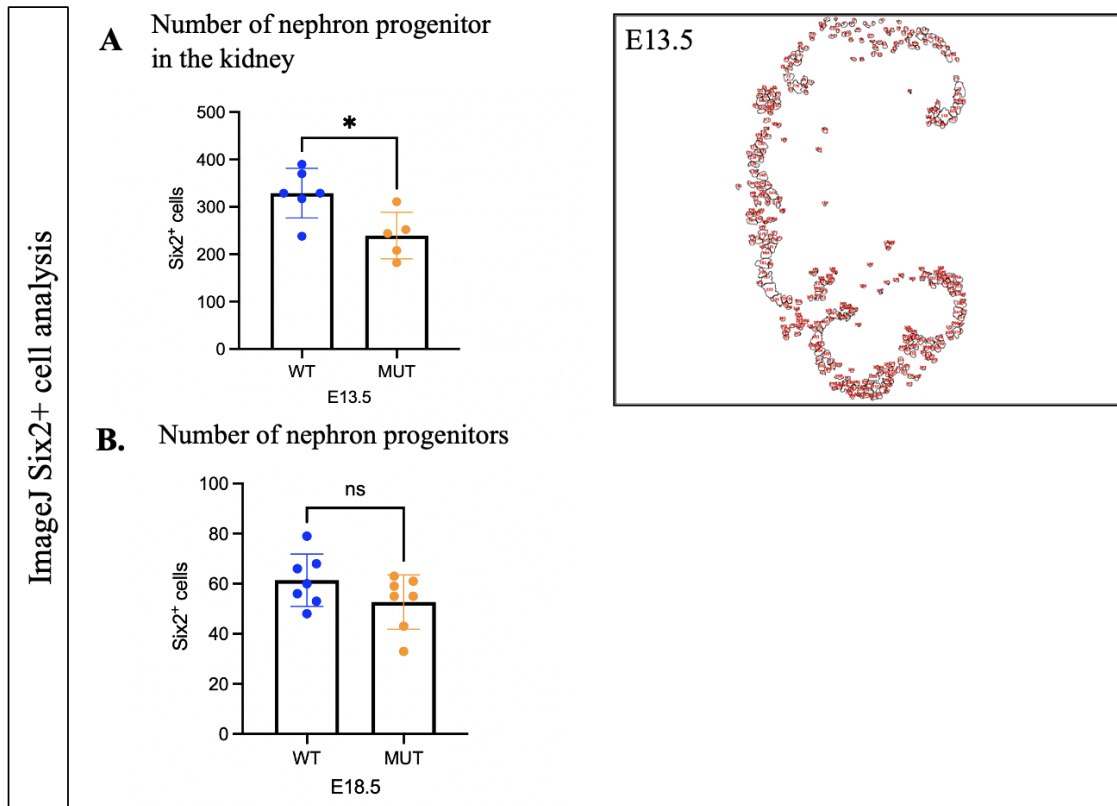
Six2 immunofluorescence of E13.5 mouse kidneys. Wild Type (A, B) and Shroom3^{-/-} (C, D) E13.5 kidneys stained for Six2 (green) and Dapi. The nephron progenitors in the wildtype (arrow) are tightly clustered compared to the nephron progenitors in the Shroom3^{-/-} kidney (arrow).

Figure 12: High power images of E13.5 mouse kidneys with Six2 staining



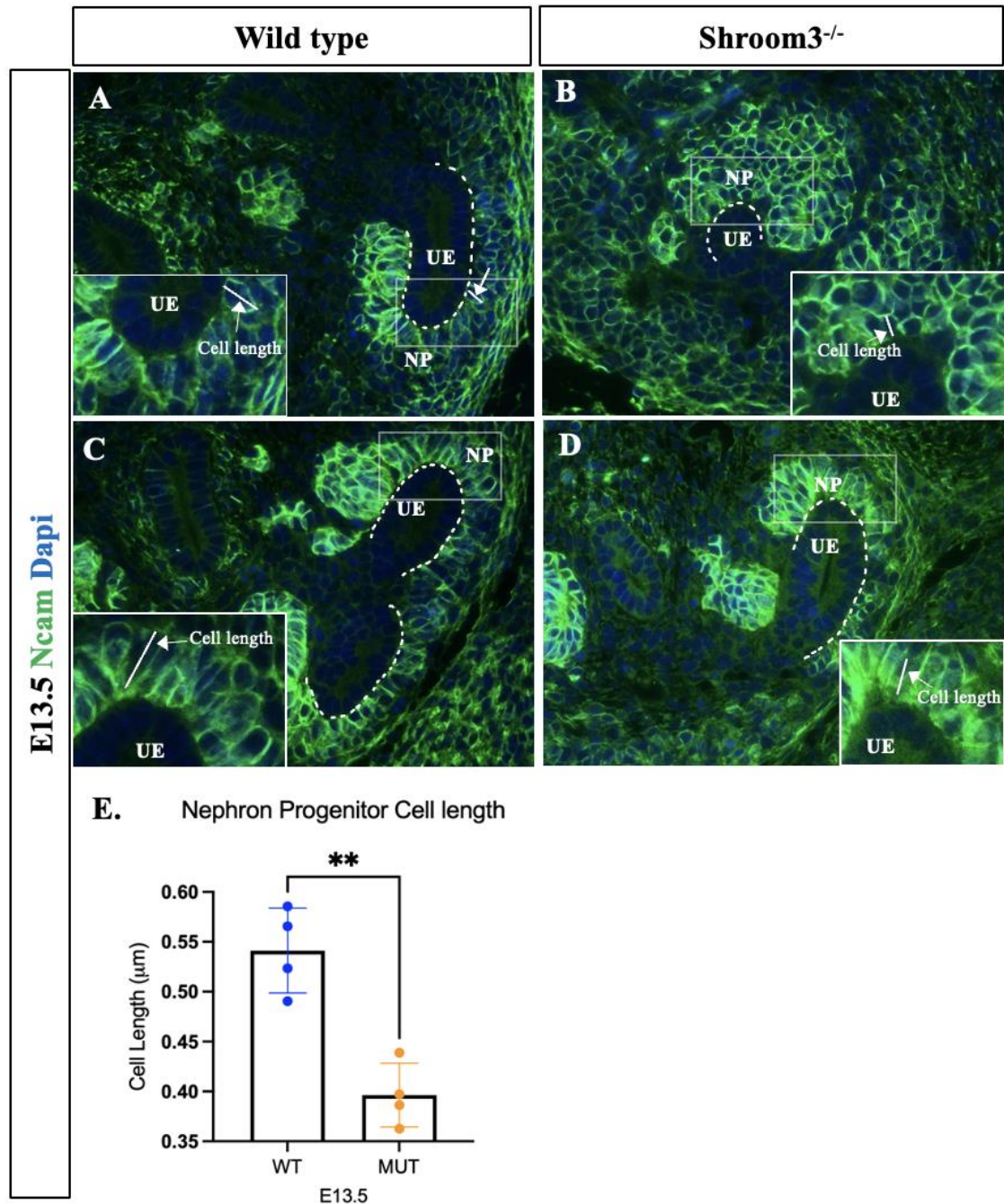
High power images of E13.5 mouse kidneys with Six2 staining. Wild Type (A, B) and Shroom3^{-/-} (C, D) E13.5 kidneys stained for Six2 (green) and Dapi. The nephron progenitors (NP) in the wildtype (arrow) appear to be tightly clustered and organized around the ureteric epithelium (UE). The nephron progenitors of Shroom3^{-/-} kidney are more loosely packed around the UE.

Figure 13: Statistical analysis of Six2+ cell in of Shroom3 knockout E13.5 mouse kidneys



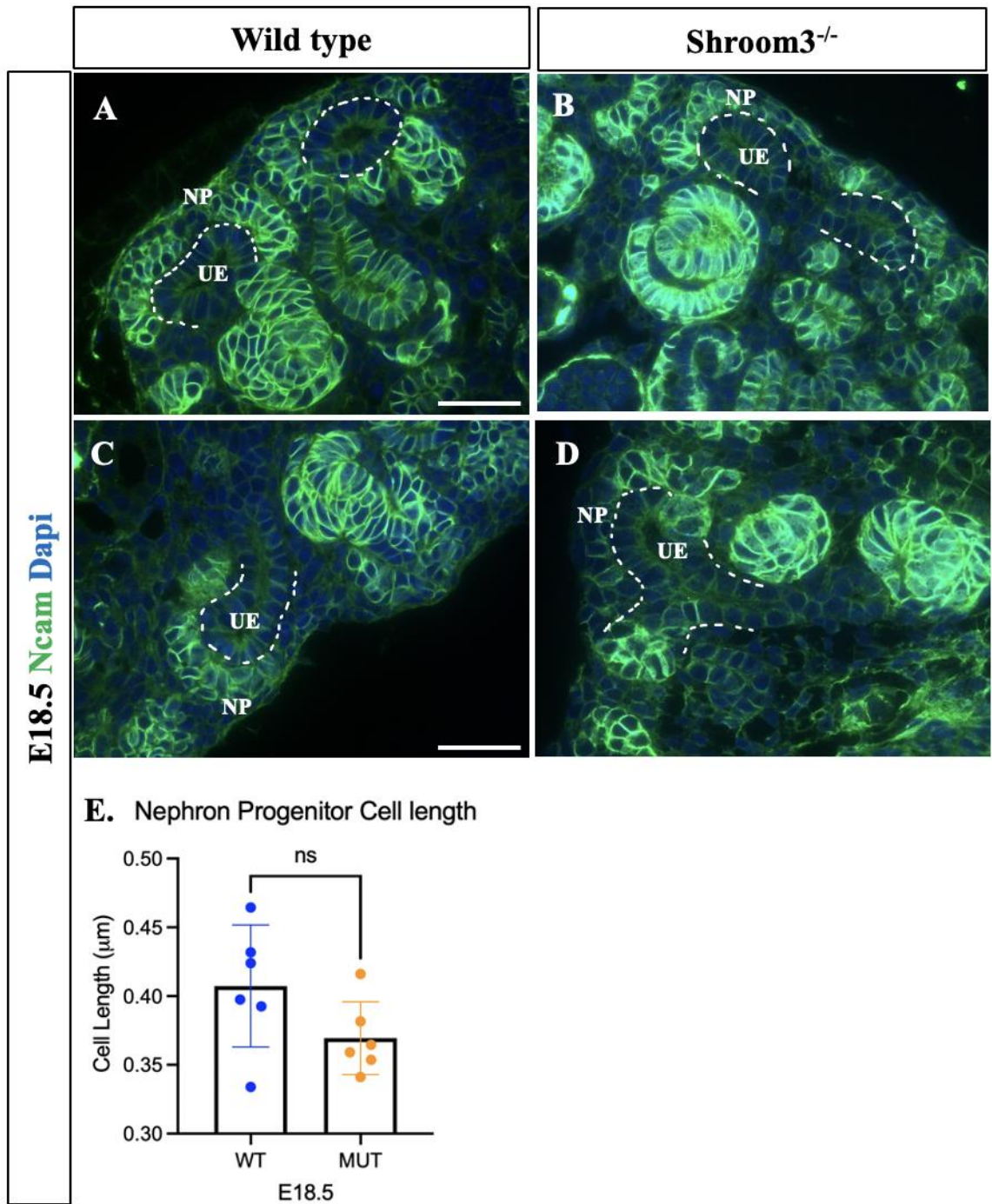
Statistical analysis of Six2+ cell in of Shroom3 knockout E13.5 mouse kidneys. (A) Graph represents the number of Six2+ (nephron progenitors) in E13.5 kidneys. Shroom3^{-/-} kidneys have reduced number of nephron progenitors. For this analysis, five difference cap mesenchyme of 6 kidneys were analyzed. The image on the right is an example of the kidney analyzed using Image J. (B) Graph represents the number of Six2+ in E18.5 kidneys. The Shroom3^{-/-} kidneys at E18.5 did not represent a significant decrease in the number of nephron progenitors. For E18.5, 20x images were analyzed to count the number of Six2+ cells. The results were analyzed through ImageJ and graphs were generated using Prism8.

Figure 14: Ncam immunofluorescence of Shroom3 knockout E13.5 mouse kidneys display reduced number of nephron progenitors



Ncam immunofluorescence of E13.5 mouse kidneys. (A, B) Wild Type and (C, D) Shroom3^{-/-} E13.5 kidneys stained for Ncam (green) and Dapi. The nephron progenitors (NP) in the wildtype display an elongated cell morphology (UE). NP of Shroom3^{-/-} kidney appear shorter in length. E) The graph represents the average cell length of 8 nephron progenitors from 6 cap mesenchyme populations from 4 different E13.5 kidneys. Nephron progenitors of Shroom3^{-/-} are significantly smaller in length than the wild types. The results were analyzed through ImageJ and graphs were generated using Prism8.

Figure 15: Ncam immunofluorescence of Shroom3 knockout E18.5 mouse kidneys displays no difference in nephron progenitor cell number



Ncam immunofluorescence of Shroom3 knockout E18.5 mouse kidneys displays no difference in nephron progenitor cell number. (A, B) Wild Type and (C, D) Shroom3^{-/-} E18.5 kidneys stained for Ncam (green) and Dapi. The nephron progenitors (NP) in the wildtype display an elongated cell morphology (UE). NP of Shroom3^{-/-} kidney appears shorter in length. Nephron progenitors of Shroom3^{-/-} are not significantly smaller in length

than the wild types. The graph represents the average cell length of 8 nephron progenitors from 6 cap mesenchyme populations from 6 different E18.5 kidneys. Image J analysis was used to analyze the cell length, and graphs were generated using Prism8.

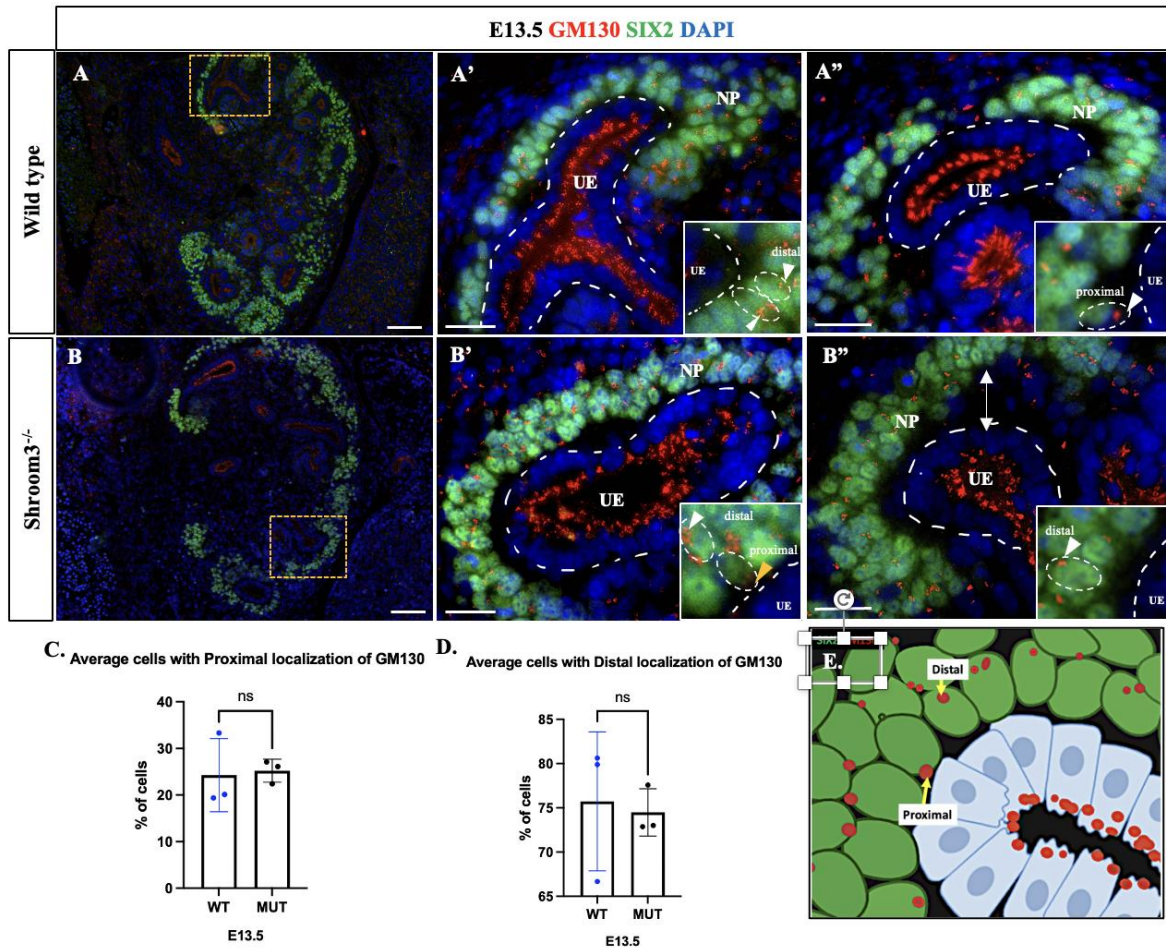
4.4 Shroom3 mutant nephron progenitors display altered cell orientation

The nephron progenitors are a dynamic group of cells that undergo cell shape changes, cell migration (O'Brien et al. 2014, Combes et al., 2016). Generally, a polarized cell can re-orient itself to undergo direction migration. Although it is well established that nephron progenitors migrate and change shape during development, if they exhibit properties of a polarized cell is unknown. Our lab has previously demonstrated that Shroom3^{-/-} renal vesicles do not form wedge-shaped morphology and lack cellular polarity. These findings indicate that Shroom3 plays a role in apicobasal polarity of the renal vesicles, likely before their development (Sup. 15). In this study, we investigated nephron progenitors to determine whether nephron progenitors also exhibit altered polarity in Shroom3^{-/-} mice. Since previous studies have also highlighted that nephron progenitors exhibit a specific orientation represented by a leading edge and a trailing edge (O'Brien et al., 2014) thus, in our analysis, we analyzed their orientation. To do this, we examined the distal and proximal ends of the nephron progenitor. To identify the distal region of the cell, we used Golgi matrix protein to identify the proximal region (Fig.16E) while the proximal region of the cell was examined through integrin α -8 localization (Fig. 22E). For my analysis, I first performed IF co-immunofluorescence using antibodies against the Golgi matrix marker (GM130) and Six2, a marker of nephron progenitor cells. By analyzing the position of the Golgi apparatus, a distal marker, we can understand how the cell is orientated. Analysis of wildtype E13.5 and E18.5 demonstrated localization of Golgi apparatus towards the distal end, also the area of the cell furthest to the ureteric epithelium. Analysis of E13.5 and E18.5

Shroom3^{-/-} kidneys demonstrated no significant difference in distal and proximal localization of GM130 (Fig.16 $p=0.8529$; Fig.17 $p=0.5505$, $p=0.4382$). However, during our quantitative analysis, we found it challenging to evaluate the precise cells that localized GM130 and thus found it difficult to perform a quantitative analysis.

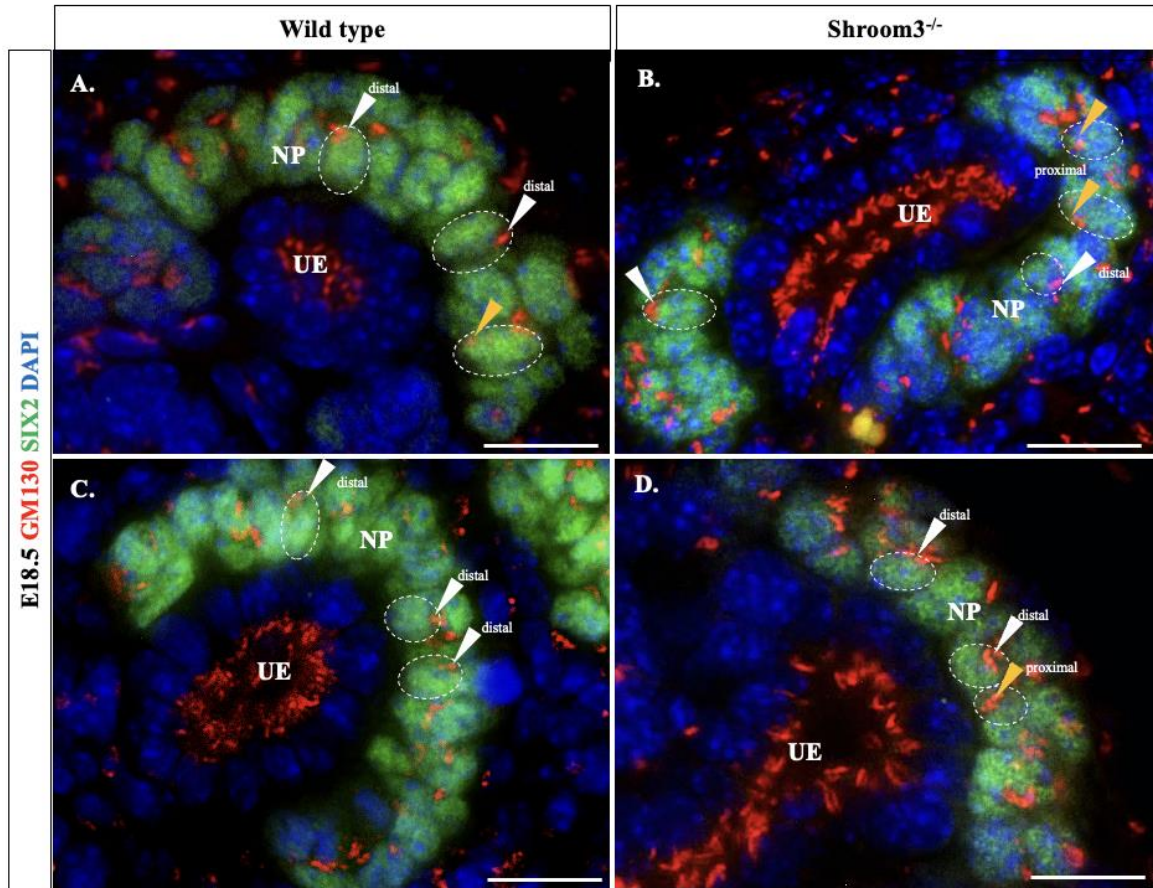
Therefore, next, I performed NCAM and GM130 IF since Ncam specifically outlines the nephron progenitor cell membrane, making the cells that express GM130. In this analysis, wildtype E13.5 and E18.5 kidneys stained with GM130 and Ncam consistently displayed a distal localization of GM130 in the nephron progenitor cells. A consistent localization was also observed in the ureteric epithelium (Fig.18, 19). These results were consistent with previous reports on GM130 expression in wildtype nephron progenitors (O'Brien et al., 2014). In contrast, the analysis of Shroom3^{-/-} E13.5 kidneys GM130 was not consistently expressed in the distal region of the nephron progenitor cells. Although the GM130 continued to be expressed apically in the ureteric epithelium. Quantification of the E13.5 kidneys revealed a significant decrease in the number of nephron progenitors that had a distal localization of GM130 in Shroom3^{-/-} ($n=4$, $p=0.0109$, Fig 18). Analysis of E18.5 Shroom3^{-/-} kidneys also revealed similar results as E13.5 Shroom3^{-/-} ($p=0.0037$, $n=4$ Fig19). These results show that in the absence of Shroom3, the normal localization of GM130, which is the distal area of the nephron progenitor, or the cell's leading edge, is reduced. The abnormal distribution of the Golgi marker suggests a role of Shroom3 in regulating nephron progenitor cell orientation.

Figure 16: Six2 and GM130 co-immunofluorescence of E13.5 Shroom3 mutant kidneys suggests no differences in cell orientation

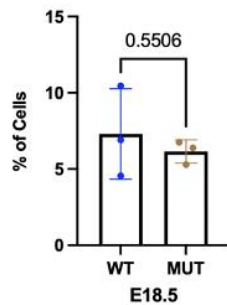


Six2 and GM130 co-immunofluorescence of E13.5 Shroom3 mutant kidneys suggests no differences in cell orientation. Wild Type (A, B) and Shroom3^{-/-} (C, D) E13.5 kidneys stained for GM130 (red) and Six2 (green). Localization of GM130 in nephron progenitors (NP) either in proximal (yellow arrow) or distal (white arrow). (E, F) Graph representing no difference in proximal and distal location of GM130 in nephron progenitors (n= 3, p= 0.8529; n=3, p=0.8081).

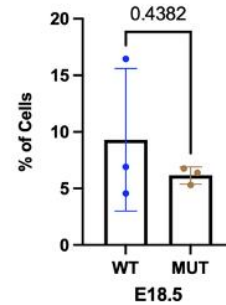
Figure 17: Six2 and GM130 co-immunofluorescence of E18.5 Shroom3 mutant suggests no differences in cell orientation



E. Average cells with Proximal localization of GM130

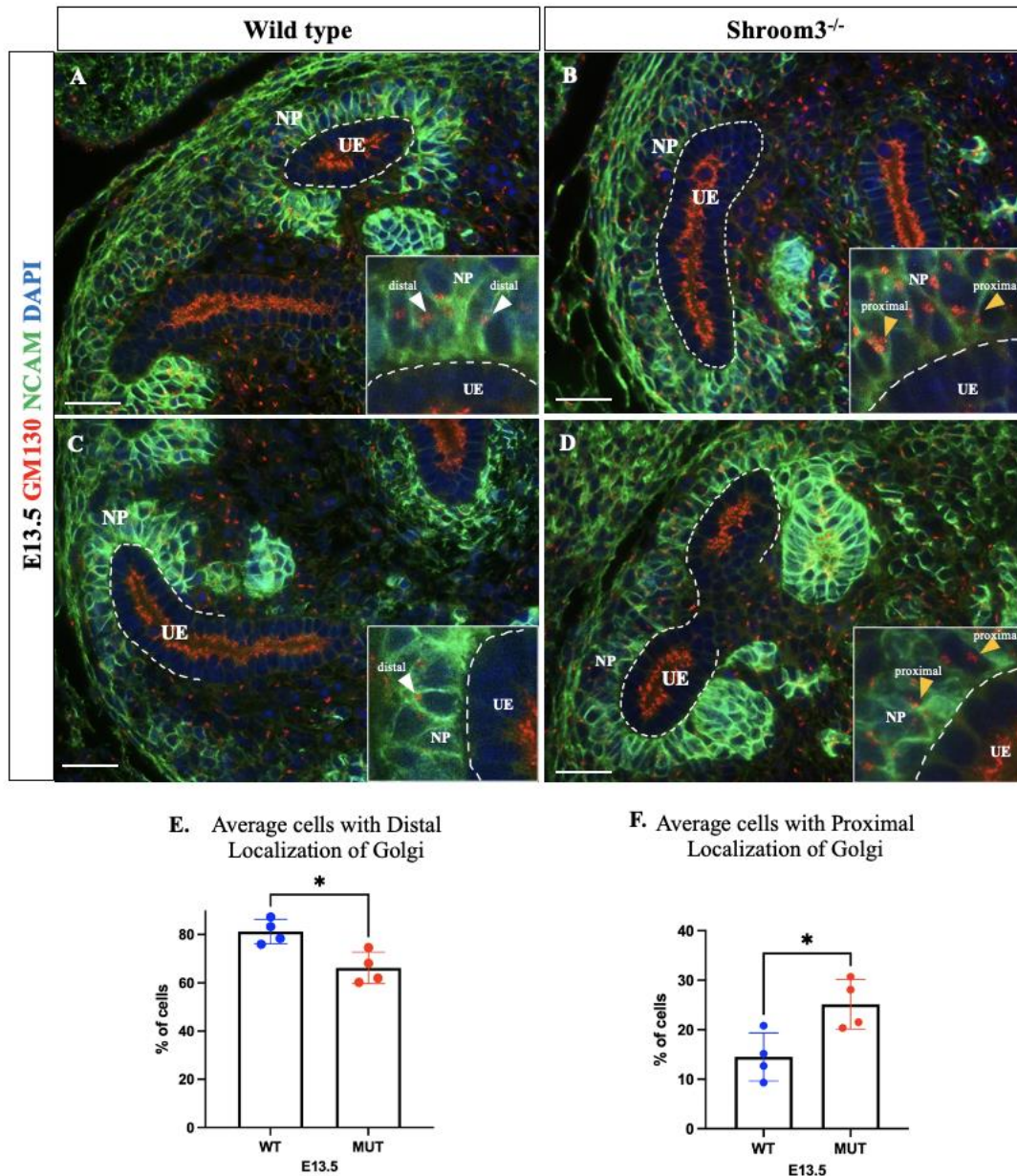


F. Average cells with Proximal localization of GM130



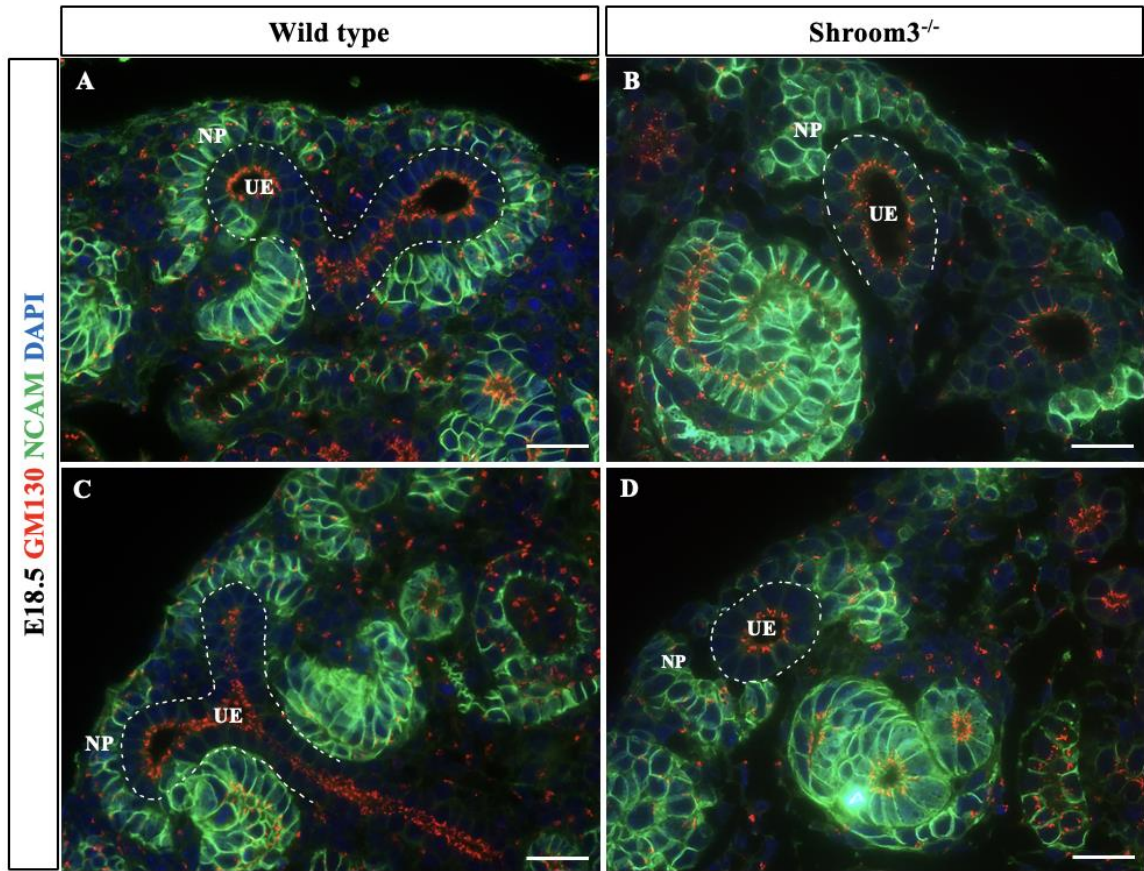
Six2 and GM130 co-immunofluorescence of E18.5 Shroom3 mutant suggests no differences in cell orientation. Wild Type (A, B) and Shroom3^{-/-} (C, D) E18.5 kidneys stained for GM130 (red) and Six2 (green) The encircled nephron progenitor cells (NP) are randomly picked to highlight the GM130 expression (arrow). Localization of GM130 in NP either in proximal (yellow arrow) or distal (white arrow) end. (E, F) No differences in proximal and distal location of GM130 in NP.

Figure 18: Shroom3 mutant E13.5 mice display altered GM130 expression pattern

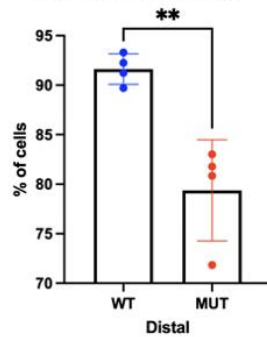


Shroom3 mutant E13.5 kidneys display altered GM130 expression: Immunofluorescence of Wild Type (A, C) and Shroom3^{-/-} (B, D) using **GM130** (red) and **NCAM** (green). Nephron progenitor cells (NP) are randomly picked to highlight the GM130 expression (arrow). Arrow points to localization of GM130 in nephron progenitor cells either Distal (white arrow) or Proximal (yellow arrow) in reference to the ureteric epithelium (UE). (E-F) Graphical representation of GM130 localization in E18.5 kidneys. E). (*p < 0.05, Student's t-test). Data expressed as mean ± SD; n= 4 WT kidneys and n= 4 MUT kidneys.

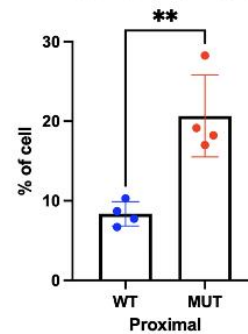
Figure 19: Shroom3 mutant E18.5 mice kidneys display altered GM130 expression pattern



E. Average cells with Distal Localization of Golgi



F. Average cells with Proximal Localization of Golgi

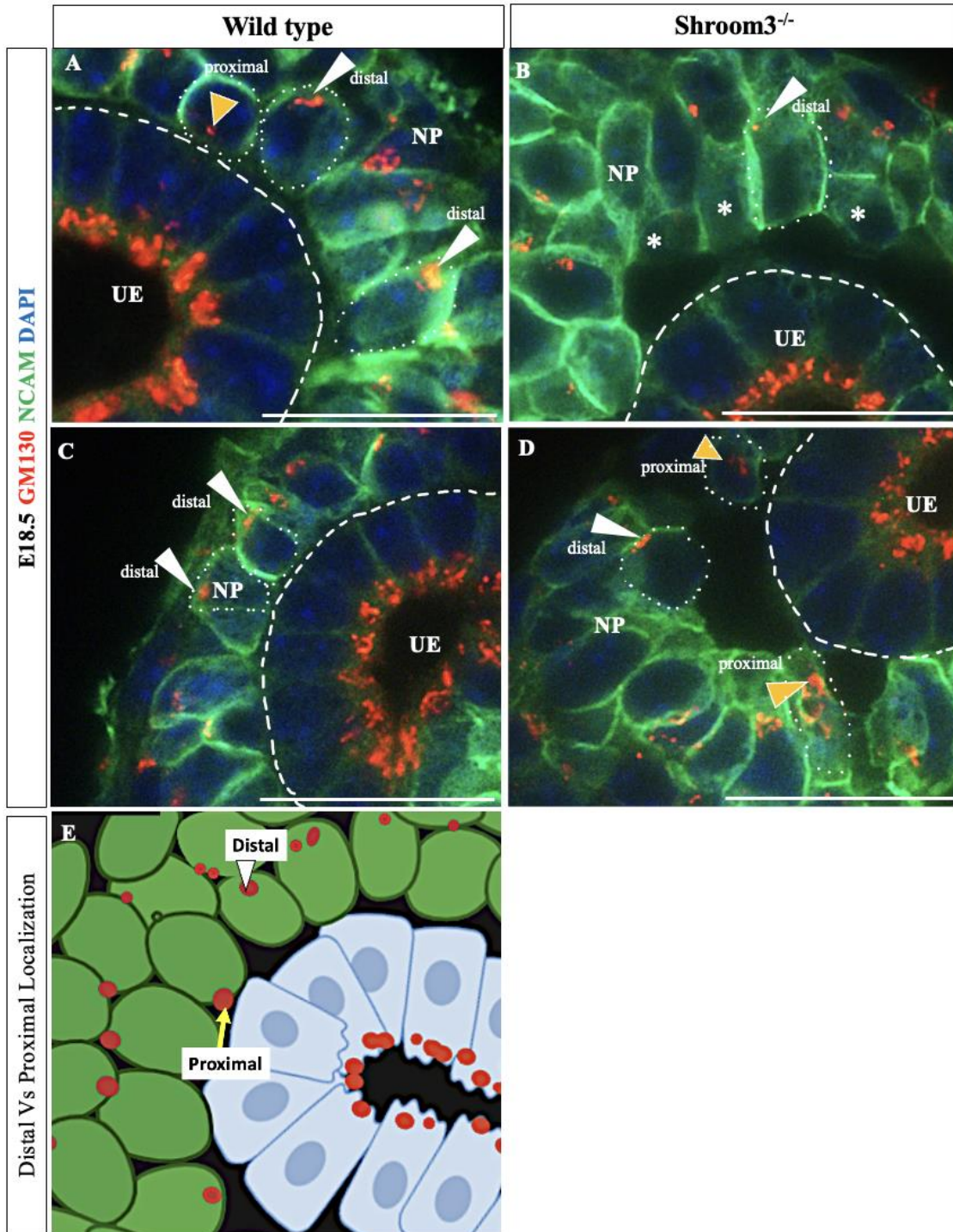


Shroom3 mutant E18.5 mice kidneys display altered GM130 expression pattern

Immunofluorescence of two Wild Type (A, C) and Shroom3^{-/-} (B, D) E18.5 kidneys using GM130 (red) and NCAM (green). Localization of GM130 in nephron progenitor (NP) cells either Distal (white arrow) or Proximal (yellow arrow) in reference to the ureteric epithelium (UE). (E) The graph illustrates a significantly lower percentage of nephron progenitors in Shroom3^{-/-} (MUT) with proximal localization of GM130 compared to wildtype (WT). While higher percentage of mutants have a proximal localization of GM130

compared to wildtypes, (*p < 0.05, **p < 0.01, Student's t-test). Data expressed as mean ± SD; n= 4 WT kidneys and n= 4 MUT kidneys)

Figure 20: High power images of E18.5 mice kidney highlight altered nephron GM130 expression



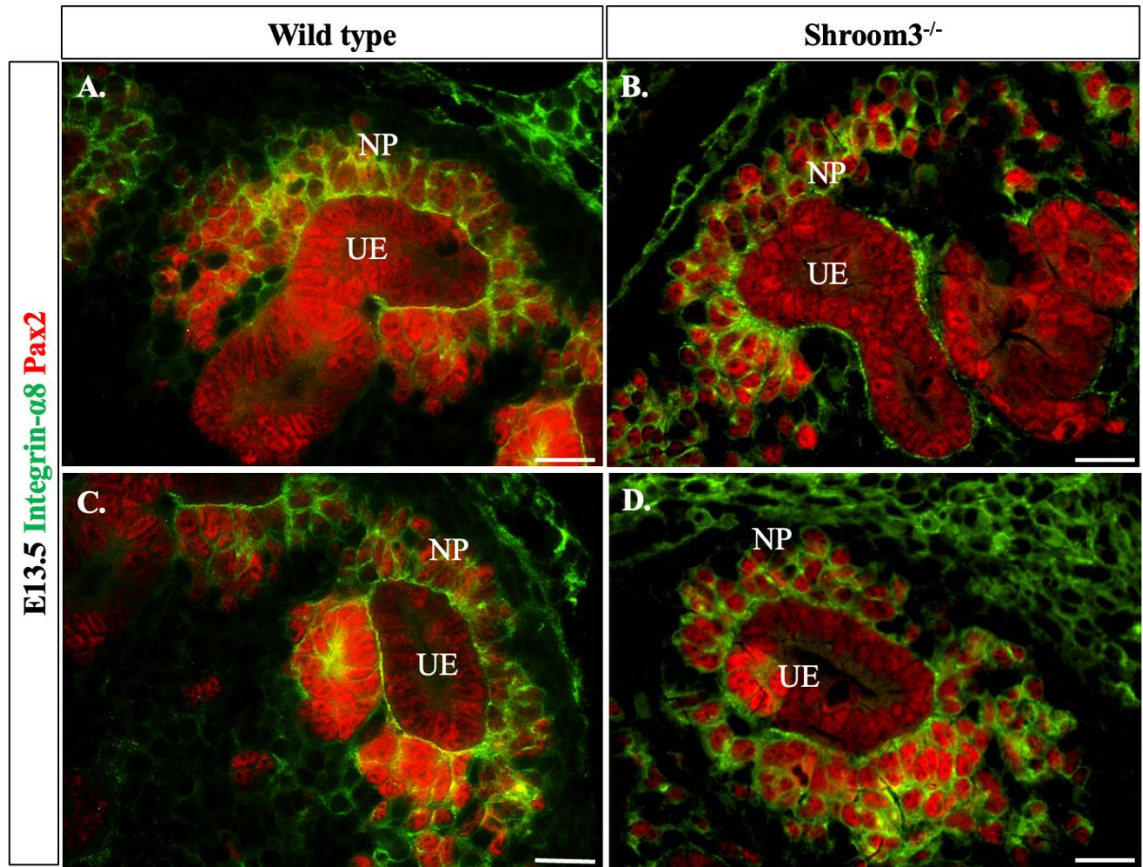
High power images of E18.5 embryonic mice kidney highlight altered nephron GM130 expression: Image is representative of different Wildtype (A, C) and Shroom3^{-/-} (B, D) embryonic kidneys stained for **GM130** (red) and **NCAM** (green). In wildtypes, GM130 is mostly expressed in the distal end (white arrow) of nephron progenitors. Whereas in the mutants, GM130 is mostly expressed in the proximal end (yellow arrow) of nephron progenitors.

Moreover, as a second measure to examine cell orientation, I co-stained wildtype and Shroom3^{-/-} kidneys (E18.5 and E13.5) with primary antibodies Integrin- α 8 and Pax2. Integrin- α 8 is a protein synthesized by nephron progenitors which binds to a nephronectin, a protein secreted by the ureteric epithelium (Muller et al., 1997; Linton et al., 2007). Studies have also demonstrated that integrin is found on polarized surfaces of nephron progenitor facing the ureteric epithelium (O'Brien et al., 2014). Therefore, we also investigated the integrin- α 8 expression pattern to complement the GM130 experiments. The analysis of E13.5 wildtype nephron progenitors demonstrated integrin- α 8 in the cell cytoplasm at proximal end of nephron progenitors, located near the ureteric bud tips (Fig. 21A,C; Fig. 22). A similar expression was found in Shroom3^{-/-} E13.5 kidneys (Fig 21B, D; Fig. 22). To determine whether this expression pattern remained consistent in the later stage, we analyzed E18.5 kidneys. However, the analysis of E18.5 Shroom3^{-/-} did not reveal a consistent expression pattern of integrin- α 8 in the area surrounding the nephron progenitors which was observed in E18.5 wildtypes (Fig.23). Based on our analysis the expression patterns in the proximal region remain consistent in the wildtype and Shroom3^{-/-} E13.5 and E18.5 kidneys.

These results are interesting as they suggest that Shroom3 is not the sole regulator of cell orientation and polarity. While integrin- α 8 did not display disruptions in its proximal localization, we did notice its expression was expanded in the space between the of nephron progenitor and the ureteric epithelium. Considering integrin is a transmembrane receptor

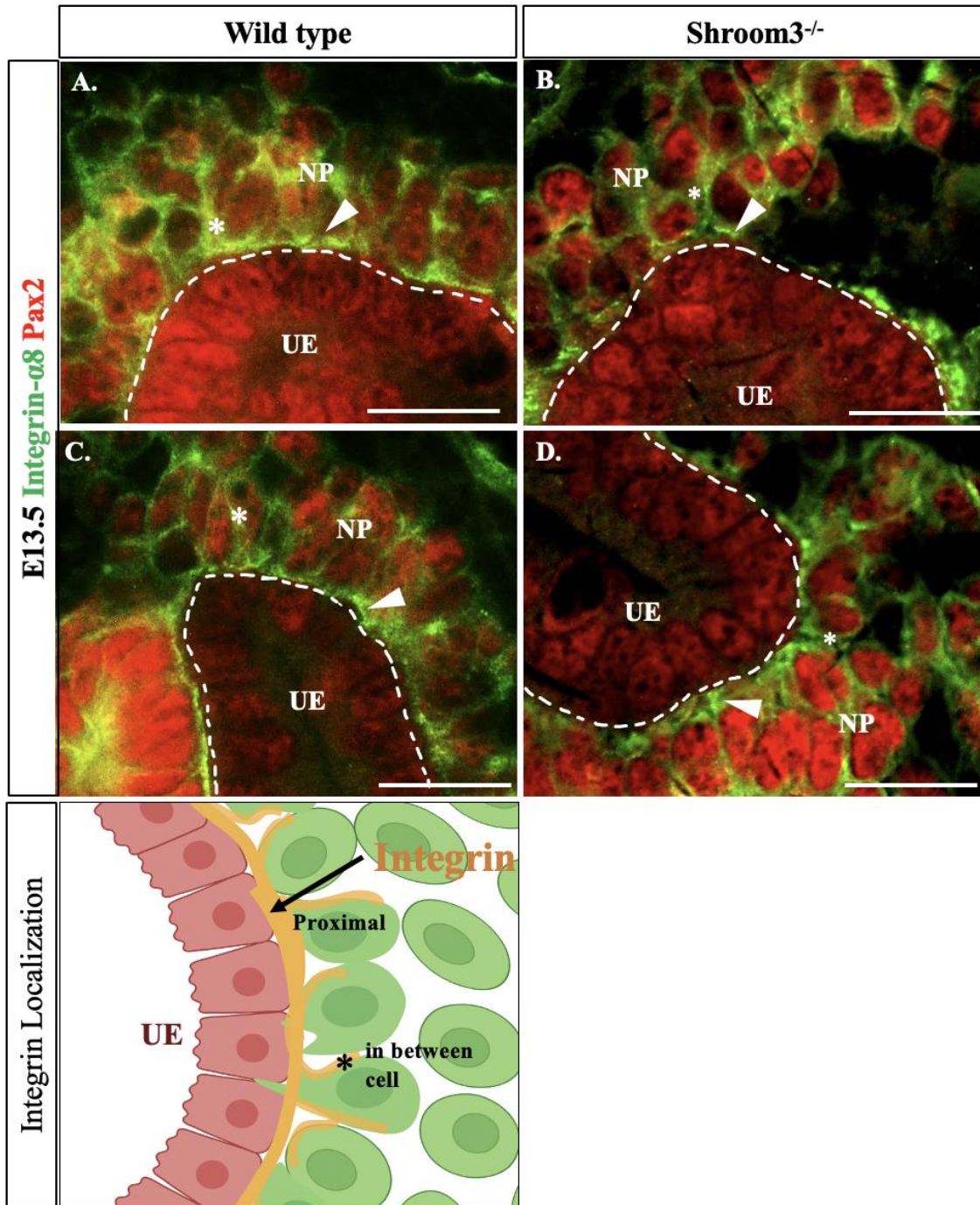
found on the nephron progenitor cell surface, and activated through a ureteric epithelium ligand, nephronectin (Linton et al., 2007), this analysis suggests that the deletion of Shroom3 disrupts proper communications between nephron progenitor and ureteric epithelium.

Figure 21: Integrin- $\alpha 8$ immunofluorescence in E13.5 kidneys



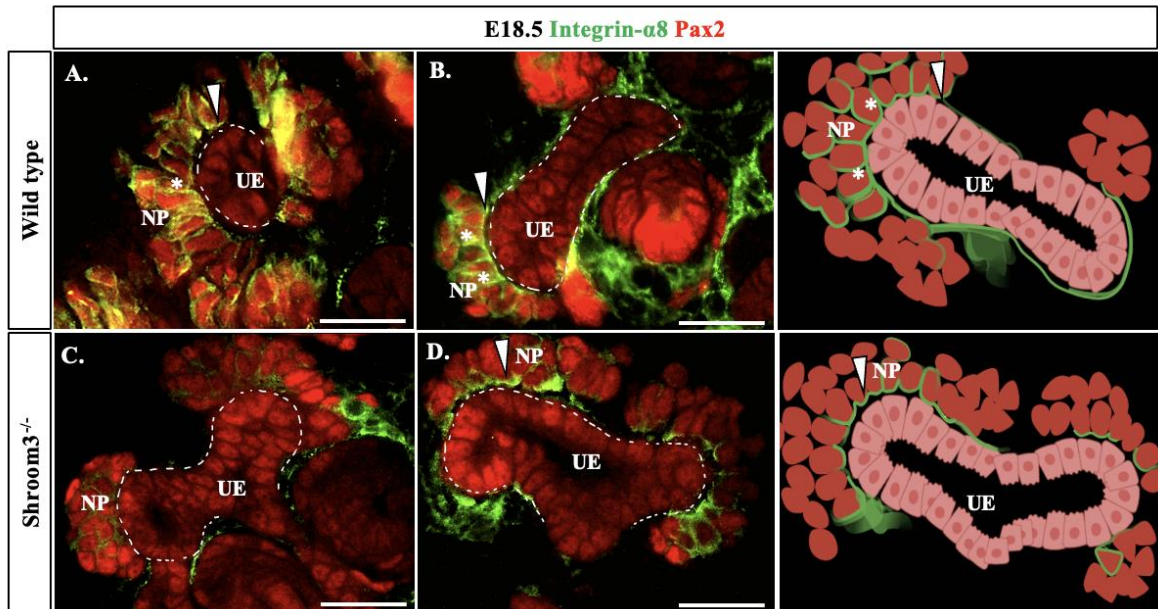
Integrin- $\alpha 8$ expression is consistent in E13.5 Shroom3 kidneys: Immunofluorescence of Integrin- $\alpha 8$ (green) and Pax2 (red) in Wildtype (A-A'') and Shroom3^{-/-} (B-B'') E13.5 kidneys. Integrin is expressed on the surface of the nephron progenitor concentrating in the membrane closest to the ureteric branch tip and surrounding the nephron progenitor cell membrane.

Figure 22: Expression of integrin- $\alpha 8$ at E13.5 is unchanged in *Shroom3*^{-/-} kidneys



Expression of integrin- $\alpha 8$ at E13.5 is unchanged in *Shroom3*^{-/-} kidneys. Immunofluorescence of **Integrin- $\alpha 8$** (green) and **Pax2** (red) in Wildtype (A, B) and *Shroom3*^{-/-} (C, D) E13.5 kidneys. Expression of integrin- $\alpha 8$ on surface of the nephron progenitor concentrating in the membrane closest to the ureteric branch tip (arrow) and surrounding the nephron progenitor cell membrane (Asterisk).

Figure 23: Shroom3 mutated E18.5 kidneys display altered expression of Integrin- $\alpha 8$



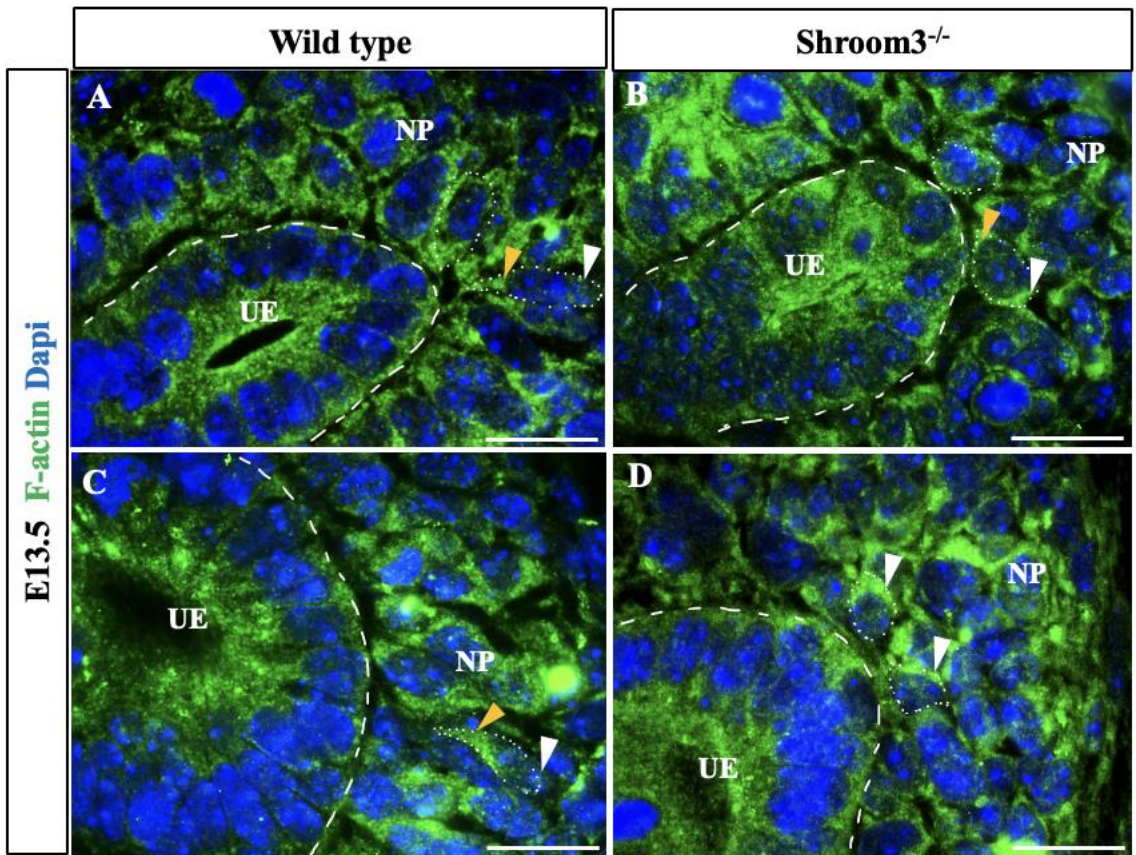
Shroom3 mutated E18.5 kidneys display altered expression of Integrin- $\alpha 8$: Immunofluorescence of Integrin- $\alpha 8$ (green) and Pax2 (red) in Wildtype (A, B) and Shroom3^{-/-} (C, D) E18.5 kidneys followed by a diagram. Integrin is expressed on the surface of the nephron progenitor concentrating in the membrane closest to the ureteric branch tip (arrow). The asterisk highlights the expression of integrin in the cell membranes of cell adjacent to each other. NP- Nephron progenitor, UB- Ureteric Bud.

4.5 Shroom3 mutation leads to changes in F-actin distribution

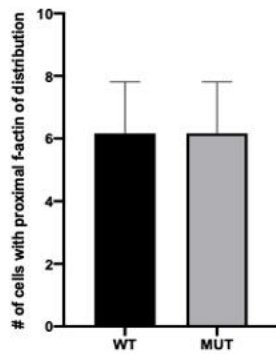
F-actin represents a significant component of the cytoskeleton. During the migration, for instance, fibroblasts cell, F-actin will accumulate at concentrated at the cells' leading edge (Svitkina, 2018) to control cell shape, orientation, and polarity. Considering Shroom3 modulates actin dynamics (Hildebrand & Soriano, 1999; Plageman et al., 2010; Chung et al., 2010), I analyzed the wildtype F-actin distribution Shroom3^{-/-} nephron progenitors. Analysis of E13.5 Wildtype kidneys displayed tightly organized nephron progenitors that appeared to be elongating towards the ureteric bud tips. In wildtypes, F-actin was primarily distributed at the proximal end of the nephron progenitors, where tiny strands of F-actin protrusions were seen reaching towards the ureteric epithelium (Fig. 24A-B). In contrast,

Shroom3^{-/-} nephron progenitors were round and loosely clustered around the ureteric epithelium. These cells also displayed altered projection formation and lack cell directionality because F-actin was localized in the distal end of the cell (Fig. 25C-D). Next, a close examination of the nephron progenitors confirmed the localization of F-actin in the proximal end of the cell (Fig. 25A-B, diagram). Whereas Shroom3^{-/-} embryonic kidneys unevenly distributed F-actin around the nephron progenitor cell. A quantitative analysis was performed by counting the number of cells with either a proximal or distal localization of F-actin. This analysis revealed that the results were not statistically significant (Fig. 25). Next, I analyzed the percentage of cells with the proximal distribution of F-actin. This analysis also revealed no significant differences in the localization of F-actin in wildtypes and Shroom3^{-/-}, therefore suggesting actin distribution was not specific to one side of the cell. While the quantification may not reveal the strong association of F-actin distribution towards a particular side of the cell, but the overall analysis does reveal that many cells have a disrupted F-actin pattern. Because a cell's cytoskeleton is critical to regulating cell shape, orientation, and polarity, Shroom3 may directly or indirectly be assisting F-actin rearrangement in the cell. Thus, these studies reveal a strong association of F-actin distribution and Shroom3, further highlighting the possible disorientation of the cells.

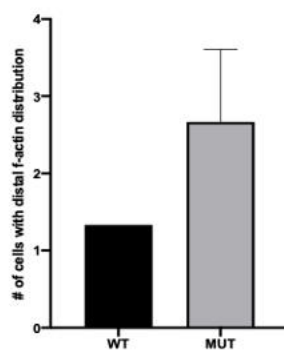
Figure 24: F-actin distribution in Shroom3 mutant embryonic kidneys is disrupted



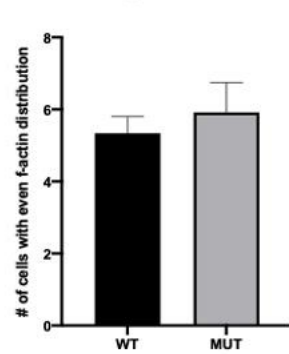
E. Proximal localization of f-actin



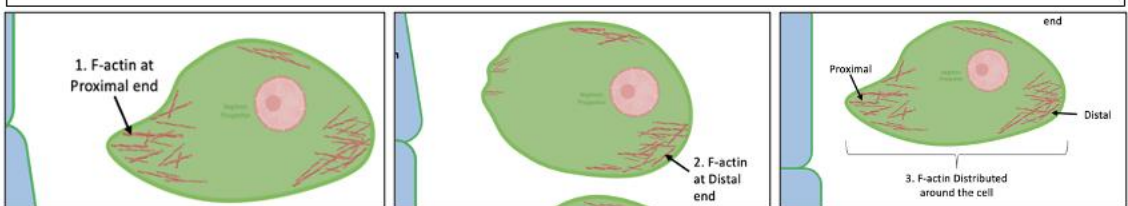
F. Distal localization of f-actin



G. F-actin distributed throughout the cell

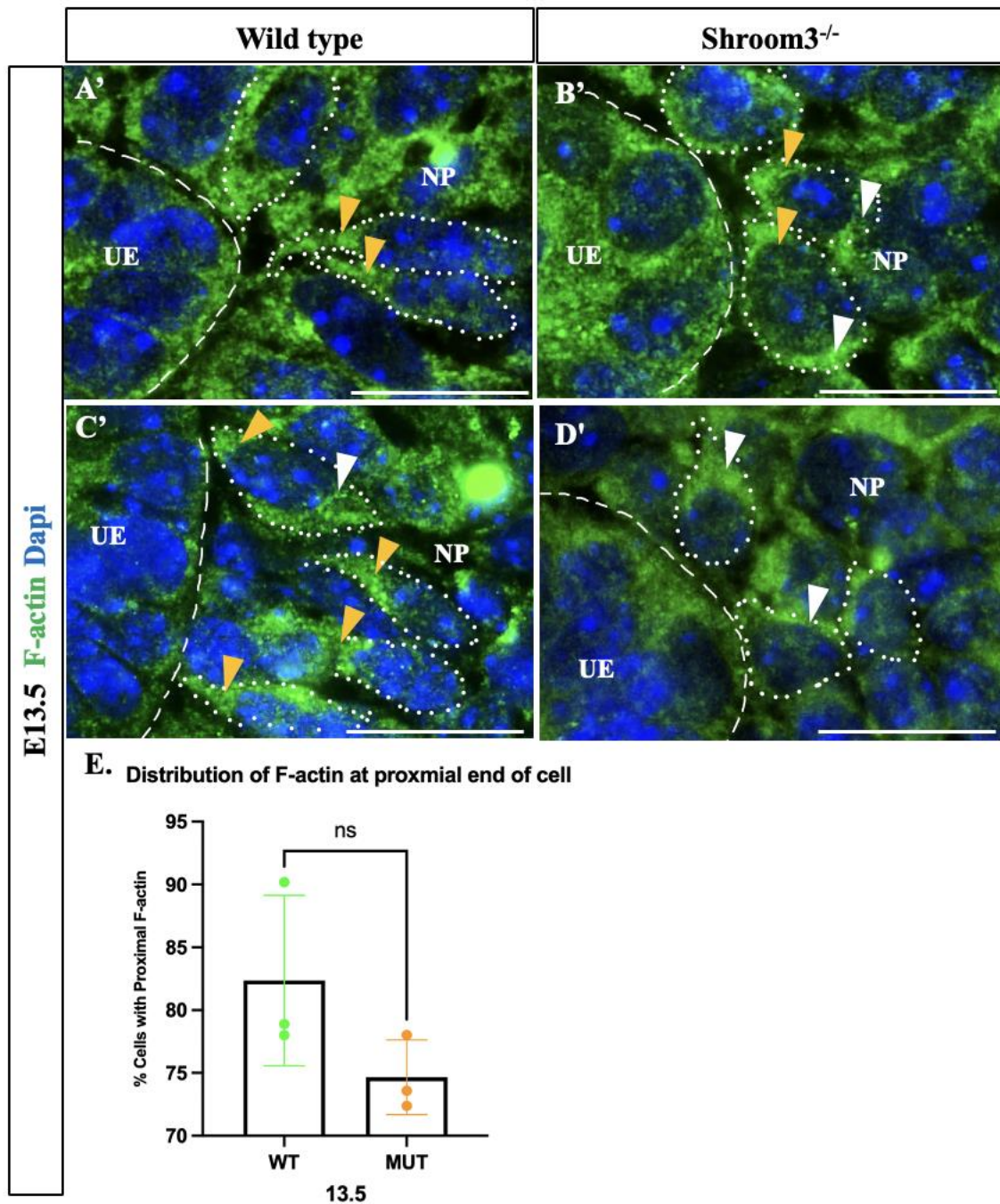


H. F-actin in Nephron Progenitor cells



F-actin distribution in Shroom3 mutant embryonic kidneys is disrupted: (A-B) Wildtype nephron progenitors (NP) are elongating towards the ureteric epithelium (UE) (C-D) *Shroom3*^{-/-} NP cells are round and disorganized around the UE. Localization of F-actin in nephron progenitor (NP) cells either in Proximal (yellow arrow) or Distal (white arrow). (E,F,G) Graphs representing number of cells that have F-actin distributed towards the proximal, middle, or distal region. H) Diagram illustrating F-actin distribution.

Figure 25: High power image of E13.5 kidneys display abnormal F-actin distribution



High power image of E13.5 kidneys display abnormal F-actin distribution: Immunofluorescence staining using F-actin (green) on (A'-C') Wild type, (B'-D') Shroom3^{-/-} kidneys (A'-B') Zoomed in images of wildtype kidney illustrates expression of F-actin (green) in the proximal region of nephron progenitor (yellow arrow). While some cells also display expression in the distal end (white arrow). (C'-D') Magnified images of Shroom3^{-/-} show F-actin is more scattered around the nephron progenitor cell membrane

and lacks expression in the proximal end. E) Graphical representation of F-actin distribution in the proximal end of cell.

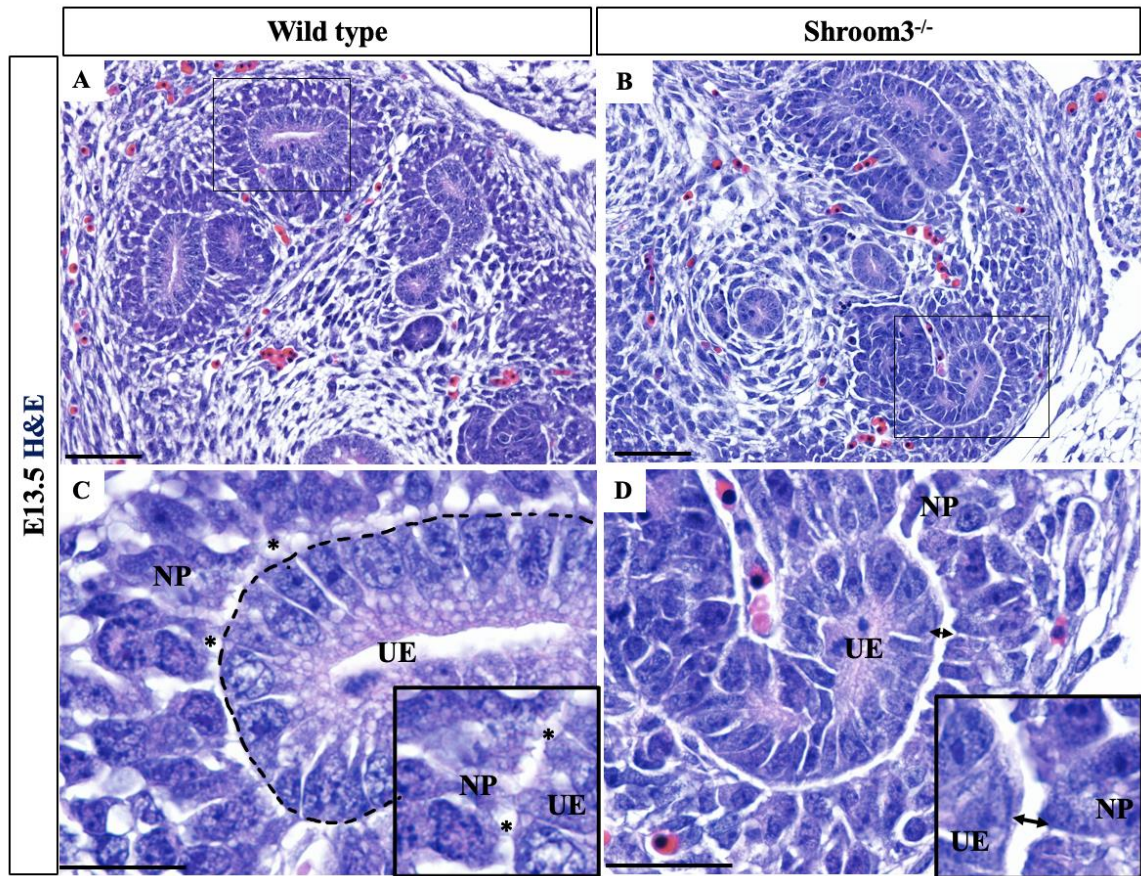
4.6 Shroom3 mutant Nephron progenitors lack cellular projections

Nephron progenitors undergo shape changes and membrane modifications to generate “membrane projections” that elongate towards the ureteric epithelium (Supplementary 8, Combes et al., 2016; Minuth & Denk et al., 2013). A study by Minuth & Denk, 2012 highlighted the presence of cellular projections in nephron progenitors of the embryonic rabbit kidneys using transmission electron microscopy. O’Brien et al., demonstrated that homozygous deletion of Wnt11 (Wnt11^{-/-}), a ureteric tip-derived protein, prevented nephron progenitors from clustering and elongating towards the ureteric epithelium. The study also highlighted that Wnt11^{-/-} nephron progenitors consistently lacked the formation of cellular projections. As a result of these abnormalities, the nephron progenitors underwent accelerated differentiation and premature depletion of the nephron progenitor pool (O’Brien et al. 2014, O’Brien, 2019). Together, these studies highlight an essential role in cellular projections with proper nephron formation, yet the mechanisms and molecular players are not well understood.

The primary mechanism regulating lamellipodia, filopodia, blebs and invadopodia projections is an accumulation of actin filaments at the end of the cell (Svitkina, 2018). Since Shroom3 regulates actin dynamics (Halabi, 2013), I hypothesized that Shroom3 assists nephron progenitors in generating cell projection formation. To investigate whether Shroom3 is a molecular player in nephron progenitor projection formation, I closely analyzed wildtype and Shroom3^{-/-} using H&E at E13.5 and E18.5. The wildtype E13.5 kidneys revealed numerous thin membrane projections reaching out from the nephron progenitors towards the ureteric epithelium (Fig.26C). Analysis of Shroom3^{-/-} E13.5

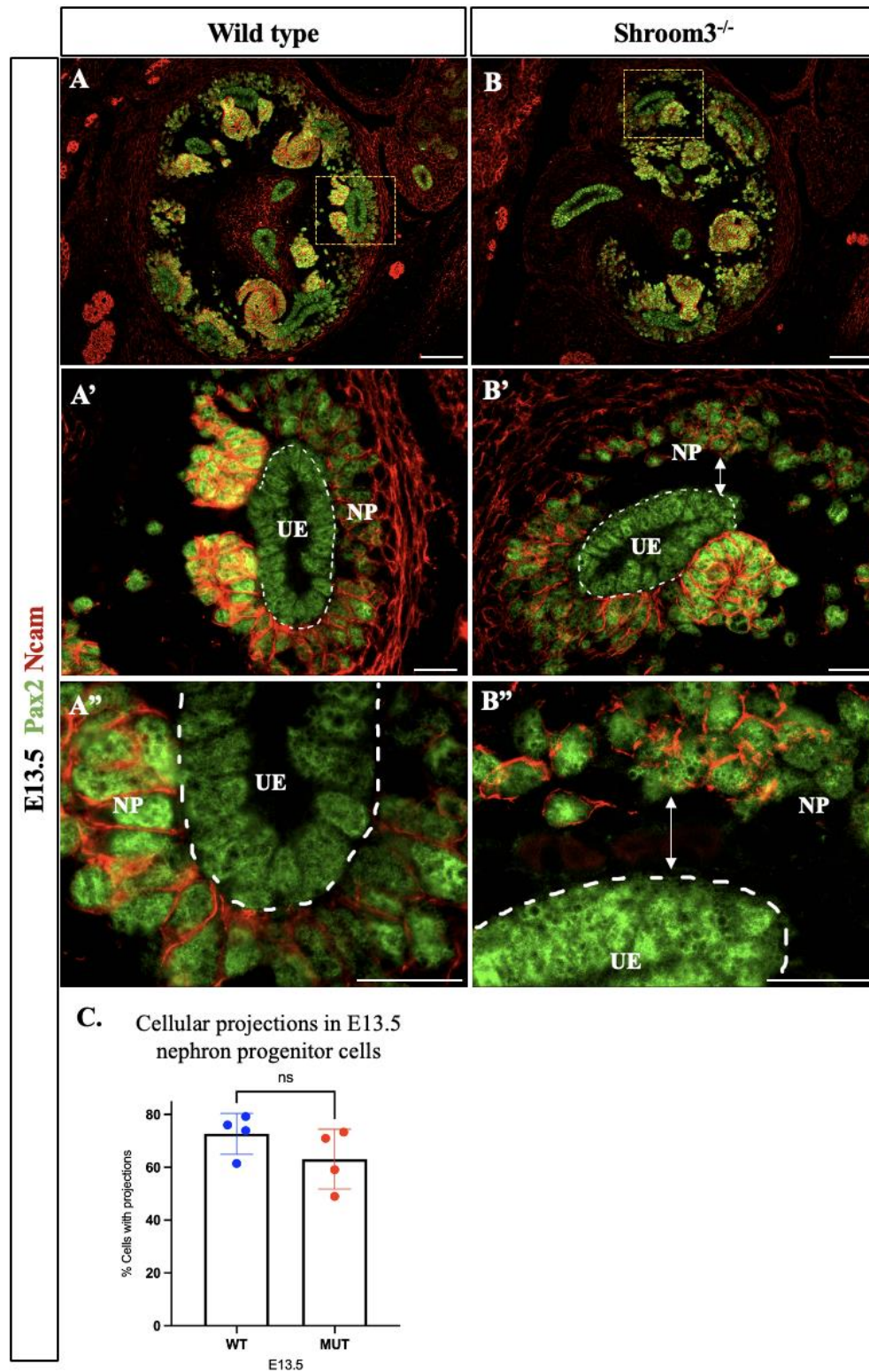
displayed irregularly shaped, distanced, and abnormally condensed nephron progenitors that did not exhibit many of these cellular projections (Fig. 26D). Furthermore, analysis of *Shroom3*^{-/-} E18.5 nephron progenitors revealed a similar phenotype and lack of projections. I next performed IF for the nephron progenitor membrane marker *Ncam* to outline the nephron progenitor cell membrane and *Pax2*, a marker of all progenitor cells. The analysis confirmed the presence of cellular projections in the wildtype (Fig. 27A). The analysis of *Shroom3*^{-/-} mutants revealed the absence of cellular projections and large space that separated the nephron progenitors from the ureteric epithelium. To determine if the difference was significant, I used the cells most adjacent to the ureteric epithelium and counted the number of cells with projections. For my analysis, I analyzed three different cap mesenchyme regions of 4 wildtypes and 4 *Shroom3*^{-/-} kidneys. The quantification revealed no differences in the number of cellular projections between the wildtype and *Shroom3*^{-/-} E13.5 and E18.5 kidneys. However, during this analysis, I did not think the *Ncam* stain accurately represented all the projections and therefore performed transmission electron microscopy on embryonic kidneys.

Figure 26: Lack of cellular projections in Shroom3 mutant E13.5 nephron progenitors



Lack of cellular projections in Shroom3 mutant E13.5 nephron progenitors: (A, C) Wild Type nephron progenitors sending out thin cellular projections (asterisks) towards the ureteric epithelium. (B, D) The space between the Shroom3^{-/-} NP and UE lacking projections (arrow).

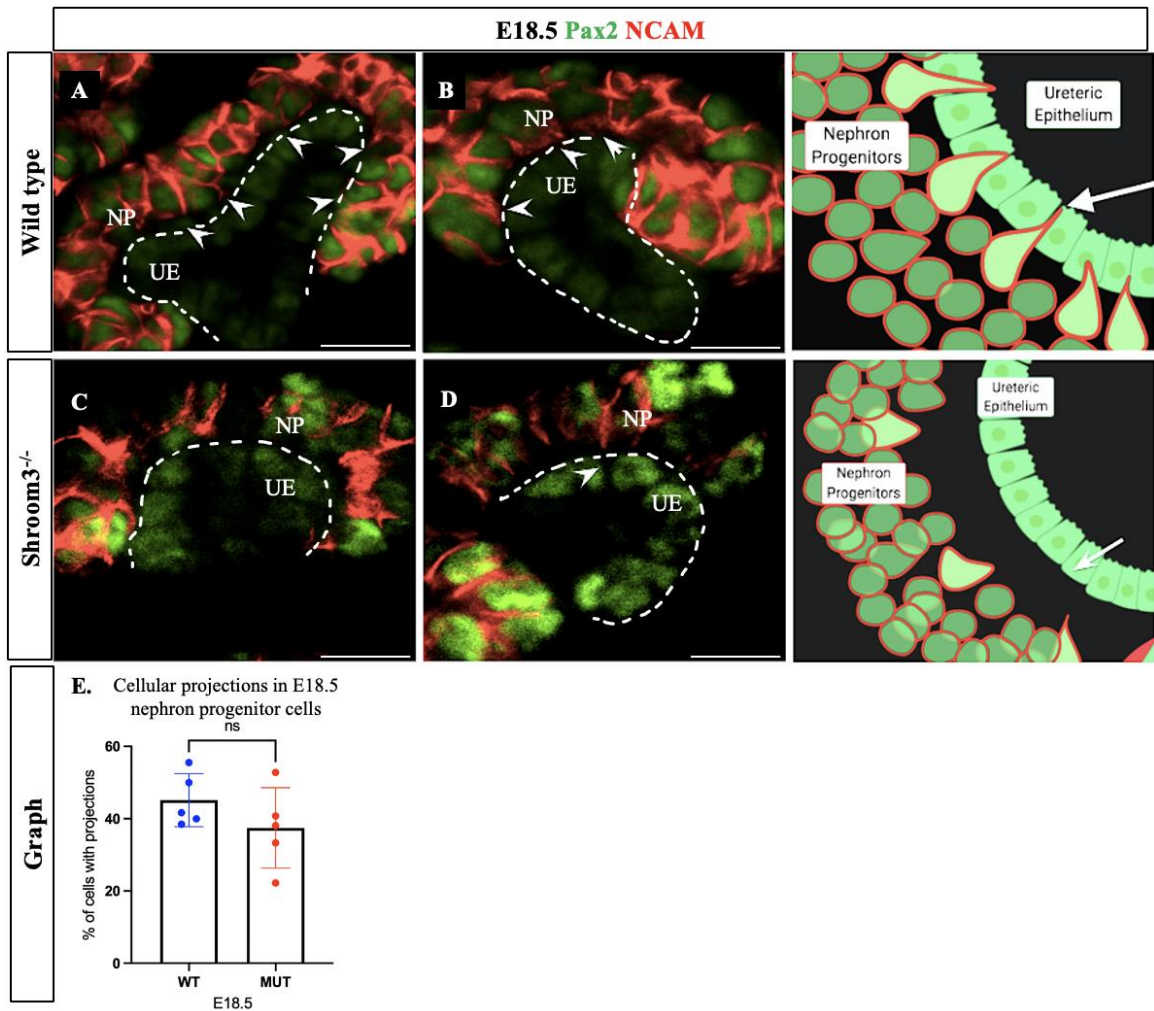
Figure 27: Ncam immunofluorescence on E13.5 kidneys to detect cellular projections



Ncam immunofluorescence on E13.5 kidneys to detect cellular projections: (A) Wild type, (B) Shroom3^{-/-} E13.5 kidneys stained for NCAM (red), Pax2 (green) stain. Wildtype

nephron Progenitors (NP) are sending out thin projection (red lines) reaching the Ureteric Epithelium (UE). The large gap in the *Shroom3*^{-/-} tissue seems to prevent the nephron progenitors from reaching towards the UE.

Figure 28: Ncam immunofluorescence on E18.5 kidneys display no change in projection formation.



Ncam immunofluorescence on E18.5 kidneys display no change in projection formation. NCAM (red), Pax2 (green) stain on E18.5 (A) Wild type, (B) Mutant kidneys. In wildtype, Nephron Progenitors (NP) can be seen forming projections (arrows) reaching the Ureteric Epithelium (UE). The large gap seems to prevent the nephron progenitors from forming or preventing them from reaching towards the UE in the mutants. The last panel represents a schematic diagram to help explain the results.

4.7 Lack of cellular projections in the absence of Shroom3

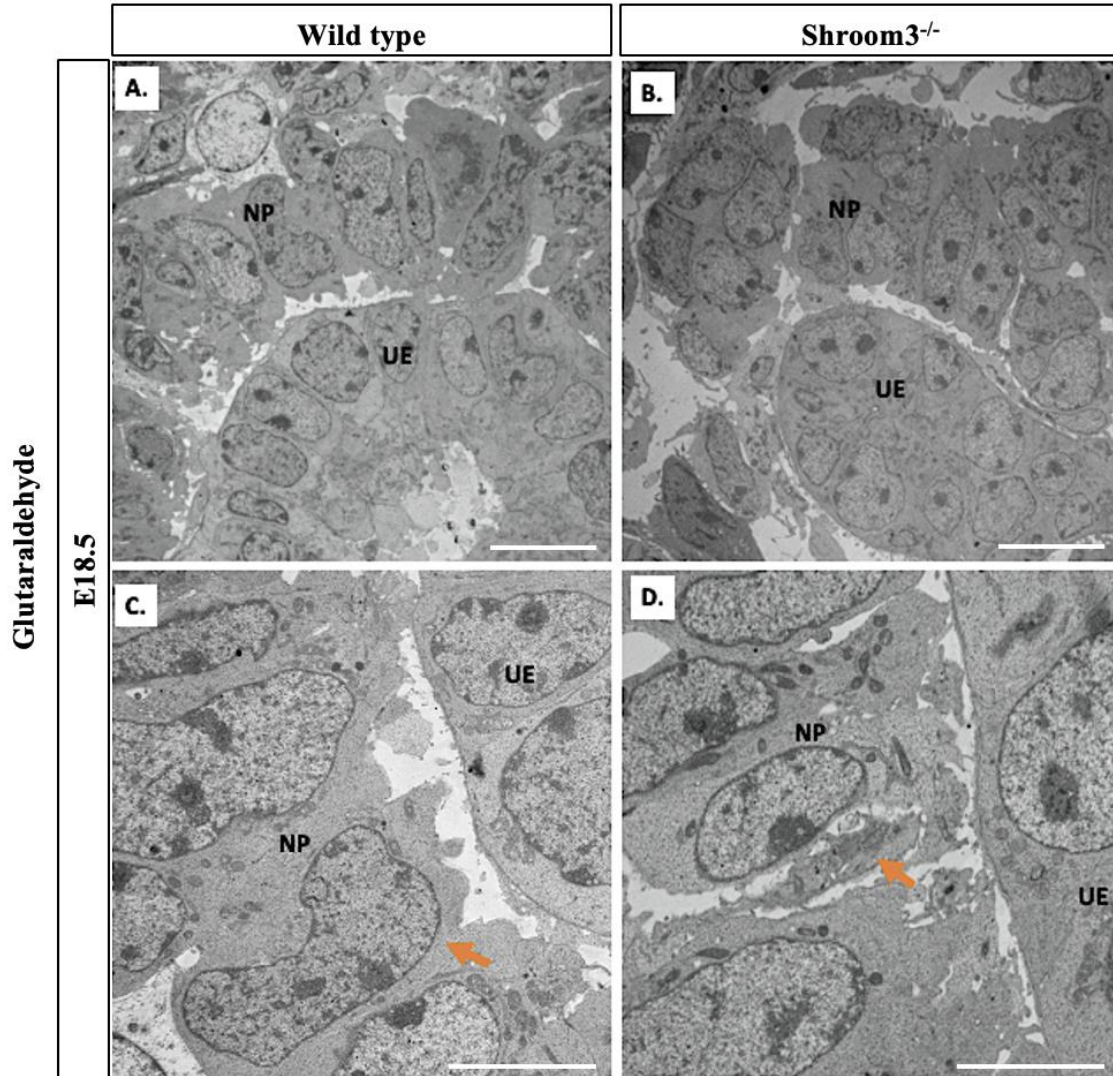
To examine cellular projections using transmission electron microscopy, I fixed embryonic kidney tissue in glutaraldehyde. The tissue was prepared for ultrastructural analysis by the Electron Microscopy Facility in the Health Science Centre at McMaster University. The initial analysis of WT kidneys demonstrated that the nephron progenitors exhibited an elongated cell shape well organized in a sheet-like fashion (Fig. 25A). In contrast, the TEM analysis of Shroom3^{-/-} kidneys confirmed that the nephron progenitors were abnormally shaped and did not exhibit an elongated cell shape. More specifically, Shroom3^{-/-} nephron progenitors appeared rounder and more spaced apart in the cap mesenchyme and confirmed the nephron progenitors phenotype at the Ultrastructural level. Interestingly, in E18.5 WT nephron progenitors, we observed many membrane modifications consistent with cellular protrusions (Fig. 30, arrow). The wildtype nephron progenitors cells exhibited thick and thinner membrane projections consistent with lamellipodia and filopodia, respectively (Kim et al., 2019). Nephron progenitors of wildtype kidneys also demonstrated the presence of blebs, which are specialized rounded membrane protrusions found in migrating cells (Kardash et al., 2010). Just outside of the cell membrane, we also observed small vesicles that seemed to carry cargo from one cell to another. These studies are the first to demonstrate that wildtype nephron progenitor cells exhibit different types of cellular projections. Next, I analyzed five nephrogenic zones from two different wildtypes and Shroom3^{-/-} E18.5 kidneys and quantified the number of projections present in each nephron progenitor near the ureteric epithelium. Quantitative analysis from wildtype and Shroom3^{-/-} E18.5 kidneys showed a significant decrease in the number of thin-filopodia-like projections in the Shroom3^{-/-} nephron progenitors, while the lamellipodia projections were similar in wildtype (Fig. 31E). Based on this analysis, the cellular projections

projecting from the nephron progenitors cells could be Shroom3 dependent, likely through the localization of actin-filaments.

Table 1– Characterizing E18.5 Nephron Progenitor cells using Electron Microscopy

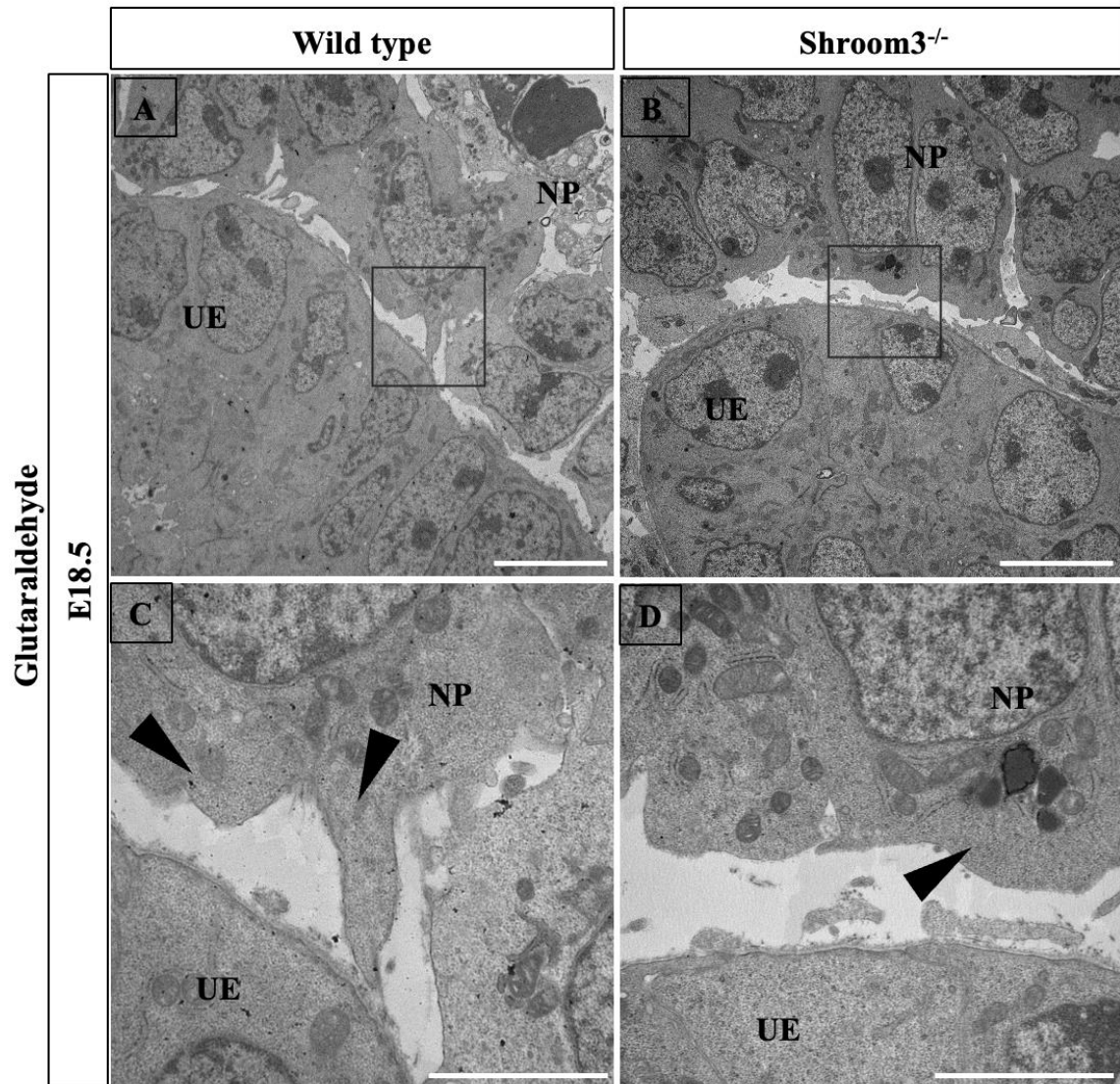
	Wild type	Shroom3 Mutant
Shape	Regular (circular and long)	Round and irregular (no consistent shape)
Organization	Condensed around UB	Further distanced from UB Unable to cluster around the ureteric epithelium
Protrusions	Lamellipodia Filopodia	Few lamellipodia Lack of Filopodia
Protrusions multidirectional	Yes	Yes
Nuclei	Round and smooth elongated	Irregular shape
Mitochondria	Located at the proximal end of NP cell	Located at the proximal end of NP cell

Figure 29: Transmission Electron Microscopy of E18.5 Shroom3 mutant nephron progenitors display irregular cell shape and organization



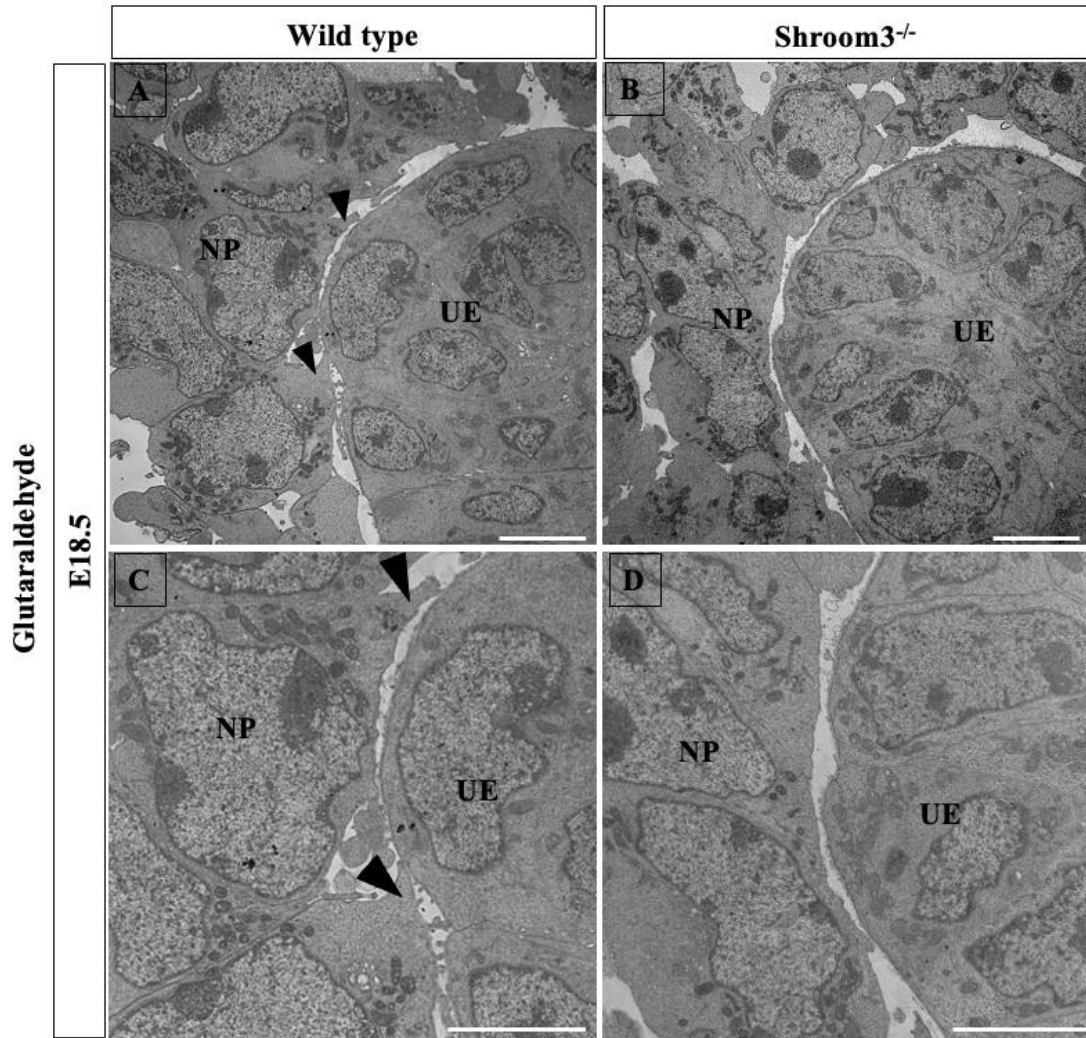
Transmission Electron Microscopy of E18.5 Shroom3 mutant nephron progenitors display irregular cell shape and organization: Transmission electron microscopy of the nephron progenitor cell niche in embryonic mice kidney after fixation in glutaraldehyde (GA). (A, C) Wild Type NP is rectangular with multiple long and thick cellular projections reaching the ureteric epithelium (UE). (B, E) Shroom3 mutant NP is irregular in shape (arrow) and separated from adjacent cells. NP – nephron progenitor, UE – ureteric epithelium

Figure 30: Embryonic kidneys display presence of Lamellipodia-like thick protrusions

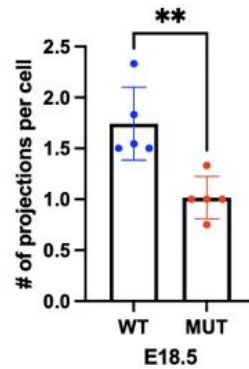


Embryonic kidneys display presence of Lamellipodia-like thick protrusions: Transmission electron microscopy of the nephron progenitor cell niche in E18.5 mice kidney after fixation in glutaraldehyde (GA). (A, C) Wildtype nephron progenitors (NP) sending out multiple long and lamellipodia-like thick protrusions (arrow) reaching the ureteric epithelium (UE). (B, D) Shroom3^{-/-} NP cells have fewer, shorter protrusions (arrow).

Figure 31: Transmission Electron Microscopy of the E18.5 Shroom3 mutant kidney show lack of cellular projection formation



E Average number of projections per cell (TEM)

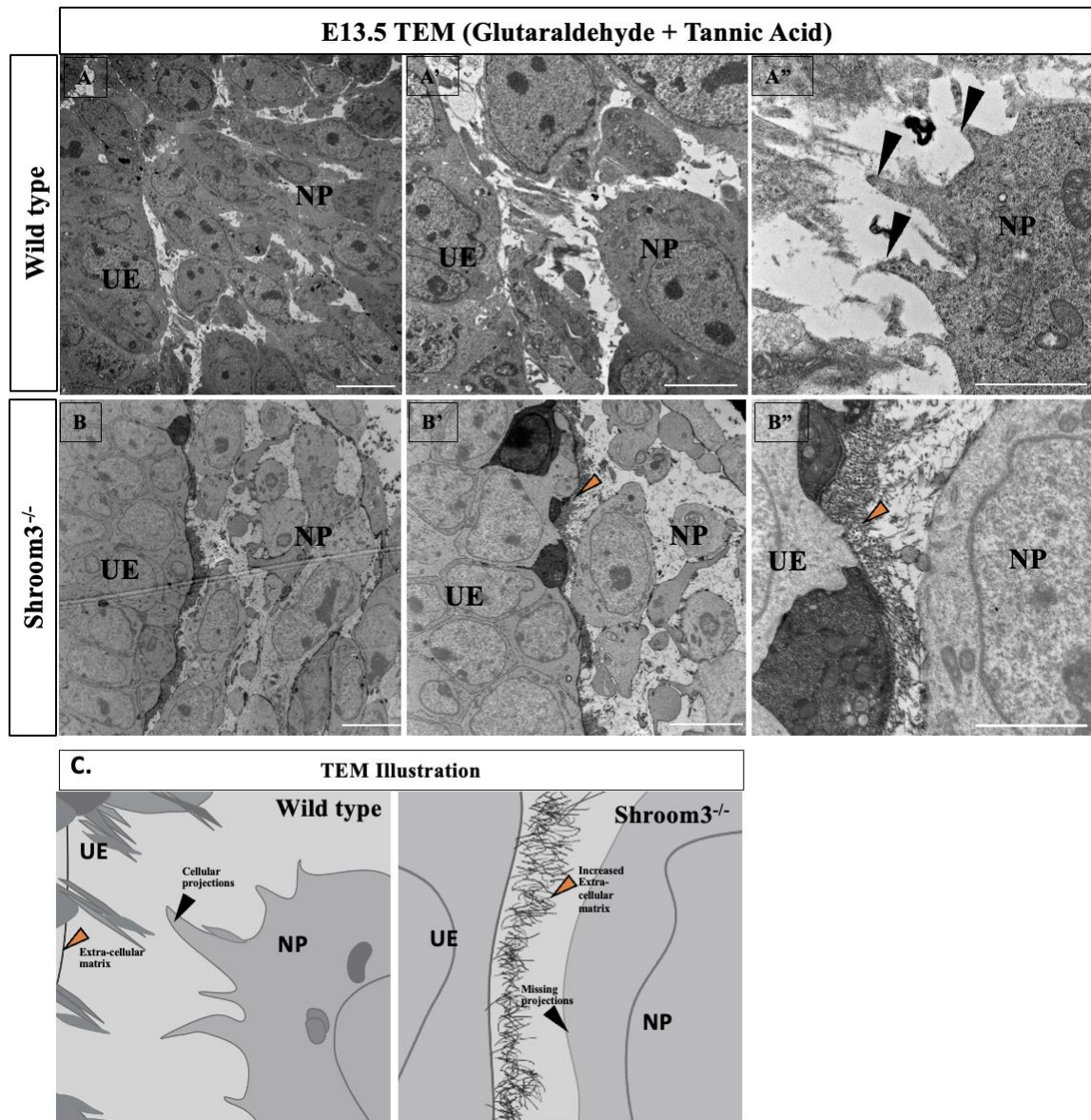


Transmission Electron Microscopy of the E18.5 kidney show lack of cellular projection formation in the absence of Shroom3: Transmission electron microscopy of

the nephron progenitor cell niche in E18.5 mice kidney after fixation in glutaraldehyde (GA). (A, C) Wildtype nephron progenitor (NP) with increasing magnification. C) Higher magnification illustrates thin projections (arrow) coming out of the nephron progenitors and reaching the ureteric epithelium (UE). (B-D) *Shroom3*^{-/-} NP lack a clear long projection. E) the Average number of projections per cell in Wildtype (WT) and *Shroom3*^{-/-} (MUT) (A two-tailed t-test was used to calculate p-value =0.004 and mean with SD, n=5 cap mesenchyme).

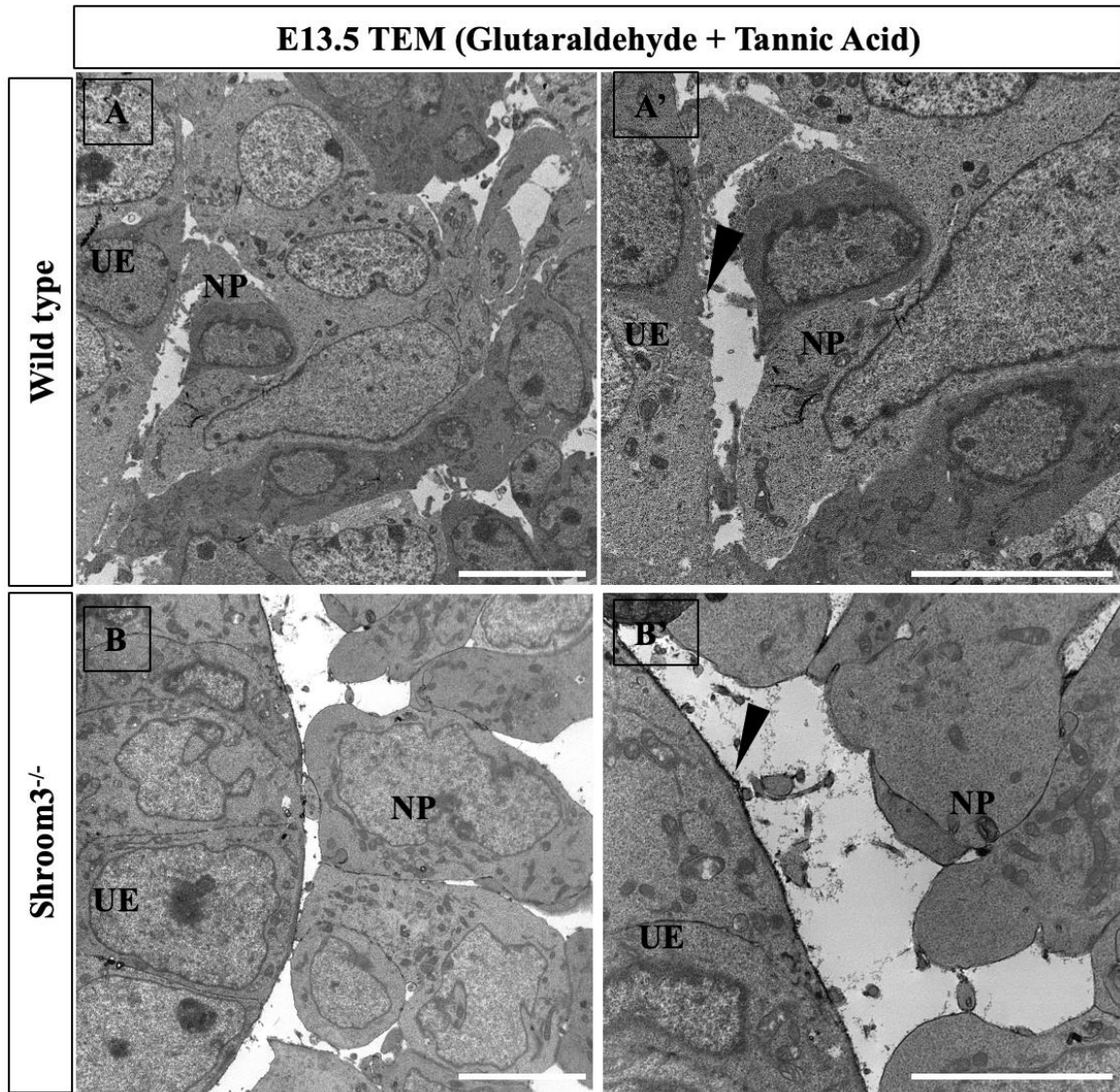
Next, based on the H&E and integrin staining, I was also interested in examining the abnormally large space between the nephron progenitors and the ureteric epithelium in some of the *Shroom3*^{-/-} kidneys. To examine the space, I fixed E13.5 kidneys in glutaraldehyde and tannic acid, which preserved the extracellular matrix of the tissue. Analysis of the wildtype kidneys displayed a very thin rim of what appeared to be an extracellular matrix that lined the basal aspect of the ureteric epithelium (Matsuura et al., 2011) (Fig. 32A', Fig. 33B', arrow). In contrast, in *Shroom3*^{-/-} mutant kidneys, the extracellular matrix surrounding the ureteric epithelium was much more prominent and was characterized by being much thicker and electron-dense (Fig 32B', 33C"). Further, I observed that the extracellular spaces surrounding the nephron progenitors in the *Shroom3*^{-/-} mutants contained many fibres consistent with extracellular matrix (Matsuura et al., 2011) (Fig.32B") and this pattern was rarely observed in wildtype. These results suggest that *Shroom3* may be involved in regulating the extracellular matrix production and degradation around the nephron progenitors.

Figure 32: Shroom3 mutant E13.5 nephron progenitors display increased ECM and decreased filipodia formation



Shroom3 mutant E13.5 mice kidneys fixed in tannic acid display absence of filipodia formation in nephron progenitors: Transmission electron microscopy E13.5 mice kidney fixed in glutaraldehyde and tannic acid. (A-A'') Wildtype kidneys illustrated in increasing in magnification show nephron progenitors (NP) sending out multiple long and thin and thick protrusions (black arrow) reaching the ureteric epithelium (UE). (B-B'') Shroom3^{-/-} kidney displayed with a gradual increase in magnification show fewer, shorter nephron progenitors lacking protrusions (black arrow) and increased extracellular matrix (orange arrow) C). Diagram illustrations extracellular matrix (orange arrow) and projection formation (black arrow).

Figure 33: Shroom3 mutant E13.5 display increased extracellular matrix



Shroom3 mutant E13.5 displays an increased extracellular matrix. Transmission electron microscopy E13.5 mice kidney fixed in glutaraldehyde and tannic acid. (A-A'') The basement membrane of wildtype ureteric epithelium (UE) does not have an increased extracellular matrix (arrow). (B-B'') Shroom3^{-/-} ureteric epithelium display an increased extracellular matrix (arrow). The dark line around the ureteric epithelium is only prominent in the mutant tissue.

5. DISCUSSION

Overall Findings

Nephron progenitor cells undergo substantial changes in cell morphology to achieve proper cell migration and cell communication. However, the mechanisms behind these dynamic morphological changes are not fully understood. Shroom3 is an actin-binding protein that regulates cell morphology by modulating the actin cytoskeleton. Our previous work has demonstrated Shroom3 null mice have reduced glomerular number and abnormal developing nephrons. However, the molecular mechanisms by which Shroom3 contributes to abnormal nephron formation are not known. In this study, we analyzed embryonic Wildtype and Shroom3 deficient mice (termed Shroom3^{-/-}) at the molecular and ultrastructural levels to investigate functional roles for Shroom3 in nephron progenitor cells. Our study demonstrated for the first time that in the absence of Shroom3, nephron progenitors exhibit abnormal cell shape, disrupted actin dynamics and altered polarity and cellular projection formation. Taken together, we have elucidated the effects of Shroom3 loss on kidney development which could explain why Shroom3 mutations are highly associated with chronic kidney disease.

5.1 Spatial expression pattern of Shroom3 in select nephron progenitor cells may influence specific cell fate changes during nephron formation

While several studies have identified Shroom3 protein localization in neural, cardiac, lateral line morphogenesis (Hildebrand & Soriano, 1999, Durbin et al., 2020, Ernst et al., 2012), the localization in the nephron progenitors has never been investigated. Our lab was the first to identify Shroom3 expression using LacZ in the cap mesenchyme region of the developing kidney (Hadiseh et al., 2016). Although Shroom3 is found in a long and a short

isoform, past studies have primarily examined the shorter isoform of Shroom3. Prokop et al. 2018 demonstrated localization of the shorter Shroom3 isoform isolated glomerulus cells and HEK293. However, in our study, because our antibody only detected Shroom3 at the N-terminus end, we localized the longer isoform of Shroom3 to select regions of nephron progenitor cells and not the short form. The long isoform contains the PDZ domain, which is a domain that might be involved in enhancing the role of Shroom3 in regulating the structure of cells by binding to the cytoplasmic tail of membrane proteins such as receptor tyrosine kinase receptors which can modulate various signalling pathways (Ponting et al. 1997). Since we detected the longer isoform of Shroom3 with the PDZ domain in select nephron progenitors, this suggests that the large isoform is regulating the structure of select nephron progenitor through an unknown mechanism which is overseen by the PDZ domain. However, since the function of the PDZ domain of Shroom3 remains a mystery, further research will help better interpret the data.

Furthermore, our findings form Shroom3 localization also build on the existing evidence that Shroom3 localization is specific to cell types and, in some cases, to a specific area of the cells to regulate cell morphogenesis. (Ernst et.al, 2012, Hildebrand & Soriano,1999, Durbin et.al, 2020). For instance, a group of researchers found that during lateral line (LL) morphogenesis of zebrafish, Shroom3 regulates apical constriction of cells, and in those cells, Shroom3 is localized in the central region. When assembling, these cells express Shroom3 cluster and apically constrict to form rosettes; however, once the rosettes assembly is complete, Shroom3 expression is downregulated (Ernst et al., 2012). Since the cells involved in lateral line (LL) morphogenesis are migrating cells that cluster together and change cell shape to form the rosettes, these findings suggest a similar role in nephron progenitors. Interestingly, nephron progenitors also migrate, form clusters, and undergo

cell shape changes to form the renal vesicles. I also found that Shroom3 expression is specific to regions within the nephron progenitors but not other regions of the developing kidney. These observations are also similar to findings from a study that examined the expression of Shroom3 in neural tube closure events. A study by Hildebrand and Soriano demonstrated that Shroom3 expression is specific to the cranial neuroepithelium and is not expressed in the surrounding head mesenchyme (Hildebrand & Soriano 1999). In the study, the researchers made similar conclusions that Shroom3 might regulate only some aspects of neural tube closure or only specific cell types. Another study demonstrated that during essential stages of cardiac development, Shroom3 is only expressed in specific cells such as cardiac neural crest cells and cardiomyocytes specific to the ventricles and interventricular septum (Durbin et al., 2020). These studies support our findings that Shroom3 expression is specific to certain cell types. These findings highlighted that Shroom3 might only regulate some aspects of nephrogenesis. For instance, the spatial distribution of Shroom3 in nephron progenitors might regulate their cell fate. Shroom3 may determine whether the cells proliferate to repopulate the nephron progenitor pool, or become induced to migrate, cluster, and eventually differentiate into epithelial cells of the renal vesicles. Combes et al. established that nephron progenitors undergo stochastic migration events, but they also raised the question regarding how nephron progenitor cell fate is controlled in a dynamic environment (Combes et al. 2016). We suggest that the Shroom3 maintains cell shape and proper cell-cell communication, which is important for the stochastic migration of nephron progenitor cells. As an actin regulator, Shroom3 can induce apical constriction in a cell (Hildebrand & Soriano, 1999). The microenvironment of the cells may activate Shroom3 in nephron progenitors, and those select cells can then migrate to areas where they receive more signals to undergo cell differentiation. The fate

of the cells that lack Shroom3 expression may only be to repopulate the nephron progenitor pool. We have evidence suggesting that Shroom3 is only required by cells that will undergo mesenchymal-to-epithelial transition with the previous findings that a mutation of Shroom3 results in abnormal renal vesicle formation (Khalili et al., 2016). Taken together, we postulate that Shroom3 regulates cell shape and cellular movement of specific nephron progenitors that will undergo cell differentiation and proceed to nephron formation.

5.2 Shroom3 might regulate the balance between nephron progenitor self-renewal and differentiation

Nephrogenesis is regulated by the right balance between Six2 dependent self-renewing and canonical Wnt signalling-directed nephron progenitors (Park et al., 2012). Nephron progenitors that express the transcriptional factor Six2 self-renew to ensure a supply of cells for nephrogenesis. In contrast, signalling factors Wnt4 and Fgf8, secreted from the ureteric epithelium, act downstream of Wnt9b signals, and regulate nephron progenitor cell differentiation and their transition to epithelial cells. My data show disorganized, abnormally spaced, and reduced number of Six2 positive cells in the absence of Shroom3. These are important findings because regulation of the self-renewing of nephron progenitors is critical for nephron formation. Previous studies have demonstrated that a reduction of Six2 positive cells ceases nephron progenitors from self-renewing and causes the remaining cells to undergo rapid depletion and premature differentiation (Self et al., 2006, Kobayashi et al., 2008). In my study, I observed a significant decrease in Six2 positive cells only at E13.5 of kidney development; in contrast, the number of Six2 positive cells at E18.5 did not significantly differ. This is interesting because my Pax2 analysis also demonstrates similar findings that Shroom3 plays an age-dependent role of Shroom3. In

support of our findings, a recent study indicated that the balance of self-renewal and differentiation is age-dependent (Liu et al., 2017). For instance, older nephron progenitors, found in postnatal day 0, differentiate at a higher rate than the younger E13.5 nephron progenitors. This is interesting because our studies also demonstrate a more significant impact of Shroom3 in the earlier nephron progenitors than the more mature nephrogenic structures. Therefore, our studies suggest that the self-renewing capacity of the nephron progenitors decreases in the absence of Shroom3. However, since the right balance between proliferation and differentiation is critical for nephron formation, can a decrease in self-renewal capacity of the cell influence or change the process of cell differentiation? While several factors regulate the cell renewal and differentiation of the nephron progenitors, one secreted factor critical that controls both are ureteric bud derived Wnt9b (Kispert et al., 1998). Wnt9b induces select nephron progenitors, typically those with reduced Six2 expression, to cluster together and form the pre-tubular aggregates under the tip-stalk junction. (Ramalingam et al., 2018). Wnt9b upregulates Wnt4 to induces the pre-tubular aggregates to undergo mesenchymal-to-epithelial transition. (Park et al., 2007). Previous studies from our lab have also demonstrated abnormal renal vesicle formation, which suggests improper cell differentiation in the absence of Shroom3. Additionally, in my studies, I show a deletion of Shroom3 during kidney development results in the formation of rounder, shorter and abnormally clustered nephron progenitors. Since nephron progenitor cell clustering and changes in cell morphology are the first steps for initiating nephron formation, the observed abnormalities suggest Shroom3 might act downstream of Wnt9B signalling. Thus, my findings add to the growing body of data on the importance of cell-cell signalling and can help identify novel molecular players and pathways that regulate nephron formation.

5.3 Shroom3 influences nephron progenitor cell orientation

Studies have shown that nephrons exhibit apical, basal polarity patterns, which help maintain fluid homeostasis. Cellular polarity is thought to be first established during renal vesicle stage formation (Georgas et al., 2009). During normal development, select nephron progenitor cells move around and create attachments and detachments to the ureteric epithelium, a characteristic of a polarized cell (Combes et al., 2016). Researchers also suggest that nephron progenitors have an intrinsic cell polarity. (O'Brien et al., 2016). They demonstrated that mutation of Wnt11, can cause the nephron progenitors to lose their polarity, cell organization and ability to form attachments which eventually can lead to abnormal nephron formation. In our study, we questioned whether the observed abnormalities of Shroom3^{-/-} nephron progenitors resulted due to lack of polarity and orientation. Similar to the findings by O'Brien et al., we demonstrated that wildtype nephron progenitor cells exhibit a specific orientation, whereas this polarity was altered in Shroom3^{-/-} nephron progenitors. A change in cell orientation suggests that the intrinsic polarity of the cell has altered. These changes can be due to changes in the cell actin cytoskeleton. As an actin regulator, we proposed that Shroom3 may facilitate the re-arrangement of F-actin in such a manner that orients the nephron progenitors. As a result, this affects the position of polarity markers such as the Golgi matrix marker. During migration, the Golgi re-orientes to the front of the cell, and this process is dependent on Rho-kinase. Many studies demonstrate that Shroom3 works through the Rho-associated coiled-coil kinase (Rock) and myosin II pathway to regulate the actin cytoskeleton and induces apical constriction (Nishimura and Takeichi, 2008, Plageman et al., 2011, Chung et al., 2010). Taken together, these studies suggest that genetic deletion of Shroom3 can prevent

the activation of non-muscle myosin, leading to the disrupted actin cytoskeleton, nephron progenitor shape changes, and changes to the cell orientation.

5.4 Shroom3 mutation may be disrupting ECM dynamics and cross talk between cells

Studies have established that nephron progenitors are motile cells that can attach and then detach from the ureteric epithelium during development (O'Brien et al., 2016; Combes et al., 2016). However, there is still limited understanding of the cell microenvironment, such as the extracellular matrix and other factors influencing motility and cell-cell communication. Integrins facilitate cell-extracellular matrix adhesion during kidney development and regulate cell cytoskeleton (Matsuura et al., 2011). In this study, observation of E13.5 Shroom3^{-/-} embryonic kidneys displayed no changes in integrin expression from the wildtype. However, E18.5 Shroom3^{-/-} embryonic kidneys demonstrated a lack of integrin expression between adjacent nephron progenitor cells. We suspected that integrins are not localized appropriately due to hindered communication between the nephron progenitors, the interstitial space surrounding the cells and the ureteric epithelium. Integrin- α 8 is a transmembrane receptor found on the nephron progenitor cell surface, which assists epithelial-mesenchymal interactions (Müller et al., 1997). My study also demonstrated that Shroom3^{-/-} nephron progenitors appear disoriented and separated by a large space from the ureteric epithelium. We suspected that these observations might be due to the large gaps between the cells, hindering cell-communicating. A study highlighted that nephronectin is an extracellular matrix protein that binds that functions as a ligand that binds to integrin- α 8 β 1 of nephron progenitors (Linton et al., 2007). As a result, integrin- α 8 β 1 activates the Glial cell line-derived neurotrophic factor (GDNF), which regulates branching morphogenesis. Thus, this study further highlights that integrin

function may be hindered in the absence of Shroom3 because the signals responsible for activating integrins, such as extracellular matrix secreted factors, are not functioning to activate the integrin receptors. Linton et al. also predict that ligand-binding integrins activate the cellular signal transduction mechanism, regulating actin cytoskeletal organization and dynamics (Linton et al., 2007). In conjunction with our findings, these studies suggest that deletion of Shroom3 affects the crosstalk between cells, primarily by interrupting the communication between the integrin and integrin-to-matrix proteins.

In addition, our transmission electron microscopy analysis of Shroom3^{-/-} embryonic mouse kidneys also suggest abnormal cell-cell communication in the absence of Shroom3. Our study demonstrated increased extracellular matrix production (ECM) between nephron progenitor cells and around the ureteric epithelium. This suggests that a deletion of Shroom3 might prevent the breakdown of the extracellular matrix, and therefore hindering cell movement and communication. However, these results contradict the claims of Minuth et al., who demonstrated that strands of the extracellular matrix visibly retraction out from the ureteric epithelium in neonatal rabbit kidneys. However, our analysis saw an increased ECM outlining the ureteric epithelium Shroom3^{-/-} kidneys, which was not observed in the Wildtype. While we used the same fixation method, glutaraldehyde and tannic acid solution, our animal models differed. We used a mouse model with a CD1 background mouse, whereas this study used neonatal rabbit kidneys. For our analyses, we also considered the E13.5 wildtype kidneys as our control, to which we compared the Shroom3^{-/-} E13.5 kidneys. These results show increased ECM had increased in the absence of Shroom3, suggesting that the extra ECM may hinder cell communications across development. As ECM turnover would be critical for proper nephron progenitor clustering

and migration, these studies could help explain the inability of the nephron progenitor cells to cluster and develop into renal vesicles.

5.5 Shroom3 modulates nephron progenitor cell cytoskeleton and influences nephron projection formation.

Cellular projections are critical for modulating communications between cells. Recent studies demonstrate that nephron progenitors change shape and create cellular protrusions that elongate towards the ureteric epithelium (O'Brien et al., 2019). However, the molecular mechanisms that drive cell shape changes and projections formation are still poorly understood (Lawlor et al., 2019). My study demonstrated that Shroom3^{-/-} progenitors lack proper shape and display altered filipodia-like cellular projection formation. A recent investigation of Shroom3 in cardiac development demonstrated that the septal cardiomyocytes appear rounder and lacked lamellipodia and filopodia in the absence of Shroom3 (Durbin et al., 2020). Interestingly, our observation of Shroom3 mutant nephron progenitors is identical to those observed in the study. Therefore, this study provides further evidence that Shroom3 modules cellular projection formation.

Filopodia and lamellipodia develop when F-actin filaments accumulate at the cells' leading edge. The accumulation of actin and protrusion formation at the cell membrane then exert a mechanical force to drive cell movement (Fletcher and Mullins, 2010; Johnson et al., 2015). Interestingly, a study by Hildebrand and Soriano demonstrated that Shroom3 recruits F-actin to ectopic sites of epithelial cells to induce apical constriction (Hildebrand and Soriano, 1999). These studies suggest that Shroom3 may module localization of actin-filaments, further suggesting that it controls a significant component of projection formation. Our study demonstrates that F-actin is abnormally distributed in nephron

progenitors in Shroom3 mutant mice, suggesting Shroom3 may control nephron progenitors' cytoskeleton. Previous studies from our lab demonstrated that a deletion of Shroom3 leads to the distorted Rho–kinase/myosin II signalling and loss of actin localization in podocytes, overall decreasing their function (Khalili et al. 2016). Other studies show that epithelial to mesenchymal transition (EMT) occurs because of actin-dependent protrusions, which propel cell migration (Shankar et al., 2010).

These studies together confirm our findings that Shroom3 regulates actin distribution. Additionally, the Rho–kinase/myosin II signalling also facilitates the transition of columnar-shaped cells found in tubular epithelial cells of the kidney into a wedge-shaped form. Studies show that in the absence of myosin II, human keratinocytes that are typically motile fail to generate lamellar protrusions and migrate (Sarkar et al., 2009). Kurosaka et al. suggested that although many actin-binding proteins participate in the leading-edge actin dynamics, such as actin assembly, disassembly, sequestering, and crosslinking, many of these proteins do so are yet to be identified (Kurosaka et al., 2008). Together these findings indicate a role of Shroom3 modulating changes to nephron progenitor cell morphology by regulating subcellular distribution of F-actin, which can also mediate cellular projection formation and cell shape changes.

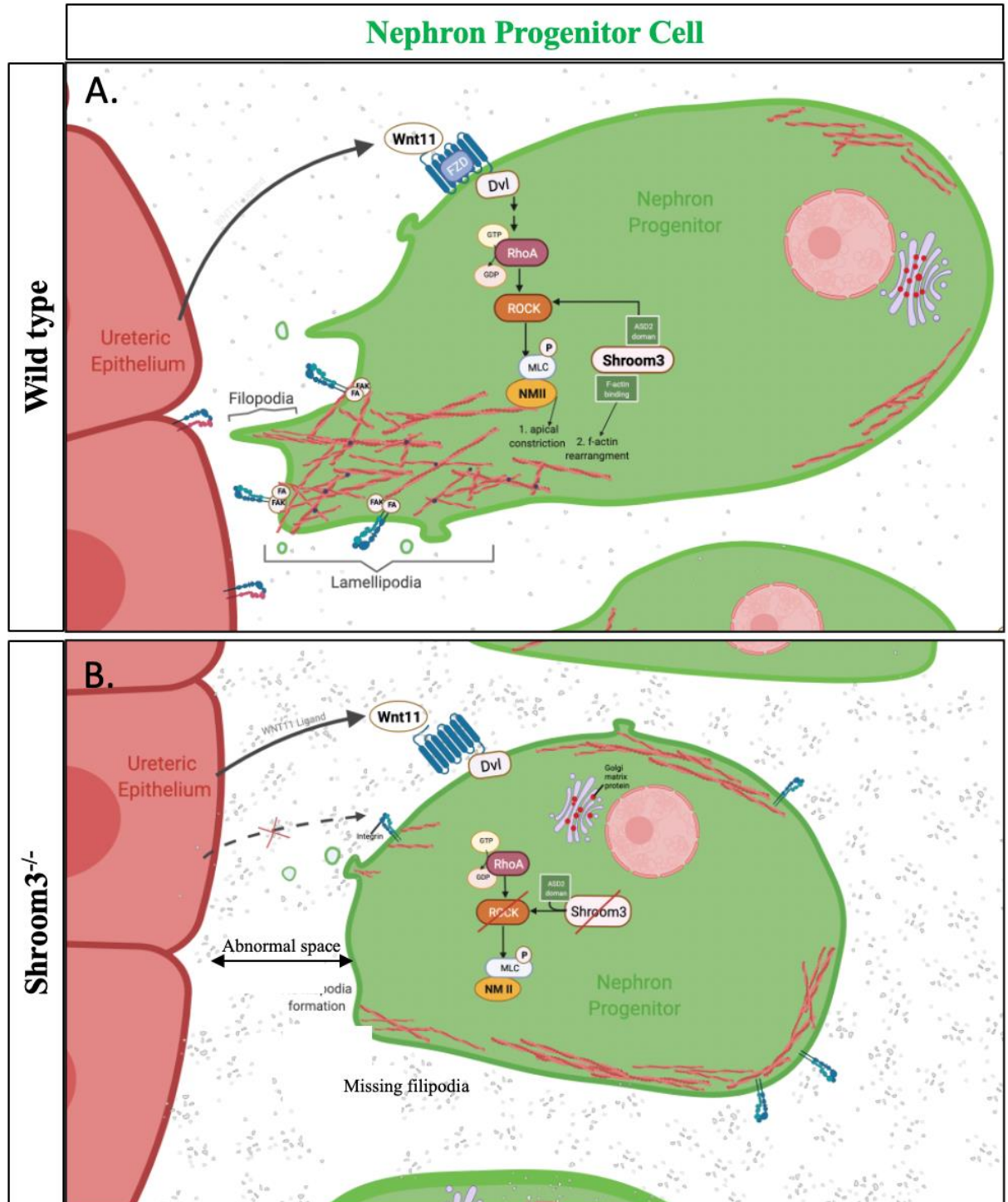
5.6 Potential Mechanism of Shroom3

Studies have demonstrated that Wnt signalling controls nephron progenitor cell differentiation and ureteric bud development (Torres et al., 2000). A part of the Wnt family of proteins secreted by the ureteric epithelium is Wnt11, which functions to modulate nephron progenitor cell differentiation during kidney development (O'Brien et al., 2018). Non-canonical Wnt11 signalling also controls cell motility, adhesion, and re-arrangements

of the cytoskeleton (Wiese et al., 2018; van Amerongen, 2012). A study demonstrated that homozygous deletion of Wnt11 results in changes to nephron progenitor cell morphology. More specifically, Wnt11 null nephron progenitors displayed loss of cell polarity, reduced cell clustering, and reduced nephron progenitor projections (O'Brien et al., 2014), identical to the kidney phenotype of Shroom3^{-/-} embryonic kidneys. The similarities suggest that Wnt11 and Shroom3 maintain the cellular dynamics of nephron progenitors, by regulating the generation of cellular projections. Interestingly studies show that Shroom3 and Wnt11 regulate Rock/myosin light chain pathway through the Planar Cell Polarity (PCP) pathway (Hildebrand et al., 1999, Ernst et al., 2012, Rodriguez-Hernandez et al., 2020). The PCP signalling pathway can alter the actomyosin cytoskeleton, cellular morphology, organization, and movement. The PCP pathway is activated when Wnt-ligands, Wnt11 and Wnt5a bind to their receptors such as Frizzled, activate downstream proteins Dishevelled, which signal activation of DAAM1, members of RHOA and ROCK1. Studies showed that Wnt11 binds receptor Frizzled in neural tube development, which activates Dishevelled2 and downstream regulatory factors Rock and myosin II to regulate the actin dynamics (Rodriguez-Hernandez et al., 2020). McGreevy et al. also investigated Shroom3 as a downstream regulator of the PCP pathway in neural tube development. In this study, researchers demonstrated that during neural tube development, Shroom3 and Dishevelled2 co-localize to form a physical complex (McGreevy et al., 2015). A recent study by Durbin et al. confirmed that Shroom3 directly interacts with Dsihevelled2. In addition to that, this study also showed that a genetic mutation of Shroom3 leads to a disrupted cardiomyocytes organization, polarity, roundedness, and formation of lamellipodia and filopodia (Durbin et al., 2020). Interestingly, my studies also show that filipodia formation is hindered in the absence of Shroom3. Together, these studies support the role of Shroom3 in regulating

cellular projection formation. These studies demonstrate that Shroom3 modulates cell movement, likely acting downstream of the Wnt11 PCP pathway.

Figure 34: Model of Shroom3 function in nephron progenitors



Model of Shroom3 function in nephron progenitors. Schematic represents potential mechanisms of Shroom3 regulating nephron progenitor cell morphology downstream of the non-canonical Wnt11 and Planar cell polarity pathway A) In a normal wildtype nephron progenitor, it is suspected that Wnt11 ligand binds to receptor Frizzled, which activates the Rock-Myosin pathway through direct interaction with Shroom3. Shroom3 ensures Rock-myosin pathway activation at the leading edge (proximal) end of the cell, where it helps cells with apical constriction. This induces the cell shape changes and gives the nephron progenitors an elongated cell shape. It is proposed that Shroom3 also recruits F-actin to an area of the cell to help generate F-actin-based filipodia formation. B) In the absence of Shroom3, Rock-Myosin pathway activation is hindered, and F-actin does not get recruited to the apical side of the cells to help induce shape changes and generate thin-filopodia projections. Thus, these alterations prevent nephron progenitors from reaching the ureteric epithelium. The increased ECM and lack of projection formation further blocks the communication between the cells.

5.7 Future directions and implications

The genome-wide association studies demonstrated that mutations of the Shroom3 gene are highly associated with chronic kidney disease. Several recent studies have also demonstrated that genetic variation of Shroom3 leads to reduced glomerular filtration rate, increased albumin-to-creatinine ratio, low serum magnesium levels and overall, with risk for developing chronic kidney disease (Wuttke et al., 2019, Graham 2019). Studies analyzing the genetic variation of Shroom3 have increased our understanding of the mechanisms that govern the function of Shroom3, many aspects of Shroom3 remain unclear. For instance, published data from our lab has confirmed the importance of Shroom3 in developing functioning nephrons (Hadiseh et al., 2015). However, limited research labs study the kidney progenitor cell population and disease progression in Canada. Therefore, with our work, we aim to decipher the mechanisms of Shroom3 action in kidney development to help future researchers generate therapies that may potentially rescue or prevent kidney abnormalities.

Researchers have advanced developmental biology research by investigating cell-cell communication, morphological and biochemical changes, and functional properties for many years. Despite this knowledge, however, the cellular communication, changes in cell morphology and migration events, the molecular processes that derive many of these changes during kidney development remain unclear. In our study, we demonstrated for the first time that Shroom3 plays an essential role in regulating nephron progenitor cell shape and cell polarity. In addition to that, we highlighted a novel role of Shroom3 in regulating cellular projection formation. Since the re-arrangement of F-actin and intrinsic polarity of a cell are the underlying mechanisms that help generate projections, we believe that the absence of Shroom3 hinders the activity of ROCK/Non-muscle myosin resulting in an abnormal arrangement of actin cytoskeleton dynamics. These novel findings and the potential mechanism of Shroom3 in nephron progenitors will aid future researchers in understanding mechanisms associated with cell protrusions and how they drive further nephrogenesis. We suspect that subtle abnormalities in cell morphology, localization and overall regulation of nephron progenitors can alter nephron formation and function during development.

However, despite these findings, our current Shroom3 model includes involves a global knockdown of Shroom3. Future studies should consider using the Cre-loxP system to create a model with a conditional knockout of Shroom3 in the nephron progenitors. This mouse model can be achieved by crossing Shroom3 LoxP mice with Six2CRE^{GFP+} mice. The cross will generate mice that are homozygotes for Shroom3 or heterozygous. The Six2CRE^{GFP} mice have been used many times in the past to study nephron progenitors (Kobayashi et al., 2008). Thus, by using this model, future studies can build on our current findings to identify the underlying mechanism of shroom3 in regulating nephron progenitor

cell morphology. We hope that our studies can help uncover the mechanisms regulating kidney development to assist with early disease prevention and treatment investigation.

6. Conclusions:

Our study demonstrated for the first time that nephron progenitors in Shroom3 null embryonic kidneys exhibit abnormal cell shape, disrupted actin dynamics, and altered polarity and cellular projections. During kidney development, nephron formation is dependent on changes in nephron progenitor cell morphology which mitigates cell clustering and migration. Our study demonstrated for the first time that nephron progenitors in Shroom3 null embryonic kidneys exhibit abnormal cell shape, cell clustering, disrupted actin dynamics, and altered polarity and cellular projections. Thus, this shows that Shroom3 regulates nephron progenitor cell morphology and projection formation. Furthermore, our findings suggest these abnormalities in nephron progenitors translate to a poorly polarized nephron epithelium and poor nephron function. Although years of research has identifying and understanding genetics and kidney disease, the underlying mechanisms of disease progression remain unclear. Using the findings from this study, we hoped to understand better the structural abnormalities that arise due to genetic mutation of Shroom3 during kidney development. We hope to build a foundation to aid the investigation, prevention, and treatment of kidney disease.

7. References

1. Anderson, L. R., Owens, T. W., & Naylor, M. J. (2014). Structural and mechanical functions of integrins. *Biophysical reviews*, 6(2), 203-213.
2. Brophy PD, Ostrom L, Lang KM, Dressler GR. Regulation of ureteric bud outgrowth by Pax2-dependent activation of the glial derived neurotrophic factor gene. *Development*. 2001;128:4747–4756.
3. Brown, A. C., Muthukrishnan, S. D., Guay, J. A., Adams, D. C., Schafer, D. A., Fetting, J. L., & Oxburgh, L. (2013). Role for compartmentalization in nephron progenitor differentiation. *Proceedings of the National Academy of Sciences*, 110(12), 4640-4645.
4. Cai Y, Lechner MS, Nihalani D, Prindle MJ, Holzman LB, Dressler GR. Phosphorylation of Pax2 by the c-Jun N-terminal kinase and enhanced Pax2-dependent transcription activation. *The Journal of biological chemistry*. 2002;277:1217–1222.
5. Carroll, T. J., Park, J. S., Hayashi, S., Majumdar, A., & McMahon, A. P. (2005). Wnt9b plays a central role in the regulation of mesenchymal to epithelial transitions underlying organogenesis of the mammalian urogenital system. *Developmental cell*, 9(2), 283-292.
6. Cebrian C, Asai N, D'Agati V, Costantini F. The number of fetal nephron progenitor cells limits ureteric branching and adult nephron endowment. *Cell Rep*. 2014;7(1):127–137. doi:10.1016/j.celrep.2014.02.033
7. Combes, A. N., Lefevre, J. G., Wilson, S., Hamilton, N. A., & Little, M. H. (2016). Cap mesenchyme cell swarming during kidney development is influenced by attraction, repulsion, and adhesion to the ureteric tip. *Developmental biology*, 418(2), 297-306.
8. Dressler GR. Advances in early kidney specification, development and patterning. *Development*. 2009;136(23):3863-3874. doi:10.1242/dev.034876
9. Dressler, G. R. (2006). The cellular basis of kidney development. *Annu. Rev. Cell Dev. Biol.*, 22, 509-529.
10. Durbin, M. D., O’Kane, J., Lorentz, S., Firulli, A. B., & Ware, S. M. (2020). SHROOM3 is downstream of the planar cell polarity pathway and loss-of-function results in congenital heart defects. *Developmental biology*, 464(2), 124-136.
11. Erica M. McGreevy, Deepthi Vijayraghavan, Lance A. Davidson, Jeffrey D. Hildebrand; Shroom3 functions downstream of planar cell polarity to regulate myosin II distribution and cellular organization during neural tube closure. *Biol Open* 15 February 2015; 4 (2): 186–196. doi: <https://doi.org/10.1242/bio.20149589>
12. Ernst, S., Liu, K., Agarwala, S., Moratscheck, N., Avci, M. E., Dalle Nogare, D., ... & Lecaudey, V. (2012). Shroom3 is required downstream of FGF signalling to mediate proneuromast assembly in zebrafish. *Development*, 139(24), 4571-4581
13. Gong, K.-Q., Yallowitz, A. R., Sun, H., Dressler, G. R., and Wellik, D. M. (2007). A Hox-Eya-Pax complex regulates early kidney developmental gene expression. *Mol. Cell. Biol.* 27, 7661–7668. doi: 10.1128/mcb.00465-07
14. Habas, R., Kato, Y., & He, X. (2001). Wnt/Frizzled activation of Rho regulates vertebrate gastrulation and requires a novel Formin homology protein Daam1. *Cell*, 107(7), 843-854.

15. Heier, J. A., Dickinson, D. J., & Kwiatkowski, A. V. (2017). Measuring protein binding to F-actin by co-sedimentation. *JoVE (Journal of Visualized Experiments)*, (123), e55613.
16. Hildebrand, Jeffrey D., and Philippe Soriano. "Shroom, a PDZ domain– containing actin-binding protein, is required for neural tube morphogenesis in mice." *Cell* 99.5 (1999): 485-497
17. Johnson, H. E., King, S. J., Asokan, S. B., Rotty, J. D., Bear, J. E., & Haugh, J. M. (2015). F-actin bundles direct the initiation and orientation of lamellipodia through adhesion-based signaling. *Journal of Cell Biology*, 208(4), 443-455.
18. Kanwar, Y. S., Wada, J., Lin, S., Danesh, F. R., Chugh, S. S., Yang, Q., Banerjee, T., & Lomasney, J. W. (2004). Update of extracellular matrix, its receptors, and cell adhesion molecules in mammalian nephrogenesis. *American journal of physiology. Renal physiology*, 286(2), F202–F215. <https://doi.org/10.1152/ajprenal.00157.2003>
19. Kardash, E., Reichman-Fried, M., Maitre, J.L., Boldajipour, B., Papusheva, E., Messerschmidt, E.M., Heisenberg, C.P., and Raz, E. (2010). A role for Rho GTPases and cell-cell adhesion in single-cell motility in vivo. *Nat. Cell Biol.* 12, 47–53, supp. 1–11.
20. Khalili, Hadiseh, et al. "Developmental origins for kidney disease due to Shroom3 deficiency." *Journal of the American Society of Nephrology* 27.10 (2016): 2965-2973.
21. Kim, J. K., Shin, Y. J., Ha, L. J., Kim, D. H., & Kim, D. H. (2019). Unraveling the mechanobiology of the immune system. *Advanced Healthcare Materials*, 8(4), 1801332.
22. Kimura S, Hase K, Ohno H. The molecular basis of induction and formation of tunneling nanotubes. *Cell Tissue Res.* 2013;352(1):67-76. doi:10.1007/s00441-012-1518-1
23. Kispert, A., Vainio, S., & McMahon, A. P. (1998). Wnt-4 is a mesenchymal signal for epithelial transformation of metanephric mesenchyme in the developing kidney. *Development*, 125(21), 4225-4234.
24. Kitala, P., Cunanan, J., & Bridgewater, D. (2019). Characterization of the Role of Shroom3 in Nephron Formation. *The FASEB Journal*, 33(1_supplement), 208-2.
25. Kobayashi, A., Valerius, M. T., Mugford, J. W., Carroll, T. J., Self, M., Oliver, G., & McMahon, A. P. (2008). Six2 defines and regulates a multipotent self-renewing nephron progenitor population throughout mammalian kidney development. *Cell stem cell*, 3(2), 169-181.
26. Kondo, T., & Hayashi, S. (2015). Mechanisms of cell height changes that mediate epithelial invagination. *Development Growth and Differentiation*, 57(4), 313–323. <https://doi.org/10.1111/dgd.12224>
27. Kurosaka, S., & Kashina, A. (2008). Cell biology of embryonic migration. *Birth Defects Research Part C: Embryo Today: Reviews*, 84(2), 102-122.
28. Kuure, S., Vuolteenaho, R., & Vainio, S. (2000). Kidney morphogenesis: cellular and molecular regulation. *Mechanisms of development*, 92(1), 31-45.
29. Lee, C., Scherr, H. M., & Wallingford, J. B. (2007). Shroom family proteins regulate - tubulin distribution and microtubule architecture during epithelial cell shape change. *Development*, 134(7), 1431–1441. <https://doi.org/10.1242/dev.02828>

30. Lelongt, B., & Ronco, P. (2003). Role of extracellular matrix in kidney development and repair. *Pediatric nephrology*, 18(8), 731-742.
31. Linton, J. M., Martin, G. R., & Reichardt, L. F. (2007). The ECM protein nephronectin promotes kidney development via integrin α 8 β 1-mediated stimulation of Gdnf expression. *Development*, 134(13), 2501-2509.
32. Liu, J., Edgington-Giordano, F., Dugas, C., Abrams, A., Katakam, P., Satou, R., & Saifudeen, Z. (2017). Regulation of nephron progenitor cell self-renewal by intermediary metabolism. *Journal of the American Society of Nephrology*, 28(11), 3323-3335.
33. M. Self, O. Lagutin, B. Bowling, J. Hendrix, Y. Cai, G. Dressler, G. Oliver Six2 is required for suppression of nephrogenesis and progenitor renewal in the developing kidney *EMBO J.*, 25 (2006), pp. 5214-5228
34. Matsuura, S., Kondo, S., Suga, K., Kinoshita, Y., Urushihara, M., & Kagami, S. (2011). Expression of focal adhesion proteins in the developing rat kidney. *Journal of Histochemistry & Cytochemistry*, 59(9), 864-874.
35. McGreevy, E. M., Vijayraghavan, D., Davidson, L. A., & Hildebrand, J. D. (2015). Shroom3 functions downstream of planar cell polarity to regulate myosin II distribution and cellular organization during neural tube closure. *Biology Open*, 4(2), 186–196. <https://doi.org/10.1242/bio.20149589>
36. Menon, M. C., Chuang, P. Y., Li, Z., Wei, C., Zhang, W., Luan, Y., ... Murphy, B. (2015). Intronic locus determines SHROOM3 expression and potentiates renal allograft fibrosis. *Journal of Clinical Investigation*, 125(1), 208–221. <https://doi.org/10.1172/JCI76902>
37. Minuth W, W, Denk L: Cell Projections and Extracellular Matrix Cross the Interstitial Interface within the Renal Stem/Progenitor Cell Niche: Accidental, Structural or Functional Cues? *Nephron Exp Nephrol* 2012;122:131-140. doi: 10.1159/000351129
38. Mugford JW, Yu J, Kobayashi A, McMahon AP. High-resolution gene expression analysis of the developing mouse kidney defines novel cellular compartments within the nephron progenitor population. *Dev Biol.* 2009;333(2):312–323. doi:10.1016/j.ydbio.2009.06.043
39. Müller, U., & Brändli, A. W. (1999). Cell adhesion molecules and extracellular-matrix constituents in kidney development and disease. *Journal of cell science*, 112 (Pt 22), 3855–3867.
40. Nemethova, M., Auinger, S., & Small, J. V. (2008). Building the actin cytoskeleton: filopodia contribute to the construction of contractile bundles in the lamella. *The Journal of cell biology*, 180(6), 1233-1244.
41. O'Brien LL, McMahon AP. Induction and patterning of the metanephric nephron. *Seminars in Cell & Developmental Biology.* 2014 Dec; 36:31-38. DOI: 10.1016/j.semcd.2014.08.014.
42. O'Brien, L. L. (2019). Nephron progenitor cell commitment: Striking the right balance. *Seminars in Cell & Developmental Biology*, 91, 94–103. doi: 10.1016/j.semcd.2018.07.017
43. Park, J. S., Ma, W., O'Brien, L. L., Chung, E., Guo, J. J., Cheng, J. G., Valerius, M. T., McMahon, J. A., Wong, W. H., & McMahon, A. P. (2012). Six2 and Wnt regulate self-renewal and commitment of nephron progenitors through shared gene regulatory networks. *Developmental cell*, 23(3), 637–651.

44. Park, J. S., Valerius, M. T., & McMahon, A. P. (2007). Wnt/ β -catenin signaling regulates nephron induction during mouse kidney development. *Development*, 134(13), 2533-2539.
45. Pasapera, Ana M et al. "Myosin II activity regulates vinculin recruitment to focal adhesions through FAK-mediated paxillin phosphorylation." *The Journal of cell biology* vol. 188,6 (2010): 877-90. doi:10.1083/jcb.200906012
46. Ponting, C. P., Phillips, C., Davies, K. E., & Blake, D. J. (1997). PDZ domains: targeting signalling molecules to sub-membranous sites. *Bioessays*, 19(6), 469-479.
47. Preuss, H. G. (1993). Basics of renal anatomy and physiology. *Clinics in Laboratory Medicine*, 13 (1), 1-11
48. Prokop, J. W., Yeo, N. C., Ottmann, C., Chhetri, S. B., Florus, K. L., Ross, E. J., ... & Lazar, J. (2018). Characterization of coding/noncoding variants for SHROOM3 in patients with CKD. *Journal of the American Society of Nephrology*, 29(5), 1525-1535.
49. Ramalingam, H., Fessler, A.R., Das, A., Valerius, M.T., Basta, J., Robbins, L., Brown, A.C., Oxburgh, L., McMahon, A.P., Rauchman, M., et al. (2018). Disparate levels of beta-catenin activity determine nephron progenitor cell fate. *Dev Biol* 440, 13–21.
50. Ravichandran, Y., Goud, B., & Manneville, J. B. (2020). The Golgi apparatus and cell polarity: Roles of the cytoskeleton, the Golgi matrix, and Golgi membranes. *Current opinion in cell biology*, 62, 104-113.
51. Reidy, K. J., & Rosenblum, N. D. (2009, July). Cell and molecular biology of kidney development. In *Seminars in nephrology* (Vol. 29, No. 4, pp. 321-337). WB Saunders.
52. Sakai, T., Li, S., Docheva, D., Grashoff, C., Sakai, K., Kostka, G., ... & Fässler, R. (2003). Integrin-linked kinase (ILK) is required for polarizing the epiblast, cell adhesion, and controlling actin accumulation. *Genes & development*, 17(7), 926-940.
53. Sarkar, S., Egelhoff, T., & Baskaran, H. (2009). INSIGHTS INTO THE ROLES OF NON-MUSCLE MYOSIN IIA IN HUMAN KERATINOCYTE MIGRATION. *Cellular and molecular bioengineering*, 2(4), 486–494. <https://doi.org/10.1007/s12195-009-0094-2>
54. Sawyer, J. M., Harrell, J. R., Shemer, G., Sullivan-Brown, J., Roh-Johnson, M., & Goldstein, B. (2010). Apical constriction: a cell shape change that can drive morphogenesis. *Developmental biology*, 341(1), 5-19.
55. Seely, J. C. (2017). A brief review of kidney development, maturation, developmental abnormalities, and drug toxicity: juvenile animal relevancy. *Journal of toxicologic pathology*, 30(2), 125-133.
56. Shankar, J., Messenberg, A., Chan, J., Underhill, T. M., Foster, L. J., & Nabi, I. R. (2010). Pseudopodial actin dynamics control epithelial-mesenchymal transition in metastatic cancer cells. *Cancer research*, 70(9), 3780-3790.
57. Skorecki, K., Chertow, G. M., Marsden, P. A., Taal, M. W., & Alan, S. L. (2016). *Brenner &*
58. Suzuki, M., Morita, H., & Ueno, N. (2012). Molecular mechanisms of cell shape changes that contribute to vertebrate neural tube closure. *Development, growth & differentiation*, 54(3), 266-276.

59. Svitkina T. (2018). The Actin Cytoskeleton and Actin-Based Motility. *Cold Spring Harbor perspectives in biology*, 10(1), a018267. <https://doi.org/10.1101/cshperspect.a018267>
60. Torres, M. A., & Nelson, W. J. (2000). Colocalization and redistribution of dishevelled and actin during Wnt-induced mesenchymal morphogenesis. *The Journal of cell biology*, 149(7), 1433-1442.
61. Vize, P. D., Woolf, A. S., & Bard, J. B. (Eds.). (2003). *The kidney: from normal development to congenital disease*. Elsevier.
62. Wellik, D. M., Hawkes, P. J., & Capecchi, M. R. (2002). Hox11 paralogous genes are essential for metanephric kidney induction. *Genes & development*, 16(11), 1423-1432.
63. Wiese, C., & Zheng, Y. (2006). Microtubule nucleation: -tubulin and beyond. *Journal of Cell Science*, 119(20), 4143–4153. <https://doi.org/10.1242/jcs.03226>
64. Wu, C., & Dedhar, S. (2001). Integrin-linked kinase (ILK) and its interactors: a new paradigm for the coupling of extracellular matrix to actin cytoskeleton and signaling complexes. *The Journal of cell biology*, 155(4), 505-510.